UNIVERSITÀ
DEGLI STUDI
DI PADOVA

Sede Amministrativa: Università degli Studi di Padova
Dipartimento di Farmacologia ed Anestesiologia "E. Meneghetti"

SCUOLA DI DOTTORATO DI RICERCA IN SCIENZE FARMACOLOGICHE
INDIRIZZO FARMACOLOGIA MOLECOLARE E CELLULARE
CICLO XXII

Agonists of the Cannabinoid Receptor Type 1 (CB1) Promote Rat Cerebellar Neural Progenitor Cell Proliferation Through Activation of ERK and Akt Pathways

Direttore della Scuola: Ch.mo Prof. Rosa Maria Gaion

Coordinatore d'indirizzo: Ch.mo Prof. Pietro Giusti

Supervisore: Ch.mo Prof. Pietro Giusti

Dottorando: Silvia Soffia

15 Marzo 2010

ABSTRACT

Endocannabinoids represent a novel class of intercellular messengers, the function of which includes retrograde signaling in the brain and mediation or modulation of several types of synaptic plasticity. Endocannabinoid signaling not only regulates the proliferation, migration, specification, survival, and phenotypic differentiation of neural progenitors during central nervous development (Harkany,T. *et al*., 2008) but has been shown to control proliferation and differentiation of neural stem/progenitor cells in the hippocampal subgranular zone and in the subventricular zone of the adult mammalian brain (Jiang,W. *et al*., 2005; Palazuelos,J. *et al*., 2006). To elucidate the cellular and molecular mechanisms underlying cannabinoid neurogenic action, we used neural progenitor cells isolated from primary cultures of rat postnatal cerebellum as an *in vitro* model of neural cell proliferation. These cells share some of the phenotypic and genotypic properties of stem cells, as characterized by immunocytochemistry and reverse transcription-polymerase chain reaction, respectively (Zusso,M. *et al.*, 2004).

The functional presence of the two cannabinoid receptors CB1 and CB2 in cerebellar neural progenitor cells at 10 days *in vitro* (DIV) was assessed by immunocytochemistry and Western blotting. Proliferation was evaluated using a [^{3}H]-thymidine incorporation assay. A significant increase in cerebellar neural progenitor cell proliferation *vs* the corresponding vehicle control was found following 24 h incubation with the synthetic non-selective CBR agonists WIN 55,212-2 (100 nM) or CP 55,940 (1000 nM) (43 ± 22 % and 37 ± 8 %, respectively), which was completely abolished by treatment with 1000 nM AM 251 (1 h pre-incubation), a selective CB1 receptor antagonist.

To evaluate a direct involvement of the CB1 receptor in the proliferative response, cerebellar neural progenitors were incubated for 24 h with ACEA (1-1000 nM), a potent selective CB1 receptor agonist. ACEA (1 nM and 10 nM) significantly increased [^{3}H]-thymidine incorporation (by 50.59 ± 6.72 % and 35.77 ± 4.48 %, respectively) and this effect was completely reverted by 10 nM AM 251. To investigate the involvement of the mitogen-activated protein kinase kinase/extracellular signal-regulated kinase (ERK)1,2 and phosphatidylinositol 3-kinase/Akt/glycogen synthase kinase-3-β signaling pathways in CB1 receptor-induced cerebellar neural progenitor proliferation, we performed SDS-PAGE Western blotting. Fifteen minutes incubation of cerebellar neural progenitor cells with 1 nM

ACEA produced a significant activation of Akt (36.54 ± 7.21%) that persisted up to 30 min (21 ± 5 %). A significant, concomitant ERK1,2 activation (32 ± 4 %) was observed at this time, as well. A 1 h pre-incubation with 10 nM AM 251 *per se* did not affect Akt and MAPK phosphorylation levels but did inhibit the ACEA agonistic effect on both kinases.

The existence of cross-talk between the two pathways was confirmed by using the corresponding selective inhibitors, LY294002 (75 μM, 3 h pre-incubation) and U0126 (10 μM, 1 h pre-incubation). The phosphatidylinositol 3-kinase inhibitor LY294002 not only inhibited 1 nM ACEA-induced cerebellar neural progenitor Akt activation but also ERK phosphorylation, while the mitogen-activated protein kinase kinase inhibitor U0126 inhibited ERK activation without affecting the Akt pathway, both in untreated and ACEA-treated cells.

Preliminary experiments have been performed to investigate the potential role of ACEA in cerebellar neural progenitor cell differentiation, evaluating the expression pattern of the transcript variants of the ARE-binding protein AUF1, which is regulated during postnatal cerebellar development (Hambardzumyan,D. *et al*., 2009).

RIASSUNTO

Gli endocannabinoidi rappresentano una nuova classe di messaggeri intercellulari che mediano la conduzione retrograda del segnale sinaptico e regolano così varie forme di plasticità sinaptica. Il segnale endocannabinoide non solo controlla la proliferazione cellulare, la migrazione, il destino decisionale, la sopravvivenza, ed il differenziamento ad un fenotipo maturo dei progenitori neurali durante lo sviluppo del sistema nervoso centrale (Harkany,T. *et al*., 2008), ma è stato dimostrato possedere un ruolo nella proliferazione e nel differenziamento di cellule staminali/progenitrici neurali esistenti nella zona subgranulare di ippocampo e nella zona subventricolare del cervello di mammifero adulto (Jiang,W. *et al*., 2005; Palazuelos,J. *et al*., 2006). Allo scopo di definire i meccanismicellulari e molecolari che sottendono all'azione neurogenica di questi composti, è stato utilizzato un modello di proliferazione cellulare neurale *in vitro* rappresentato da cellule progenitrici neurali isolate da colture primarie di cervelletto di ratto postnatale. La caratterizzazione di queste cellule, sia genotipica, tramite RT-PCR, che fenotipica, tramite analisi immunocitochimica, ha evidenziato che esse possiedono proprietà tipiche delle cellule staminali (Zusso,M. *et al*., 2004).

La presenza funzionale dei due recettori cannabici CB1 e CB2 nelle cellule progenitrici neurali cerebellari a 10 giorni in coltura (10 days *in vitro*, DIV) è stata confermata tramite analisi immunocitochimica e Western blotting. La proliferazione cellulare è stata valutata tramite saggio d'incorporazione di timidina triziata. Tramite questo saggio è stato riscontrato un aumento significativo rispetto al controllo della proliferazione dei progenitori neurali cerebellari, per trattamento di 24 ore con gli agonisti sintetici non selettivi dei recettori cannabici, WIN 55,212-2 (100 nM) o CP 55,940 (1000 nM) (43 ± 22 % e 37 ± 8 %, rispettivamente), completamente inibito dal pretrattamento di un'ora con l'antagonista selettivo del recettore CB1 AM 251 (1000 nM).

Al fine di valutare il diretto coinvolgimento del recettore CB1 nella risposta proliferativa, le cellule progenitrici neurali cerebellari sono state incubate per 24 ore con ACEA, potente agonista selettivo del recettore CB1. ACEA, alla concentrazione di 1 e 10 nM, ha indotto una significativa incorporazione del radionuclide rispetto alle cellule non trattate (50.59 ± 6.72 % e 35.77 ± 4.48 %, rispettivamente), ma la risposta è stata completamente inibita da AM 251 allaconcentrazione 10 nM.

Allo scopo di studiare il coinvolgimento delle cascate di trasduzione del segnale MEK/ERK1,2 ed IP3K/Akt/GSK3-β nella risposta proliferativa delle cellule progenitrici mediata dall'attivazione del recettore CB1, è stata usata la tecnica del SDS-PAGE Western blotting. L'incubazione delle cellule progenitrici con 1 nM ACEA ha prodotto un incremento significativo dei livelli di attivazione di Akt a 15 minuti (36.54 ± 7.21%) che persiste fino a 30 minuti di trattamento (21 ± 5 %), tempo a cui si registra un concomitante aumento dei livelli di fosforilazione della proteina ERK (32 ± 4 %). Il trattamento di 60 minuti con AM 251 alla concentrazione 10 nM non influenza i livelli basali di attivazione delle due chinasi, ma inibisce completamente l'effetto mediato da ACEA.

Successivamente è stato possibile confermare l'esistenza di un "cross-talk" tra le due cascate di trasduzione del segnale tramite impiego dei rispettivi inibitori selettivi. L'inibitore della fosfatidilinositolo-3 chinasi, LY294002 (75 μM, 3 ore di preincubazione), ha inibito l'attivazione di entrambe le chinasi nelle cellule progenitrici trattate con ACEA, mentre l'inibitore di MEK, U0126 (10 μM, un'ora di preincubazione), ha inibito l'attivazione di ERK in cellule trattate e non, senza influenzare la fosforilazione di Akt.

Sono stati eseguiti alcuni esperimenti preliminari per valutare un potenziale ruolo di ACEA nel differenziamento delle cellule progenitrici neurali cerebellari, tramite analisi dell'espressione delle varianti trascrizionali della proteina AUF1 che lega sequenze ricche di adenina e uracile dell'RNA messaggero ed è regolata durante lo sviluppo cerebellare postnatale (Hambardzumyan,D. *et al*., 2009).

INDEX OF CONTENTS

INDEX OF FIGURES

CHAPTER 1:

CHAPTER 3:

INDEX OF TABLES

LIST OF ABBREVIATIONS

ABH	αβ-hydrolase
AC	adenylate cyclase
2-AG	*sn*-2-arachidonoylglycerol
AEA	*N*-arachidonoylethanolamine
2-AGE	2-arachidonyl glyceryl ether
AMPARs	α-amino-3-hydroxyl-5-methyl-4-isoxazole-propionate receptors
AMT	AEA membrane transporter
ANOVA	analysis of variance
APS	ammonium persulfate
AUF1	AU-rich element/poly(U)-binding/degradation factor 1
BDNF	brain-derived neurotrophic factor
bFGF	basic fibroblast growth factor
BG	Bergman glia
BME	eagle's basal medium
Bq	Becquerel
BSA	bovine serum albumin
cAMP	cyclic adenosine monophosphate
CBR	cannabinoid receptor
CCK	cholecystokinin
cDNA	complementary DNA
CF	climbing fibres
CGC	cerebellar granule cells
CNS	central nervous system
COX-2	cyclooxygenase-2
CREB	cAMP response element binding protein
CSF	cerebrospinal fluid
D	dilution factor
DAG	1-acyl-2-arachidonoylglycerol
DAGL	diacylglycerol lipase
DAPI	4'-6-Diamidino-2-phenylindole
dATP	deoxyadenosine triphosphate
dCTP	deoxycytidine triphosphate
DEPC	diethylpyrocarbonate
dGTP	deoxyguanosine triphosphate
DIV	days *in vitro*
DNMT1	DNA methyltransferase I
dNTP	deoxyribonucleotide triphosphates
D_2R	D_2-type receptors
dsDNA	double-stranded DNA
DSE	depolarization-induced suppression of excitation
DSI	depolarization-induced suppression of inhibition
DTT	Dithiothreitol
dTTP	deoxythymidine triphosphate
E	embryonic day
eCB	endocannabinoid

ECL	enhanced chemiluminescence
EGF	epidermal growth factor
EGL	external granular layer
EMT	endocannabinoid membrane transporter
ERK	extracellular signal-regulated kinase
FAAH	fatty acid amide hydrolase
GABA	γ-aminobutyric acid
GAD	glutamate decarboxylase
GAPDH	glyceraldehyde 3-phosphate dehydrogenase
GC	granule cells
GDE1	glycerophosphodiester phosphodiesterase 1
GFAP	glial fibrillary acidic protein
GLAST	astrocyte-specific glutamate transporter
GPCR	G protein-coupled receptor
GPR55	G protein-coupled receptor 55
GSK-3β	glycogen synthase kinase 3β
h	hours
HAEA	hydroxy-*N*-arachidoylethanolamine
HDACI	histone deacetylase
HNSC	human neural stem cell
HRP	horseradish peroxidase
5-HT	5-Hydroxytryptamin
IGF1	insulin-like growth factor 1
IGL	internal granular layer
iNOS	inducible NOS
LIPOX	lipoxygenase
LPS	lipopolysaccharide
LTD	long-term depression
LTP	long-term potentiation
MAGL	monoacylglycerol lipase
MAP2	microtubule-associated protein 2
MAPK	mitogen activated protein kinase
MEK	MAPK kinase
MF	mossy fibres
mGluR1	metabotropic glutamate receptor 1
ML	molecular layer
NADA	*N*-arachidonoyl-dopamine
NAE	*N*-Acylethanolamine
NAPE	*N*-acyl phosphatidylethanolamine
NAPE-PLD	*N*-acyl phosphatidylethanolamine- specific phospholipase D
Nar-lysoPE	*N*-arachidonoyl-lysoPE
N-ArPE	*N*-arachidonyl phosphatidylethanolamine
NAT	*N*-acyltransferase
NF	neurofilament
NGF	nerve growth factor
NIH	National Institutes of Health
NMDA	N-methyl-D-aspartate
nNOS	neuronal NOS

NO	nitric oxide
NOS	nitric oxide synthase
NTC	no template control
ODA	*cis*-9,10-octadecenoamide
P	postnatal day
Pa	Pascal
PA	phosphatidic acid
PBS	phosphate buffered saline
PBS-T	phosphate buffered saline with Triton
PC	Purkinje cells
PCL	Purkinje cell layer
PEA	palmitoiletanolamide
PF	parallel fibres
PG	prostaglandin
PI	phosphatidylinositol
PI3K	phosphoinositide 3'-kinase
PKC	protein kinase C
PLA	phospholipase A
PLC	phospholipase C
PLD	phospholipase D
PMSF	phenylmethylsulfonyl fluoride
PNS	peripheral nervous system
PSA-NCAM	polysialic acid–neural cell adhesion molecule
PTPN22	protein tyrosine phosphatase, non-receptor type 22
PTX	pertussis toxin
PVDF	polyvinylidene difluoride
qPCR	quantitative PCR
RDB	RNA binding domain
RMS	rostral migratory stream
ROX	6-carboxy-X-rhodamine
RT-PCR	Reverse Transcription-Polymerase Chain Reaction
SD	standard deviation
SDS-PAGE	Sodium Dodecyl Sulphate-PolyAcrylamide Gel Electrophoresis
S.E.M	standard error medium
SGZ	subgranular zone
Shh	sonic hedgehog
sp	synapse
sPLA2	soluble phospholipase A2
SVZ	subventricular zone
TAE	Tris-acetate-EDTA
TBS-T	Tris buffered saline with Tween-20
Δ^9-THC	Δ^9-tetrahydrocannabinol
TNFα	tumor necrosis factor α
Trk	tropomyosin-related kinase
TRPV1	transient receptor potential vanilloid subtype 1
Tuj1	beta III-tubulin
UV	ultraviolet
VSCCs	voltage-sensitive calcium channels

CHAPTER 1

INTRODUCTION

1.1 The endocannabinoid signaling system.

The last twenty years have seen a rapidly growing body of studies confirming the existence of an endogenous cannabinoid system consisting of cannabinoid receptors (CBRs), their endogenous ligands (endocannabinoids, eCBs), and the enzymes responsible for eCB biosynthesis, degradation, and transport. Prior to the eighties, the term "cannabinoids" referred to a group of diterpenic C_{21} compounds contained in *Cannabis sativa*, their carboxylic acids, analogs, and transformation products. Among the 60 phytocannabinoids present in *C. sativa*, only a few are bioactive, and interact with specific plasma membrane receptors. Δ^9-tetrahydrocannabinol (Δ^9-THC, dronabinol), which is responsible for the majority of the psychoactive and addictive effects of *C. sativa,* was isolated, stereochemically characterized, and synthesized in 1964 (Mechoulam,R. *et al*., 1965). At first, the high lipophilic nature of Δ^9-THC suggested that it acts by altering cell membrane fluidity, stimulating or inhibiting associated enzymes, and influencing the physical state of ion channels.

In 1984, Howlett and Fleming first demonstrated the existence of cannabinoid receptors by incubating a neuroblastoma cell line with Δ^9-THC and measuring a reduced cyclic adenosine monophosphate (cAMP) level as a consequence of adenylate cyclase (AC) inhibition (Howlett,A.C. and Fleming,R.M., 1984). This effect was blocked by pertussis toxin (PTX), suggesting the involvement of a $G_{i/o}$ protein in the cannabinoid action. The existence of cannabinoid receptors was strenghtened by the discovery of Δ^9-THC (-)-enantiomer stereoselectivity and concentration-dependent agonist binding specificity (CP 55,940, *Pfizer* Inc., Groton, CT) in rat brain membranes. In 1990 the first cannabinoid receptor was cloned from rat cerebral cortex. This receptor, negatively coupled to AC and belonging to the G protein coupled receptor (GPCR) superfamily, was subsequently cloned from human and mouse brain. A second cannabinoid receptor was later discovered on the basis of sequence structure homology. It was cloned from human leukemic promyelocytic cells (HL-60) and resembles the other CBRs in its seven transmembrane domain structure and PTX-sensitive G protein coupling. The transmembrane amino acid sequence of the human receptors shares

68% homology, reduced to 44% when considering the whole protein structure: human/rat and rat/mouse pairs show a homology of 81%. The first CBR was identifed as being CNS (central nervous system) specific, while the second as the peripheral one. CB1R was later cloned, its molecular structure characterized, and cerebral distribution analysed, allowing one to infer the existence of cannabinoid receptors and their role in mediating most of Δ^9-THC actions in central and peripheral tissues.

Until the 1990s, the term cannabinoid defined any molecule able to bind one of the CBRs, named CB1 and CB2 according to NC-IUPHAR (International Union of Pharmacology Committee on Receptor Nomenclature and Drug Classification) nomenclature. The endogenous cannabinoid receptor identification suggested that the brain itself produced chemical compounds, the eCBs, able to interact with the CB1 receptor during normal brain functions. The eCBs represent a new family of signaling lipid mediators that includes amides, esters, and ethers of long-chain polyunsaturated fatty acids, particularly arachidonic acid. Because of structure similarities (a polar group (ethanolamine or glycerol) and a polyunsaturated chain) they resemble the eicosanoids, inflammation mediators involved in neural communication.

In 1992 the first endogenous CBR ligand was isolated from chloroform/methanol extracts of porcine brain. It was characterized as the arachidonic acid ethanolamide (C20:4) (*N*-arachidonoylethanolamine, AEA), called anandamide (taken from the Sanskrit word ananda, which means "bliss, delight", and amide) (Fig. 1). AEA is distributed in many peripheral regions: adult rat neural tissues involved in peripheral nociceptive transmission (dorsal root ganglia, sciatic nerve, and spinal cord) (Lever,I.J. *et al*., 2009), human adipose tissue (Spoto,B. *et al*., 2006), human heart and spleen, rat skin and spleen (Felder,C.C. *et al*., 1996), rat liver, kidney, thyme, and testis (Koga,D. *et al*., 1997), mouse uterus (Schmid,P.C. *et al*., 1997), many limphocyte cell lines, blood platelets (Kunos,G. *et al*., 2000), human mammary cancer cells, rat pheochromocytoma (Bisogno,T. *et al*., 1998), and human cerebral tumors (Maccarrone,M. *et al*., 2001). The greatest quantity of AEA is found in human and rat cerebral areas with the highest CBR density, for example hippocampus, cerebellum, striatum, and cortex. Radiolabeling studies demonstrate that AEA behaves as a partial agonist at CB1 and CB2 receptors (K_i = 89 ± 10 nM and 371 ± 102 nM, respectively) (Showalter,V.M. *et al*., 1996). It resembles Δ^9-THC structure and has the key features that define an endogenous cannabinoid compound: parenteral (intravenous, intrathecal, and intraperitoneal) injection of

AEA in mouse produces a typical tetrad of effects consisting of analgesia, hypothermia, hypomotility, and catalepsy (Smith,P.B. *et al*., 1994). Another AEA action, ascribed to cannabinomimetic compounds, is the reduction of mouse *vas deferens* electrically-evoked contractile activity *in vitro* (Devane,W.A. *et al*., 1992). Moreover, AEA can activate the transient receptor potential vanilloid subtype 1 (TRPV1), behaving as a full agonist provided with a low binding affinity.

At about the same time, different authors independently discovered the second endogenous cannabinoid ligand, *sn*-2-arachidonoylglycerol (2-AG), an arachidonic acid ester that binds both CB1 and CB2 receptors with similar affinity, thus behaving as a full agonist. Its brain distribution is analogous to AEA, but with 170-fold higher affinity (Bisogno,T. *et al*., 1999), even if only a part mediates the cannabinoid signaling because of its involvement in lipid metabolism (Fig. 1). 2-AG is present also in the rat peripheral nervous system: sciatic nerve, lumbar spinal cord, lumbar dorsal root ganglia (Huang,S.M. *et al*., 1999), and retina (Straiker,A. *et al*., 1999). Moreover, 2-AG is found in rat peripheral tissues, for example liver, spleen, lung, kidney (Kondo,S. *et al*., 1998), heart, testis (Schmid,P.C. *et al*., 2000), human milk (Di Marzo,V. *et al*., 1998), and human and rat cerebral tumors (Maccarrone,M. *et al*., 2001). 2-AG possesses anti-inflammatory (Facchinetti,F. *et al*., 2003) (Gallily,R. *et al*., 2000), analgesic (Hohmann,A.G. *et al*., 2005; Mechoulam,R. *et al*., 1995), and immobility effects. Like Δ^9-THC, 2-AG reduces rectal temperature and inhibits mouse *vas deferens* electrically-evoked contractile activity (Mechoulam,R. *et al*., 1995). As the third eCB, 2-arachidonyl glyceryl ether (2-AGE, noladin ether) was identified in porcine brain. It binds CB1R (K_i = 21.2 ± 0.5 nM) with greater affinity than CB2R (K_i > 3 μM) and displays AEA's tetrad effects following intraperitoneal injection.

Virodhamine (*O*-arachidonoyl ethanolamine), an eCB and a non-classic eicosanoid, derives from esterification between arachidonic acid and ethanolamine. (Fig. 1) Virodhamine was isolated from rat hippocampus, cortex, cerebellum, brainstem, and striatum. Its concentration is higher than AEA’s in rat peripheral tissues expressing CB2R (skin, spleen, kidney, and heart). Virodhamine behaves as a full agonist at CB2R and as a partial agonist/antagonist at CB1R, and inhibits AEA transport because both compounds compete for the same re-uptake mechanism. Following intravenous administration, virodhamine reduces rat body temperature, but neutralizes the effect mediated by AEA, thus behaving as an endogenous CBR1 antagonist in the presence of AEA. *N*-arachidonoyl-dopamine (NADA), is

a selective agonist at CB1R (K_i = 250 nM and 12 μM at CB1R and CB2R, respectively), and is more potent and effective than AEA *in vitro* (Fig. 1). In rat brain NADA is found mainly in striatum, hippocampus, and cerebellum. In murine neuroblastoma-glioma N18TG2 cell membranes, NADA behaves as a competitive inhibitor of the intracellular membrane-bound fatty acid amide serine hydrolase (FAAH), which inactivates AEA. NADA inhibits AEA facilitated transport in rat basophilic leukemia RBL-2H3 cells and in glioma C6 cells. It exhibits the typical cannabinoid tetrad effects in mouse, and activates TRPV1, and induces hyperalgesia when peripherally administered.

In 1995 oleamide (*cis*-9,10-octadecenoamide, ODA) was isolated from the cerebrospinal fluid (CSF) of sleep-deprived cats (Fig. 1). ODA is a sleep induction factor able to induce physiological sleep in rats when intraperitoneally injected (Cravatt,B.F. *et al*., 1995). Oleamide can strengthen serotonin (5-Hydroxytryptamine, 5-HT) action at 5-HT_{2A} and 5-HT_{2C} receptors. It modulates rat γ-aminobutyric acid (GABA)-induced $GABA_A$ chloride currents *in vitro*, inactivates glial cell serrated junction-mediated communication without affecting intercellular calcium current transmission, induces rat hypomotility (Basile,A.S. *et al*., 1999), hypothermia (Huitron-Resendiz,S. *et al*., 2001), memory modulation (Murillo-Rodriguez,E. *et al*., 2001), and antinociception (Fedorova,I. *et al*., 2001). Oleamide's mechanism of action is likely to be indirect, as it strengthens AEA activity *in vivo* when coadministered. Like other analogous molecules, oleamide displays an "entourage effect", whereby the biological activity of an endogenous compound can be enhanced by related endogenous compounds that themselves alone lack such activity. Such an effect can be due to the ability of the entourage compounds to prevent breakdown of the biologically active compound, or to improve affinity for the biological target. Oleamide increases the AEA concentration competing for the FAAH active site (Mechoulam,R. *et al*., 1997). Leggett *et al.* demonstrated that despite the allosteric regulation of other receptors and the "entourage effect", ODA has micromolar binding affinity at the human and rat CB1 receptors and an agonist activity similar to AEA (Leggett,J.D. *et al*., 2004).

Palmitoylethanolamide (PEA) is classified as a fatty acid-derived endogenous "eCB-like" compound because of its cannabinomimetic effects, despite the lack of direct affinity at CBRs *in vitro* (Fig. 1). PEA is known for its anti-inflammatory properties (Lambert,D.M. *et al*., 2002) it exhibits analgesia in acute and inflammatory pain (Calignano,A. *et al*., 1998; Conti,S. *et al*., 2002), and in a mouse model of chronic neuropathic pain. PEA strengthens AEA

analgesic action through an "entourage effect" at CB1 and TRPV1 receptors, and reduces mast cell mediator production (nerve growth factor, NGF, and tumor necrosis factor α, TNFα) (Costa,B. *et al*., 2008). The brain's concentration of PEA is higher than that of AEA; one study referred to PEA as a CB2R endogenous ligand (Malan,T.P.,Jr *et al*., 2002; Maccarrone,M. *et al*., 2000).

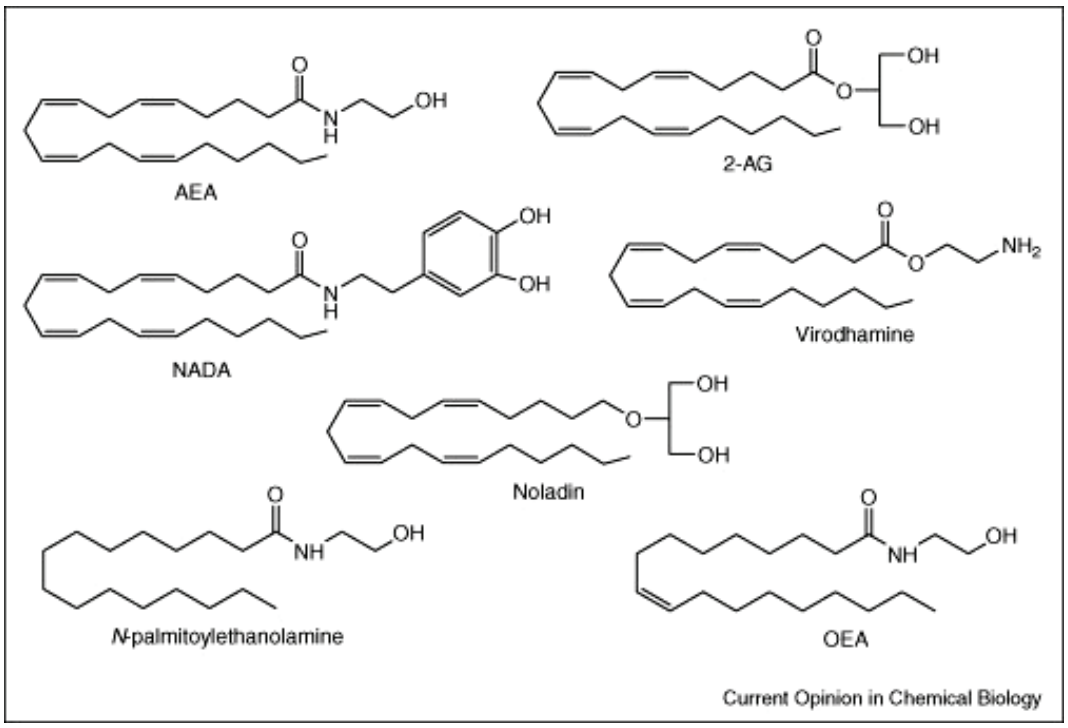

Figure 1. Chemical structures of established and proposed endocannabinoids and of some pharmacologically active *N*-acylethanolamines. (Petrosino,S. *et al*., 2009)

1.1.1 Regulation of cannabinoid GPCR signaling: the role of plasma membrane microdomains.

Growing evidence points to the influence of plasma membrane lipid composition on the conformational activity of GPCR, particularly "lipid rafts", on eCB signaling. eCBs are local neuromodulators produced "on demand" by receptor-stimulated cleavage of membrane lipid precursors and released from neurons immediately afterwards in to the synaptic cleft, without being stored in secretory vesicles. In turn, depolarizing stimuli induce postsynaptic terminal release of eCBs that behave as retrograde synaptic signaling messengers via activation of CB1Rs at the presynaptic terminal, with consequent inhibition of other neurotransmitter release. eCB signaling extinction occurs via carrier-mediated transport or simple diffusion in

the postsynaptic membrane, followed by internalization through caveola/lipid raft-mediated endocytosis and enzymatic degradation.

Lipid rafts are membrane specializations composed of tightly packaged sphingolipid and cholesterol microdomains enriched in arachidonic acid, and associated with specific proteins (Fig. 2). The localization and trafficking/internalization of receptor components by rafts can modify GPCR signaling. These microdomains spatially organize signaling molecules at the membrane (ionotropic and GPCRs, G proteins, and signaling effectors, such as second-messenger-generating enzymes), perhaps in complexes, to promote kinetically favorable interactions necessary for signal transduction, or to inhibit interactions by separating signaling molecules and dampening signaling responses. In these structures neurotransmitter signaling might occur through a clustering of receptors and components of receptor-activated signaling cascades. Moreover, the enrichment in lipid rafts of arachidonic acid-containing phospholipids implies that these compartimentalized domains may represent a localized pool of substrate for the generation of arachidonic acid in response to cell activation.

GPCR and G proteins are localized in these compartmentalized domains, and fatty acylation or caveolin interaction has been suggested as a Gα subunit transport mechanism for these microdomains. Moreover, the hydrophobic residues of the transmembrane-spanning region of proteins can favor targeting of the slightly thicker lipid raft membrane. G proteins are targeted to lipid rafts following a reversible post-translational modification consisting of cysteine-specific residue palmitoylation, with the palmitoylated state affecting receptor activity. CB1Rs possess a cysteine residue in the C-terminal domain that is 90% palmitoylated, and different protein portions interact with different $G\alpha_o$ and $G\alpha_i$ subunits. Palmitoylation affords selectivity among $G_{i/o}$ protein family members and affects CB1R localization in specific lipid bilayer domains.

Caveolin, localized to the inner leaflet of the membrane bilayer, is the coat protein of caveolae, non-clathrin-coated and flask-shaped lipid rafts consisting of plasma membrane invaginations (60-80 nm diameter) (Fig. 2), involved in modulating signal transduction, endocytosis, transcytosis, and cholesterol trafficking. Caveolins are widely expressed in the nervous system in microvessels, endothelial cells, astrocytes, oligodendrocytes, Schwann cells, dorsal root ganglia, and hippocampal neurons (Trushina,E. *et al*., 2006).

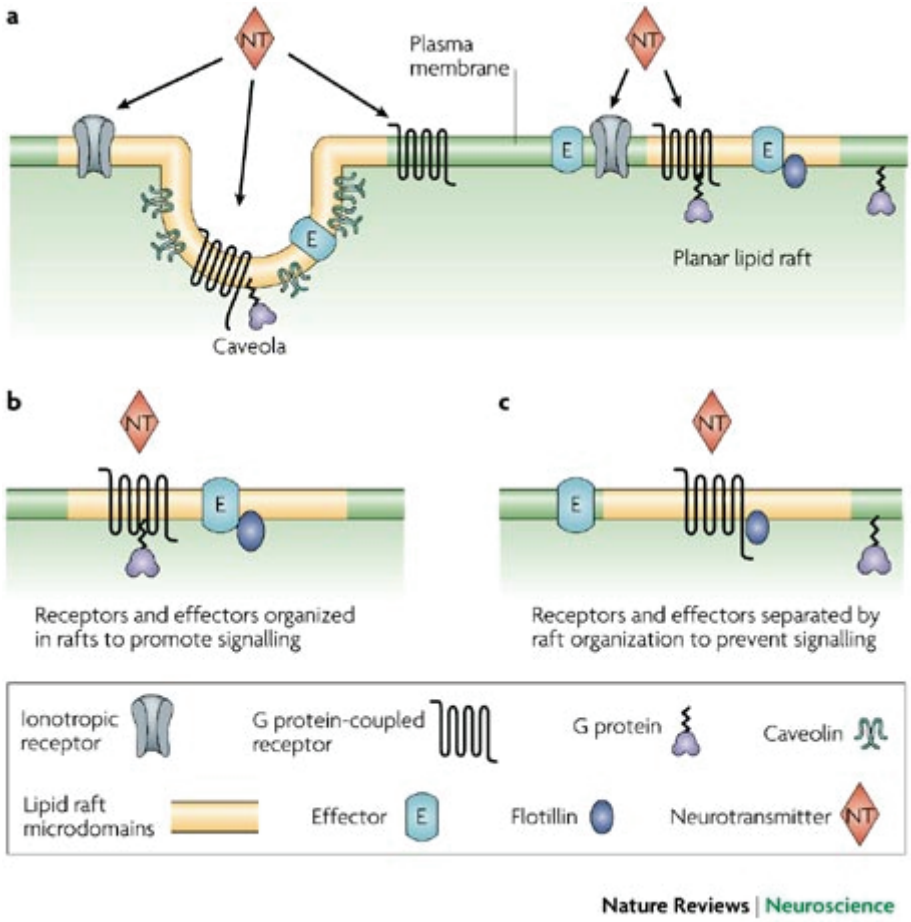

Figure 2. Plasma membrane microdomains. Lipid rafts are cholesterol- and sphingolipid-enriched, highly dynamic, submicroscopic (25–100 nm diameter) assemblies, which float in the liquid-disordered lipid bilayer in cell membranes. **a |** There are two common raft domains in mammalian cells: planar lipid rafts and caveolae. Both possess a similar lipid composition. Planar rafts are essentially continuous with the plane of the plasma membrane and lack distinguishing morphological features. By contrast, caveolae are small, flask-shaped membrane invaginations of the plasma membrane that contain caveolins. Caveolin molecules can oligomerize and are thought to be essential in forming these invaginated membrane structures. Caveolins and flotillin can recruit signaling molecules into lipid rafts. Many neurotransmitter receptors (both ionotropic and G-protein-coupled), G proteins, and signaling effectors such as second-messenger-generating enzymes are found in lipid rafts. Neurotransmitters might activate receptors that are located both within and outside lipid rafts. **b |** The lipid raft signaling hypothesis proposes that these microdomains spatially organize signaling molecules at the membrane, perhaps in complexes, to promote kinetically favorable interactions that are necessary for signal transduction. **c |** Alternatively, lipid raft microdomains might inhibit interactions by separating signaling molecules, thereby dampening signaling responses (Allen,J.A. *et al*., 2007).

Caveolin exists in 3 different isoforms, but expression of caveolin-1 (or -3, the striated muscle-specific isoform) is necessary for caveola biosynthesis. Caveolin-2 is found in hetero-oligomers with caveolin-1 and -3, but its function is still unclear. Caveolin-1 can transit the membrane lipid bilayer and cycle between the protoplasmic portion of the plasma membrane (extending both C- and N-termini in the cytosol, while the lipophilic moiety spans the lipid bilayer) and the ectoplasmic membrane of intracellular compartments (endoplasmic reticulum cisternae, *trans*-Golgi vesicles, *cis*-Golgi cisternae, inner, and outer nuclear membrane). It behaves as a scaffolding protein, with a docking site near the N-terminus that binds and inhibits signaling molecules. Caveolins not only spatially organize signaling proteins, but modulate signaling transduction itself through different mechanisms, inhibits AC and NOS (nitric oxide synthase), serine/threonine kinases, and phosphatases.

Conformational studies show that AEA assumes an extended conformation in the bilayer, aligning parallel to lipids with its ethanolamide group in the lipid-water interface and its acyl chain in the hydrophobic region of the bilayer. Arachidonyl chain flexibility is critical for reaching the binding site located in the bilayer center among the seven transmembrane helices. The great torsional mobility of this chain is due to the presence of four *cis* vinyl double bonds separated by one methylene group that permit AEA to easily adopt and change shape, facilitating its target interactions. Quantitative structure-activity studies report that 2-AG is embedded in the lipid bilayer much like AEA, because of their similar lipophilicity and polarizability properties. Rimmermann *et al.* demonstrated that 2-AG is concentrated in the caveolae of dorsal root ganglia cells, where it co-localizes with components of the diacylglycerol pathway responsible for 2-AG production, and where CB1Rs reside (Rimmerman,N. *et al*., 2008). In contrast, comparable levels of AEA have been found in lipid raft and non-lipid raft fractions, where CB2Rs are localized. The different interactions of these endogenous ligands with lipid rafts demonstrate their proximity to CB1Rs, where they can easily reach the binding site by lateral diffusion. This questions the general concept of 2-AG as the only true agonist at CB2Rs. Moreover, synaptic transmission is regulated by receptor trafficking. Many GPCRs are not totally inactive in the absence of ligands but exhibit tonic activity, with elevated basal levels of intracellular signaling. Constitutively active GPCRs are endocytosed from the plasma membrane, and under steady-state conditions are mainly localized intracellularly (endosomal).

CB1Rs display constitutive activity when heterologously expressed in neuronal and non-neuronal cells *in vitro* (Pertwee,R.G. 2005), which results in constitutive endocytosis and recycling (Leterrier,C. *et al*., 2004). In primary cultures of rat embryonic hippocampal neurons, constitutive activity-driven endocytosis occurs mostly from the somatatodendritic surface and represents the driving force for CB1R targeting to the axonal plasma membrane (Leterrier,C. *et al*., 2006). Prolonged agonist treatment induces G protein uncoupling and both clathrin- and raft/caveolae-mediated endocytosis of CB1Rs (Keren,O. and Sarne,Y. 2003). Wu *et al*. suggested a role for receptor endocytosis in counteracting CB1R desensitization by facilitating receptor recycling and reactivation in stably transfected human embryonic kidney (HEK) 293 cells. Moreover, in primary cultures of rat embryonic cortical neurons these authors demonstrated that 2-AG, as well as synthetic cannabinoid agonists with high endocytotic efficiency, can reduce the development of cannabinoid tolerance to some effects (Wu,D.F. *et al*., 2008).

Surface diffusion of presynaptic CB1Rs in cortical neurons *in vitro* (Mikasova,L. *et al*., 2008) represents an efficient means of modulating retrograde signaling, and can be considered as a mechanism of desensitization. Under resting conditions, axon terminal surface CB1Rs display a high level of lateral mobility, moving by diffusion within synaptic and extrasynaptic compartments. Prolonged exposure to non-selective cannabinoid receptor agonists significantly increases the percentage of immobile extrasynaptic CB1Rs in a CB1R-dependent manner, excluding them from synapses and reducing the number of surface receptors.

1.1.2 Biosynthetic pathways of eCBs.

The enzymes responsible for AEA biosynthesis and degradation have been characterized in many tissues. *In vivo*, the AEA precursor *N*-arachidonyl phosphatidylethanolamine (*N*-ArPE) originates from arachidonic acid transfer from the *sn*-1 position of 1,2-*sn*-di-arachidonylphosphatidylcholine to phosphatidylethanolamine, catalyzed by a calcium-dependent *N*-acyltransferase (NAT). *N*-ArPE is then cleaved by a *N*-acyl phosphatidylethanolamine (NAPE)-specific phospholipase D (PLD), which releases AEA and phosphatidic acid. NAPE-PLD is a member of the *zinc* metallo-*hydrolase* family of the beta-*lactamase* (Fig. 3). AEA production and *N*-ArPE biosynthesis are thought to proceed in parallel, because intracellular Ca^{2+} increase and/or activation of other GPCRs can stimulate both reactions (Cadas,H. *et al*., 1997; Cadas,H. *et al*., 1996). Application of dopamine D_2-

receptor agonists increases newly synthesized AEA outflow in the rat striatum. However, in hippocampus there is evidence for the involvement of muscarinic acetylcholine receptors and metabotropic glutamate receptors in Ca^{2+}-independent eCB release. AEA biosynthesis is unaffected in NAPE-PLD knockout mice (Leung,D. *et al*., 2006), suggesting the involvement of enzymes other than NAPE-PLD. A proposed alternative biosynthetic pathway occurs through a double-deacylation of NAPE to generate lyso-NAPE and then glycerophospho-*N*-acylethanolamine, which is rapidly cleaved to the corresponding *N*-acylethanolamine. This novel route is driven by the sequential action of a fluorophosphonate-sensitive serine hydrolase and a metal-dependent phosphodiesterase (Simon, G.M. and Cravatt,B.F. 2006) (Fig. 3). Another mechanism involves the conversion of NAPE into 2-lyso-NAPEs via the action of secretory phospholipase A2 (PLA2). PLA2 hydrolyses NAPE to release fatty acids and *N*-arachidonoyl-lysoPE (NAr-lysoPE), and subsequently a lyso phospholipase D (lyso-PLD) may release AEA from NAr-lysoPE (Fig. 3). Recently, it has been shown that in RAW264-7 macrophages, lipopolysaccharide (LPS)-induced AEA production appears to depend mainly on a pathway whereby NAPE is hydrolysed to yield a phospho-AEA, which is then dephosphorylated (Liu,J. *et al*., 2006).

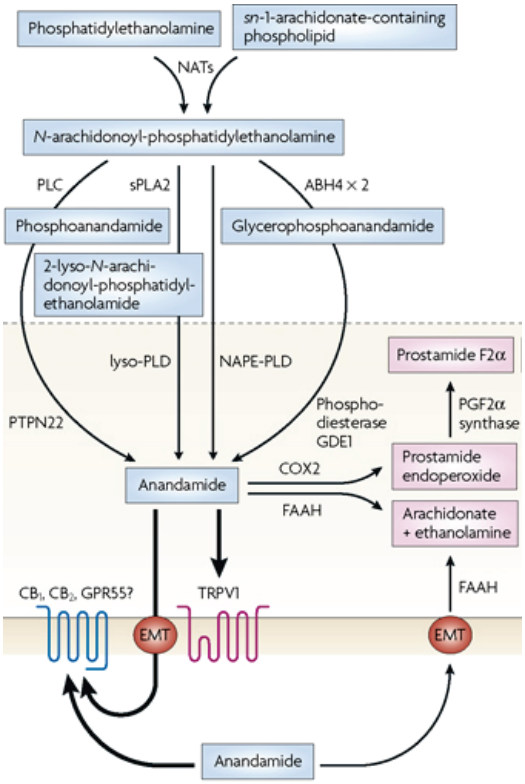

Figure 3. Biosynthesis, action, and inactivation of anandamide. The biosynthetic pathway for anandamide is shown in blue, degradative pathways are shown in pink. Thick arrows denote movement or action. ABH4, αβ-hydrolase 4; CB1/2, cannabinoid receptor 1/2; COX2, cyclooxygenase-2; EMT, "endocannabinoid membrane transporter"; FAAH, fatty acid amide hydrolase; GDE1, glycerophosphodiester phosphodiesterase 1; GPR55, G protein-coupled receptor 55; NAPE-PLD, *N*-acyl-phosphatidylethanolamine-selective phosphodiesterase; NATs, *N*-acyltransferases; sPLA2, (soluble) phospholipase A2; PLC, phospholipase C; PLD, phospholipase D; PTPN22, protein tyrosine phosphatase, non-receptor type 22; TRPV1, transient receptor potential vanilloid subtype 1 receptor (Di Marzo,V. 2008) .

2-AG biosynthesis occurs by two possible pathways in neurons: phospholipase C (PLC)-mediated hydrolysis of membrane phospholipids to produce 1-acyl-2-arachidonoylglycerol (DAG) (Di Marzo,V. 2008) which is then converted to 2-AG by *sn*-1-DAG lipase (DAGL) (Bisogno,T. *et al*., 2003); PLA1-mediated hydrolysis of phosphatidylinositol (PI) into lysoPI, followed by hydrolysis by PLC to produce 2-AG (Sugiura,T. *et al*., 2002) (Fig. 4). Two *sn*-1-specific diacylglycerol lipase (DAGL-α and -β) exist, both associated with the cell membrane and stimulated by high concentrations of Ca^{2+} (Bisogno,T. *et al*., 2003). DAGL-α appears to be primarily localized in a subdivision of the postsynaptic dendritic spine, called the perisynapse, which forms a thin border around the postsynaptic density (Yoshida,T. *et al*.,

2006). This same area also contains metabotropic glutamate receptor 1 (mGluR1) and PLCβ. In cultures of rat cortical neurons, the Ca^{2+} ionophore ionomycin and the glutamateric receptor agonist NMDA (N-methyl-D-aspartate) stimulate 2-AG synthesis in a Ca^{2+}-dependent manner. Similarly to AEA, NMDA receptor activation induces Ca^{2+} entry and consequent 2-AG production, which is synergistically increased by the cholinergic agonist charbacol. In hippocampal slices, high-frequency stimulation of the Schaffer collaterals induces a Ca^{2+}-dependent increase in 2-AG, that is prevented by Ca^{2+} medium removal, and is independent from a generalized increase in the rate of lipid turnover.

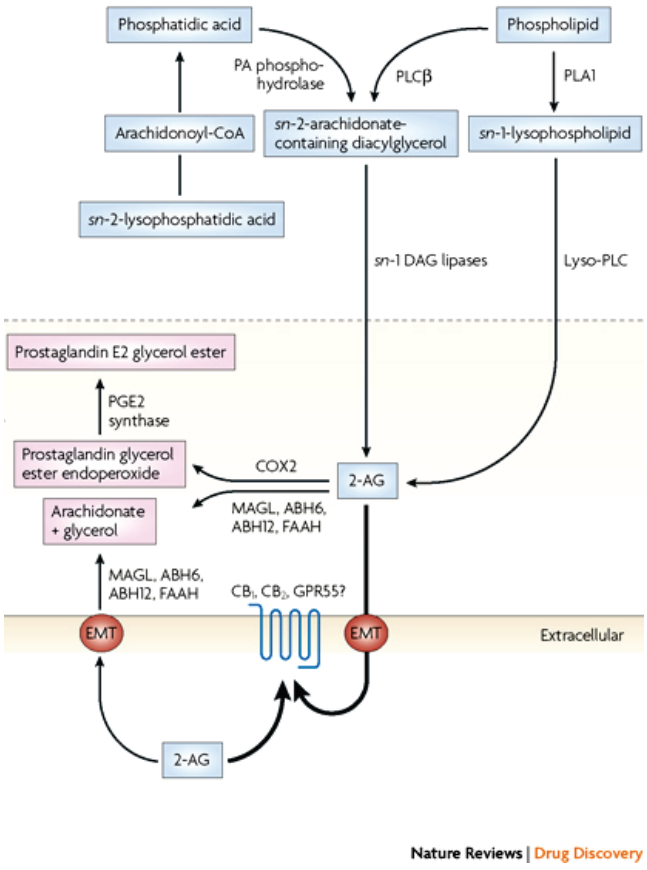

Figure 4. Biosynthesis, action, and inactivation of 2-arachidonoylglycerol (2-AG). The biosynthetic pathway for 2-AG is shown in blue, degradative pathways are shown in pink. Thick arrows denote movement or action. ABH6/12, αβ-hydrolase 6/12; CB1/2, cannabinoid receptor 1/2; COX-2, cyclooxygenase-2; DAG, diacylglycerol; EMT, "endocannabinoid membrane transporter"; FAAH, fatty acid amide hydrolase; GPR55, G protein-coupled receptor 55; MAGL, monoacylglycerol lipase; PA, phosphatidic acid; PGE2, prostaglandin E, PLA1, phospholipase A1; PLC, phospholipase C; PLCβ, phospholipase Cβ (Di Marzo,V. 2008).

1.1.3 Degradation of eCBs.

The rapid inactivation of eCB signal in the brain involves two mechanisms: carrier-mediated transport into cells and intracellular hydrolysis. AEA uptake in neuronal and glial terminals is mediated by facilitated diffusion utilizing a presynaptic energy-independent, saturable, and temperature-dependent protein carrier, which is substrate-specific (Piomelli,D. *et al*., 1999). Although AEA is rapidly hydrolyzed, its uptake into CNS cells is largely independent of an enzymatic mechanism. Different cells that do not express FAAH are still able to rapidly take up AEA (Day,T.A. *et al*., 2001). Compounds inhibiting AEA cellular uptake without affecting FAAH activity have been synthesized (Ortar,G. *et al*.,2003); however, the existence of a specific transporter can only be inferred from indirect evidence. Moreover, its substrate selectivity is still debated. Some authors suggest this transporter to be responsible for uptake of other eCBs (Bisogno,T. *et al*., 2001; Fezza,F. *et al*., 2002), with 2-AG being a competitor (Beltramo,M. and Piomelli,D. 2000; Bisogno,T. *et al*., 2001). Caveolae/lipid raft-associated endocytosis has been proposed as a new model for AEA transport (McFarland,M.J. *et al*., 2004). The involvement of lipid rafts in AEA uptake in neuronal cells (Bari,M. *et al*., 2005) has been documented. 2-AG is inactivated by reuptake via a membrane transport molecule, probably the "AEA membrane transporter" (AMT) (Bisogno,T. *et al*., 2001; Beltramo,M. and Piomelli,D. 2000), and subsequent intracellular enzymatic degradation by MAGL (Fig. 4).

Once inside the cells eCBs are hydrolysed by FAAH that breaks down AEA into arachidonic acid and ethanolamine esters like 2-AG and primary amides like ODA (Fig. 3). FAAH can also hydrolyze bioactive fatty amides that don’t bind the CBRs. These compounds coexist with AEA or 2-AG, and their levels can increase by competing for the same degradation enzyme. FAAH is a member of the amidase family, with its characteristic conserved region rich in serine, glycine, and alanine. This enzyme has a dimeric structure, and channels to allow a direct access to the active site from the lipid bilayer. FAAH is widely distributed in rat CNS neuronal cell bodies and dendrites. In neocortex, hippocampus, and cerebellum, FAAH-positive cell bodies are juxtaposed to axon terminals containing CB1R. This evidence suggests a postsynaptic role of the enzyme in degrading neuronally-generated AEA. In many other brain regions this correlation, however, does not hold, due to the involvement of FAAH in other amide catabolic reactions. 2-AG may be degraded by FAAH (Fig. 4), and some authors report increased 2-AG levels induced by FAAH inhibitors

(Ligresti,A. *et al*., 2003); however, this is not the main 2-AG-metabolizing enzyme in CNS. In fact, FAAH inhibitors do not affect 2-AG hydrolysis when used at concentrations which completely block AEA degradation (Beltramo,M. and Piomelli, D. 2000). Indeed, FAAH knockout mice are still able to hydrolyze 2-AG (Lichtman,A.H. *et al*., 2002).

MAGL is responsible for 2-AG metabolism in the brain (Fig. 4). It is a cytosolic serine hydrolase that transforms 2- and 1-monoglycerides into a fatty acid and glycerol (Karlsson,M. *et al*., 1997; Dinh,T.P. *et al*., 2002). Cerebral distribution of MAGL partly overlaps, but is more limited than that of FAAH, and is found mainly in brain areas containing the highest quantity of CB1Rs (hippocampus, cortex, and cerebellum). Whereas FAAH is predominantly located in postsynaptic structures, MAGL is mostly presynaptic in localization (Gulyas,A.I. *et al*., 2004), suggesting a role in terminating retrograde signaling mediated by 2-AG (Straiker,A. and Mackie,K. 2005). However, AEA (and other eCBs) are also susceptible to oxidative metabolism catalyzed by lipoxygenase (LIPOX), cyclooxygenase-2 (COX-2), and cytocrome P450 oxidase (Kozak,K.R. *et al*., 2002). COX-2 transforms 2-AG to prostaglandin glycerol esters, as it converts arachidonic acid to classical prostaglandins (PGs) (Fig. 4). In contrast, COX-2 metabolism of AEA produces prostaglandin endoperoxide ethanolamides, intermediates transformed to prostamides (prostaglandin-ethanolamides) (Ross,R.A. *et al*., 2002) (Fig. 3). Prostamides affect neither FAAH nor AMT, and do not bind CBRs (Fowler,C.J. 2007). Their molecular target is still unknown. 5- and 2-LIPOX convert AEA in 12-hydroxy-*N*-arachidoylethanolamine (12-HAEA) and 15-hydroxy-*N*-arachidoylethanolamine (15-HAEA), respectively, but only 12-HAEA displays affinity for CBRs (Kozak,K.R. *et al*., 2002). 2-AG is transformed into 15-hydroperoxyeicosatetraenoic glyceryl ester (Moody,J.S. *et al*., 2001). Cytochrome P450 metabolism of AEA yields more than 20 polar lipids (Burstein,S.H. *et al*., 2000).

1.1.4 Signaling via cannabinoid receptors in CNS.

1.1.4.1 The cannabinoid CB1 and CB2 receptors.

CBRs are cell surface GPCRs consisting of seven polypeptide transmembrane α helices, connected by 3 intracellular and 3 extracellular loops. The consensus sites for *N*-glycosylation are concentrated at the N-terminus of the CB1Rs; Song *et al*. reported an heterogeneous carbohydrate composition for this N-linked glycoprotein in rat brain (Song,C. and Howlett,A.C. 1995). CB1Rs predominantly couple to inhibitory G proteins (G_i and G_o), but Howlett *et al*. (Howlett,A.C. *et al*., 2002) reported G_s or G_q coupling and consequent PLC activation (Howlett,A.C. 2004). CB1R stimulation inhibits AC, N/Q (Mackie,K. and Hille,B. 1992) and L (Gebremedhin,D. *et al*., 1999) calcium channels, leading to activation of A-type and inwardly rectifying potassium channels (Mu,J. *et al*., 1999), but the inhibition of D-type ones (Howlett,A.C. and Mukhopadhyay,S. 2000). Moreover, CB1R activation can directly stimulate nitric oxide production (Stefano,G.B. *et al*.,2000). Unlike CB2Rs, CB1Rs present 4 clusters of potential cAMP-dependent protein kinase and Ca^{2+}-calmodulin-dependent protein kinase sites, and a single PKC (protein kinase C) site, all conserved across human rat, and mouse proteins. CB1Rs contain a characteristic alkyl-binding domain implicated in the recognition of lipid ligands, which is located in a region of the protein embedded within the membrane. This suggests that the ligand first enters the lipid bilayer and then reaches the binding site by lateral diffusion. Some authors reported that accessing CB1Rs through the bilayer would shorten the distance that 2-AG needs to cover in the acqueous medium, increase 2-AG density surrounding the binding site, and enhance the subsequent hydrolysis of 2-AG by MAGL associated with the cytoplasmic presynaptic membrane.

CB1Rs are mainly expressed in the brain, spinal cord, and in some peripheral tissues: ileum, testis, urinary bladder, and *vas deferens* (Lambert,D.M. and Fowler,C.J. 2005). They are distributed on sensory and autosomic fibres of the PNS (peripheral nervous system) (spinal dorsal root ganglia interneurons, myenteric neurons, urinary bladder prejunctional fibres, and superior cervical sympathetic ganglia) (Farquhar-Smith,W.P. *et al*., 2000). CB1R distribution in rat and human brain is similar, with highest levels found in limbic cortices, in accord with CB1R involvement in motivational (limbic) and cognitive (associative) information processing. High binding levels are present also in the hippocampal dentate gyrus and in the molecular layer of the cerebellum, in the basal ganglia, substantia nigra, *pars reticulata*, and globus pallidus. CB1R is the major cannabinoid receptor responsible for

cannabinoid-dependent presynaptic modulation at not only inhibitory, but also excitatory synapses in the brain. CB1Rs are localized on GABAergic interneurons (Hajos,N. *et al*., 2001) and at hippocampal excitatory synapses on pyramidal neurons, and at climbing fibres and parallel fibre synapses on cerebellar Purkinje cells (Kawamura,Y. *et al*., 2006). In some cases these receptors are also present at low levels and frequency on neuronal cell dendrites and somata (Marsicano,G. *et al*., 2003). Until a decade ago, CB2Rs were thought to be predominantly present in immune tissues (spleen, thymus, and tonsils) and circulating immune cells (Klein,T.W. *et al*., 2003) like B cells, natural killer cells, macrophages, neutrophils, and T lymphocytes. We now know that functional CB2Rs are expressed in brain neurons like cerebellar granule cells (Skaper,S.D. *et al*., 1996), perivascular microglial cells, cultured cerebrovascular endothelium (Nunez,E. *et al*., 2004; Golech,S.A. *et al*., 2004), brainstem neurons (Van Sickle,M.D. *et al*., 2005), and by activated microglia in mouse models of multiple sclerosis and Alzheimer's disease (Benito,C. *et al*., 2003).

1.1.4.2 CB1 and CB2 receptor functions in CNS.

In the mammalian brain eCBs act as neuromodulators of functions such as motor activity, emesis, nociception, motivational responses, and appetite (Mackie,K. 2006). They regulate different forms of short-term synaptic plasticity that underlie memory and learning. Brain plasticity refers to the brain's ability to change its structure and function during maturation, learning, environmental challenges or pathology. Synaptic plasticity specifically refers to the activity-dependent modification of the strength or efficacy of synaptic transmission at pre-existing synapses through attenuation or enhancement of neuronal excitability, depending on the reduction of an excitatory or inhibitory neurotransmitter release.

The eCB system signaling represents a mechanism by which neurons can communicate backwards across synapses to modulate their inputs. Different mechanisms have been proposed to explain the eCB-mediated reduction of neurotransmitter release: inhibition of N- and P/Q-type voltage-dependent conductance and consequent reduced calcium influx *per* action potential; up-regulation of potassium currents and consequent shortening of the action potential duration and increased threshold for action potential generation; mechanisms involving the release machinery pathways unrelated to calcium entry. Voltage-dependent Ca^{2+} influx into postsynaptic hippocampal pyramidal neurons (Alger,B.E. 2002) or Purkinje cerebellar cells (Llano,I. *et al*., 1991) induces depolarization and eCB synthesis that

transiently suppresses transmitter release from presynaptic GABA interneurons, reducing the amplitude of afferent GABAergic inhibitory currents. This phenomenon, called depolarization-induced suppression of inhibition (DSI) can facilitate the induction of long-term potentiation (LTP) in hippocampal pyramidal neurons and contribute to hippocampus-dependent learning (Carlson,G. *et al*., 2002). Considerable evidence supports a prominent role for 2-AG in mediating this mechanism. Depolarization-induced suppression of excitation (DSE), a similar phenomenon, occurs at glutamatergic synapses (Kreitzer,A.C. and Regehr,W.G. 2001) and postsynaptic group I mGluRs have a similar CNS expression, and the activation of glutamate receptors releases eCBs both in cerebellum and hippocampus.

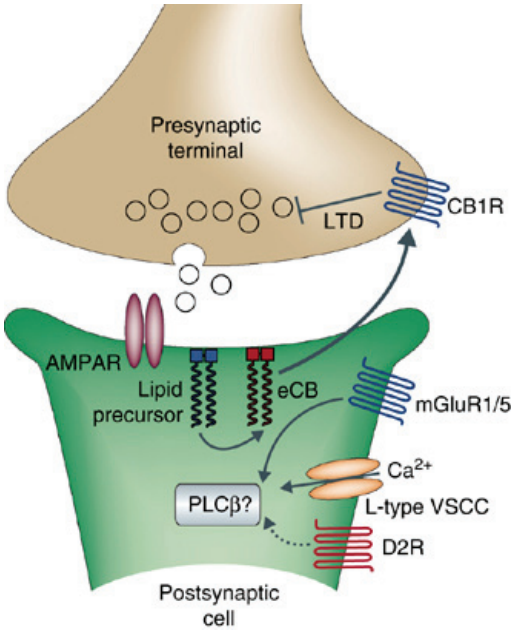

Figure 5. Model of eCB-LTD at excitatory synapses onto medium spiny neurons in the striatum. Activation of postsynaptic type I mGluRs, along with coincident subthreshold depolarization of medium spiny neurons sufficient to activate L-type voltage-sensitive calcium channels (VSCCs), stimulates the postsynaptic synthesis and release of endocannabinoids. What enzyme generates the endocannabinoids is not known; one candidate is PLCβ. Co-activation of postsynaptic dopamine D_2-type receptors (D_2R) enhances endocannabinoid production and the subsequent induction of presynaptic LTD, mediated through activation of presynaptic CB1 receptors (CB1R) (Citri,A. and Malenka,R.C. 2008).

Moreover, eCBs participate in the induction of long-term synaptic plasticity (Chevaleyre,V. *et al*., 2006). Repeated low-frequency stimulation of glutamatergic fibres induces a prolonged activation of group I mGluRs and eCB release. This results in a prolonged stimulation of CB1Rs and a long-term inhibition of neurotransmitter release that

persists longer after the stimulation (long-term depression, LTD) (Fig. 5). eCB-mediated LTD (eCB-LTD) was observed in the glutamatergic synapses which contact medium spiny neurons in the striatum. In the hippocampus, in contrast, eCBs mediate a form of LTD at inhibitory, but not excitatory, synapses. In the dorsal striatum, eCB-LTD requires postsynaptic activation of group I mGluRs, L-type calcium channels, and D_2 dopamine receptors. This leads to the production most likely of AEA. However, prolonged activation of CBRs alone is not sufficient to elicit eCB-LTD; concomitant presynaptic activity is also required. Another important feature of eCB-LTD in the dorsal striatum is that it appears to be restricted to the medium spiny neurons that primarily express D_2 dopamine receptors, and is not present at excitatory synapses on cells expressing D_1 receptors. LTD in the cerebellum was also reported to depend on retrograde eCB signaling, but the mechanistic basis for this observation is still unclear, since cerebellar LTD is expressed postsynaptically. LTP is produced when repeated glutamate release precedes postsynaptic depolarization. LTD and LTP of CA3-CA1 synaptic transmission are two *in vitro* models for learning and memory.

The eCB system appears to play a role in the neuroprotective response to a variety of insults such as traumatic brain injury, ischemia, excitotoxicity, and oxidative stress. In addition, some brain insults induce a selective increase in certain eCB species, e.g. traumatic brain injury enhances 2-AG levels. In ischemia, when oxygen and nutrient deprivation occurs, there is a large synaptic accumulation of glutamate that induces excitotoxicity by Ca^{2+} overload through NMDA receptors. Cannabinoids exert a neuroprotective action, inhibiting presynaptic glutamate release as a consequence of their inhibitory action on Ca^{2+} influx through voltage-sensitive channels. Piomelli suggested that eCB production may result from the cytotoxic environment found in brain injury, in which high intracellular calcium levels stimulate eCB release by both neurons and glia (Piomelli,D. *et al*., 2000). Skaper *et al*. reported a protective action of cannabinoids in a model of delayed postglutamate excitotoxic death in cerebellar granule neurons, which was independent of NMDA and kainate receptor antagonism, but was ascribed to CB2R activation (Skaper,S.D. *et al*., 1996). CB1R-knock-out mice are more sensitive to brain insults and neurodegenerative disorders than wild-type mice, and increased excitotoxic injury was reported in CB1R-deficient mice after brain stroke or kainic acid administration. CB1R-deficient mice have an enhanced loss of neurons in CA1 and CA3 hippocampal areas and decreased cognitive functions with aging (Bilkei-Gorzo,A. *et al*., 2005).

Other mechanisms involved in the eCB action include the inhibition of NO production and pro-inflammatory cytokine release. Cannabinoids inhibit the release of pro-inflammatory molecules (TNFα, interleukin 6, and NO) from glia and neurons and enhance the release of anti-inflammatory cytokines (Molina-Holgado,F. *et al*., 2003). This action involves also CB2R activation that decreases the *in vitro* production, and the *in vivo* release, of pro-inflammatory molecules (Benito,C. *et al*., 2008). Brain NO release is increased following stroke and the reduction of iNOS (inducible NOS) and nNOS (neuronal NOS) expression is neuroprotective. Cannabinoids reduce NO release from rat microglia activated by LPS and interferon-γ in a PTX- and SR141716A (CB1R antagonist)-sensitive manner (Fowler,C.J. 2003). LPS-treatment of cultured primary astrocytes induces expression of iNOS and AEA, and CBR agonists reduce this expression. Influx of calcium in response to K^+ depolarization activates NOS in cerebellar granule neurons, and this response is reduced by WIN 55,212-2 in a pertussis toxin- and SR141716A-sensitive manner. CB2R expression in rodent and human brain is up-regulated in chronic inflammation *in vivo*, as a direct consequence of microglia activation (Maresz,K. *et al*., 2005). Neuroinflammation occurs in myelin degenerative disorders and in neurodegenerative disorders, ischaemia, and traumatic brain injury.

Cannabinoids protect glial cells from apoptosis, e.g. they prevent oligodendrocyte death induced by growth factor deprivation. CB2R activation on glioma and astrocytoma cells induces apoptosis by promoting ceramide *de novo* synthesis, a sphingolipid second messenger that causes cell-cycle arrest and cellular stress responses (Guzman,M. 2003). Another secondary mechanism suggested to explain cannabinoid antitumoral effects through CB2R involves inhibition of angiogenesis and the vascular endothelial growth factor pathway.

The activation of cytoprotective and survival signaling pathways, and an enhanced supply of energy substrates from astrocytes to neurons, are other proposed mechanisms. Cannabinoids can activate phosphatidylinositol 3'-kinase (PI3K)/protein kinase B and extracellular signal-regulated kinase (ERK) by acting on both CB1 and CB2 receptors and is dependent on $G_{i/o}$ protein dissociation. CBRs can directly release G protein βγ subunit activating class I_B PI3K isoforms, or indirectly via transactivation of growth factor tyrosine kinase receptors and subsequent stimulation of class I_A PI3K/Akt and ERK pathways. *In vivo* acute administration of Δ^9-THC in mice activates Akt and phosphorylates/inactivates glycogen synthase kinase-3β (GSK-3β) in several brain areas, and this effect is closely related to the activation of CB1R. The Akt/GSK-3β pathway promotes cell survival by enhancing the

expression of anti-apoptotic proteins and inhibiting the activity of pro-apoptotic ones (Bad, caspase 9, Forkhead transcription factors) (Ozaita,A. *et al*., 2007). Receptor cross-talk is involved in coordinating the coincident actions of cannabinoids and growth factors in neuronal cell survival. Treatment of adult hippocampal neural progenitors *in vitro* leads to the expression of kainate receptors that mediate proliferation and neurosphere generation via CB1R. *In vivo,* CB1R ablation prevents the induction of hippocampal expression of basic fibroblast growth factor (bFGF), brain-derived neurotrophic factor (BDNF), and epidermal growth factor (EGF) (Aguado,T. *et al*., 2007). CB1Rs induce BDNF production that mediates the neuroprotective response elicited by eCBs following an excitotoxic insult in the hippocampus (Marsicano,G. *et al*., 2003). In addition, the eCB system exerts a neuroprotective action through receptor-independent mechanisms. Cannabidiol, Δ^9-THC, and other phenol-containing cannabinoids have intrinsic antioxidant properties. In addition, COX-2-mediated metabolites of eCBs generate neuroactive prostaglandins and prostamides, while brain injury increases PEA levels which exert anti-inflammatory effects through the peroxisome proliferation-activated receptor-α.

1.1.4.3 Endocannabinoid signaling functions during CNS development.

During vertebrate embryonic development different classes of neurons, glia, and ependymal cells are produced in a highly discrete spatio-temporal pattern. Most neurons in the mammalian brain are generated embryonically during restricted phases, and the mature mammalian brain is characterized by a relatively constant number of neurons. Prior to neurogenesis, the neural plate and neural tube consist of a single layer of neuroepithelial cells that forms the neuroepithelium. With the generation of neurons, the neuroepithelium transforms into a multilayer tissue, and that which lines the ventricle (the most apical cell layer that contains most of the progenitor cell bodies) represents the ventricular zone. With the switch to neurogenesis, neuroepithelial cells give rise to radial glial cells that represent more fate-restricted progenitors that successively replace the former. Most radial glial cells are restricted to the generation of a single cell type (astrocytes, oligodendrocytes, or neurons) (Gotz,M. and Hottner,W.B. 2005).

Radial glial cells exhibit residual neuroepithelial properties such as expression of the intermediate-filament protein nestin. They show several astroglial properties, expressing the astrocyte-specific glutamate transporter (GLAST), the Ca^{2+}-binding protein S100β, and glial

fibrillary acidic protein (GFAP). The transition of neuroepithelial to radial glial cells during embryonic development is associated with an increase in the length of their cell cycle, predominantly due to a lengthening of the G1 phase. Another type of neuronal progenitor appears at the onset of neurogenesis: basal progenitors originate from the mitosis of neuroepithelial and radial glial cells. During later stages of neurogenesis, basal progenitors form the subventricular zone, a mitotic cell layer that is basal to the ventricular zone, which contributes to neurogenesis by undergoing symmetric cell divisions that generate two neuronal daughter cells.

eCB signaling serves key functions during neurodevelopment by affecting neural progenitor proliferation, lineage segregation, migration, progenitor specification, and survival (Galve-Roperh,I. *et al*., 2006), phenotypic neuron differentiation (Berghuis,P. *et al*., 2005), and synapse establishment. eCBs can influence neurodevelopment through cross-talk with other signaling systems, neurotrophin and growth factor receptor dimerization, different G protein coupling, and interaction with a broad spectrum of second messengers. For example, consider the evolution of eCB metabolism molecular organization and receptor distibution during brain development. During corticogenesis eCBs act as morphogens, and establishment of a functional eCB system coincides with the generation of cortical pyramidal cells from subventricular zone (SVZ) progenitors, immature pyramidal cell-radial migration to the cortical plate, and tangential migration of GABA-containing precursors to the neocortex (Wonders,C.P. *et al*., 2006). CB1R activation promotes neural progenitor proliferation, and the eCB system regulates their primary fate-decision point. Neural progenitors have a functional eCB system (they synthesize eCBs), functional CB1 and CB2 receptors, and the catabolic enzyme FAAH (Aguado,T. *et al*., 2005).

CB1R expression is spatially and temporally coordinated with eCB synthesis during brain development. DAGL-β immunoreactivity in mouse embryonic ventricular and subventricular zones reflects eCB synthesis during neuronal progenitor proliferation. Bisogno *et al*. reported an embryonic spatial association between DAGL-α/β and CB1R expression in long-range subcortical fibres and cerebellar projection tracts, in contrast to a dendritic location in the adult. DAGL-α represents the predominant isoform in the perinatal and postnatal neocortex. 2-AG levels plateau in prenatal life. The primary role of 2-AG during neurodevelopment is suggested by the undetectable levels of NAPE-PLD until the neonatal period (Berghuis,P. *et al*., 2007), and 2-AG expression appears late in gestation in GABAergic interneurons

migrating intracortically. At mid-gestation, AEA brain concentration is low and increases during the perinatal period until adulthood. eCB signaling through CB1Rs exerts different effects on growth cone navigation, axonal elongation, and synaptogenesis of cerebral interneurons and pyramidal cells in mammals. The eCB system is instructive and permissive for neuronal migration. Cells use eCB signaling to initiate the elongation and fasciculation of their long-range axons. eCB control of axonal elongation in pyramidal cells is a cell-autonomous mechanism. DAGLs and CB1Rs are in close proximity along the axon stem, allowing direct ligand-receptor coupling. DAGLs are recruited to elongating axons of developing pyramidal cells. The primary enzyme concentrates in axonal growth cones at mid-gestation, while at late gestation it is located in postsynaptic pyramidal cells and 2-AG guides axonal growth cones. DAGL distribution is negatively associated with axon morphogenesis and accounts for an activity-dependent postnatal location of eCB synthesis and release. FAAH is present in radial glia from late gestation until the neonatal period, while it is transiently expressed in hippocampal interneurons during the intralaminar migration, suggesting a different role for AEA in neural specification. AEA induces the elongation of a leading axon while inhibiting axon branching (Harkany,T. *et al*., 2007).

The coincidence of eCB synthesis in elongating long-range and GABAergic axons suggests that eCB signaling is responsible for the initial axonal growth, while target-derived eCB signals regulate axonal navigation and positioning. In cooperation with BDNF, eCBs and CB1R agonists induce the migration of GABAergic interneurons undergoing long-distance intracortical migration to the neocortex. Berghuis *et al*. reported that AEA stimulation of CB1R on fetal rat cortical cholecystokinin (CCK)-expressing GABAergic interneurons is chemoattractive. eCB regulation of interneuron migration is mediated by Src kinase-dependent tyrosine kinase B (TrkB) receptor transactivation. Interneuron differentiation is associated with a simultaneous recruitment of CB1Rs and TrkB receptors to axon terminal segments of developing $CB1R^+$ interneurons, providing a platform for signaling interactions. AEA modulates BDNF-induced migration of $CB1R^+$ interneurons in an additive fashion. BDNF selectively expressed and released by pyramidal cells is a differentiation signal for GABAergic interneurons. Prolonged AEA exposure suppresses BDNF-dependent cortical interneuron differentiation, reduces interneuron membrane hyperpolarization, inhibits neurite extension and elongation, and attenuates BDNF-induced growth response when co-applied (Berghuis,P. *et al*., 2005). CB1Rs are concentrated in axonal growth cones of GABAergic

interneurons, suggesting their use of a target-derived eCB as directional cue. eCBs simultaneously inhibit neurite outgrowth and synaptogenesis of GABAergic interneurons, suggesting that autocrine eCB signaling controls growth cone differentiation and axon guidance, in such manner as to be most compatible with a particular stage of cell differentiation. An eCB contribution to neuronal cell differentiation is suggested also by the selective axonal targeting of CB1Rs through a domain-specific endocytosis, from the early period of acquiring neuronal polarity.

The eCB system links axonal specification in the early embryonic brain to synaptogenesis and synaptic plasticity during the neonatal period. DAGL-α/β expression in axonal growth cones during axonal navigation is down-regulated during synaptogenesis. Termination of synaptogenesis coincides with CB1R disappearance from axonal tracts and appearance in growth cones which are in the process of forming synapses. Collectively, these data support eCB signaling in the evolution of retrograde synaptic transmission, when immature neuronal networks become operational. eCB signaling can thus be viewed as a "guidance cue" for embryonic and adult neurogenesis.

The adult persistence of motor, cognitive, and social deficits induced by prenatal exposure to cannabinoids further supports eCB signaling in the regulation of neurodevelopment. In the developing rat hippocampus, GABA exerts a depolarizing effect on pyramidal cells. In cooperation with glutamate, GABA generates giant depolarizing potentials necessary for NMDA receptor activation and subsequent glutamatergic synapse maturation. During the first postnatal week eCBs are released by CCK-containing interneurons and pyramidal cells in the hippocampal CA1 region. The over-activation of CB1Rs located on GABAergic presynaptic terminals of CCK-interneurons decreases network activity, whilst their blockade generates epileptiform discharges (Bernard,C. *et al*., 2005).

1.2 Persistence of neurogenesis in the adult mammalian brain.

Adult neurogenesis comprises the entire set of events of neuronal development beginning with the division of a precursor cell, and ending with the presence and survival of a mature, integrated, functioning new neuron. In mammals, the constitutive generation of new functional neurons from endogenous pools of neural stem cells throughout life is probably confined to just two regions: the subgranular zone (SGZ) of the hippocampal dentate gyrus, and the SVZ, which contributes interneurons to the olfactory bulb. There is evidence to suggest the presence of constitutive neurogenesis in other regions of the adult brain, as well. In these two neurogenic regions, stem-like cells are not in a quiescent state but have a very slow dividing turnover (a few weeks). Transient early postnatal neurogenesis has been reported in the cerebellum and the brain stem nuclei (Kaslin,J. *et al*., 2008).

Adult CNS "stem cells" are self-renewing, with the ability to produce progeny indistinguishable from themselves. They proliferate, continuing to undergo mitosis (with quite long cell cycles) and are multipotent for the different neuroectodermal lineages of the CNS, including the different neuronal and glial subtypes. The adult SVZ develops from the embryonic and early postnatal ventricular zone and SVZ. In the postnatal period, radial glia are neural stem cells that mature into ependymocytes (whose function is to circulate the cerebrospinal fluid), and adult SVZ stem cells (astrocyte-like cells). Stem-like cells (astrocyte-like cells) in the adult SVZ expressing nestin and GFAP act as slow-dividing neural stem cells capable of generating transit-amplifying progenitors expressing nestin, and forming clusters interspaced among chains throughout the SVZ. Multipotent progenitors of the adult brain are proliferative cells with only limited self-renewal that can differentiate into at least two different cell lineages (Okano,H. and Sawamoto,K. 2008). The SVZ transit-amplifying progenitors divide very actively and mature into neuroblast precursors expressing polysialic acid–neural cell adhesion molecule (PSA-NCAM), Tuj1 (beta III-tubulin), and Hu . The neuroblasts proceed through the rostral migratory stream (RMS) into the olfactory bulb, with migration involving PSA-NCAM. In the RMS neuroblasts are not guided by radial glia, but migrate tangentially in chains through tubular structures formed by specialized astrocytes (Lois,C. and Alvarez-Buylla,A. 1994). SVZ precursors can also migrate radially to the white matter, where they differentiate into astrocytes and oligodendrocytes during postnatal myelination. The peak of gliogenic activity in the SVZ at P (postnatal day) 15 decreases as development progresses into adulthood, at which time neurogenesis predominates. Adult

oligodendrogenesis from the SVZ increases after toxic and autoimmune demyelination, as precursors are recruited to give rise to oligodendrocytes in the lesioned areas.

After detaching from these chains and migrating radially from the RMS into the olfactory bulb, adult-born cells from the SVZ mature into olfactory inhibitory GABAergic granule interneurons and periglomerular dopaminergic interneurons. Newborn olfactory bulb neurons become more complex within the first few weeks after their birth. Granule cells form more elaborate dendrites that extend into the external plexiform layer of the bulb. During this maturation, immature bulbar interneurons express transient marker proteins including Tuj1 (Carleton,A. *et al*., 2003). The SGZ of the hippocampus lines the hilar side of the granule cell layer of the dentate gyrus. In the adult SGZ, GFAP-positive stem-like cells give rise to intermediate progenitors that mature locally into granule neurons of the granular cell layer of the dentate gyrus, sending axonal projections to the CA3 area and dendritic arbours into the molecular layer. As they differentiate, the dendrites of newborn dentate gyrus cells become progressively more complex and extend deeper into the molecular cell layer. The new neurons express a series of transient markers, such as doublecortin and PSA-NCAM, which are also characteristic of immature neurons during development. Neural cell adhesion molecule facilitates hippocampal neurogenesis proliferation and the differentiation of neuronal cells through regulation of proneurogenic transcription factors.

1.2.1 AUF1: importance of RNA stabilization for cell differentiation.

AUF1 (AU-rich element/poly(U)-binding/degradation factor 1/heterogeneous nuclear ribonucleoprotein D, hnRPD) (NW_047422.1 NCBI Reference Sequence) exists as 4 alternative mRNA splice variants of a single primary transcript consisting of 7 exons in *Rattus Norvegicus* ("taxon: 10116") (corresponding to p37, p40, p42, and p45 proteins). AUF1 mRNAs contain two non-identical RNA binding domains (RNA binding domain I, RDBI, and RNA binding domain II, RDBII) with or without one or both N-terminus and C-terminus 19 and 49 amino acid inserts, respectively. p45 and p42 isoforms share exon 7 at the C-terminus, which is absent in the p40 isoform. p42 lacks the N-terminal exon 2, while p37 is devoid of both the exons. AUF1 transcript expression is regulated in the brain from the embryonic stage through adulthood (Hambardzumyan,D. *et al*., 2009). In fact, AUF1 is present in cortical progenitors of the ventricular and subventricular zones, and in differentiating post-mitotic neurons in the cortical plate during corticogenesis (E19-P2) (Lee,C. *et al*., 2008).

Numerous functions for AUF1 have been described, including the control of neuronal cell differentiation through alteration of transcription factor access to their DNA binding sites. p37 in particular binds double strand DNA regions rich in AT with high specificity, where it recruits chromatin remodeling molecules lacking DNA binding domains, such as histone deacetylase (HDACI). Chromatin deacetylation involves its condensation and inactivation, leading to inhibition of target gene transcription. The p40 isoform interacts with dsDNA TATA-binding proteins on promoter regions where transcription factors and RNA polymerase cluster, guiding transcription direction and determining which of the two strands is copied. There is some evidence supporting a role for exon 2 in transcription regulation. p42 binds single strand DNA telomeres, interact with telomerase and determines telomere length. Telomeres are short G-repeat-rich sequences in the terminal portion of the chromosome. During cell division telomeres are not replicated, but are added by telomerase. Variations in the telomer repetition number may be introduced, owing to a lack of complete fidelity by telomerase. Senescence (definitive cell cycle exit, corresponding to G0 phase) seems to correlate with the inability to maintain telomere length. Moreover, these proteins interact with the translation initiation complex and destabilize cytoplasmic -labile ARE-mRNAs coded by genes controlling cell cycle and growth, mitogen stimulation, signaling transduction, and cytokine production.

Heterogeneous nuclear RNA is covalently modified. Binding of a 7-methyl guanosine to 5'-RNA, which then undergoes ribosomal binding for protein synthesis. This step protects RNA from degradation and is important for translation. A poly-A sequence is added to 3'-RNA by poly-A-polymerase, which is necessary for mature mRNA transport to the cytoplasm, its stability, and ribosomal identification. ARE sequences behave as signals for mRNA fast turnover, because they are deadenylated and degradated. p37 and p40 possess the major destabilizing activity and p37 can drive degradation of mRNA lacking non-canonical AU rich sequences. p37 levels thus represent the limiting factor of ARE-mRNA turnover rate. Moreover, degradation rate is correlated to AUF1 turnover, being ubiquitinated and degradated by proteasome. Exon 7 changes protein conformation and sensitivity to ubiquitination, which is reflected by the different isoform binding strengths to ARE sequences. p37 is the most ubiquitinated isoform, while p42 and p45 are the most abundant isoforms *in vivo* and are poorly degradated *in vitro* (412 Sarkar,B. *et al*., 2003).

An example of AUF1 post-transcriptional regulation is represented by the destabilizing action on DNA methyltransferase I mRNA (DNMT1) that maintains DNA methylation during cell division and so is transcriptionally inactive, and it is regulated by growth factors (Torrisani,J. *et al*., 2007). AUF1 expression is regulated during the cell cycle via ubiquitin-proteasome, which contributes to maintenance of genomic methylation integrity, being inversely correlated to DNMT1 expression. AUF1 binds to non-canonical AU sequences, increased in G0/G1 phase, and is in part responsible for decreased DNMT1 transcript levels. This acts to determine cell number reduction, because DNMT1 belongs to the replication complex, which inhibits replication and cell growth. AUF1 levels decrease during S phase. Cyclin D1 is critical for G1 progression, as it binds and activates CDK4. This complex phosphorylates and inactivates retinoblastoma protein, thus allowing G1-S transition. Cyclin D1 is regulated during the cell cycle through AUF1-3' binding. Its low concentration in quiescent cells increases following serum or mitogen stimulation (Lal,A. *et al*., 2004).

1.2.2 The endocannabinoid system modulates adult neurogenesis.

Jiang *et al*. demonstrated that the synthetic non-selective CBR agonist HU210 and AEA promote proliferation of embryonic hippocampal neural stem/progenitor cells *in vitro* through CB1R-induced ERK activation, without affecting differentiation (Jiang,W. *et al*., 2005). *In vivo* chronic, but not acute, HU210 treatment increases the number of newborn neurons in the dentate gyrus of adult rat and this is correlated with anxiolytic- and antidepressant-like effects. These authors reported a HU210 mitogenic effect in the absence of exogenous EGF and bFGF, excluding an indirect action on proliferation through growth factor signaling. Jin *et al*. showed a reduction in proliferation in the dentate gyrus and SVZ of adult CB1R knockout mice *vs* wild-type levels, while the CB1R antagonists SR141716A and AM 251 increased the proliferative index in wild-type mice (Jin,K. *et al*., 2004). Interestingly, the SR141716A effect persisted in CB1R knockout mice, proposing involvement of both CBR1 and TRPV1 in the neurogenic action. Aguado *et al*. reported rat embryo cortical progenitor cultures express CB1R and FAAH, and produce AEA and 2-AG. WIN 55,212-2 treatment increased neurosphere generation via CB1R activation, and adult brain-derived neurospheres proliferated in response to cannabinoid treatment. This action was abrogated in CB1R-deficient neural progenitors. Accordingly, proliferation of hippocampal neural progenitors is increased in FAAH-deficient mice (Aguado,T. *et al*., 2005).

Molina-Holgado *et al*. reported that mouse embryo cortical neural stem cell cultures express DAGL-α and both CBRs. The selective CB1R agonist ACEA and the CB2R agonist JWH-056 each significantly stimulate neurosphere formation three days after a single exposure. Treatment of cultures alone with specific antagonists of CB1 or CB2 receptors abolished or significantly decreased neurosphere formation. The proposed mechanism involves PI3K/Akt signaling activation (Molina-Holgado,F. *et al*., 2007). These authors suggest that CB2Rs can be involved in the mantainance of the self-renewal capacity of stem cells. Palazuelos *et al*. showed CB2R expression, both *in vivo* and *in vitro*, in mouse neural progenitors from late embryonic stages to adult brain, which underwent down-regulation upon neural cell differentiation. Genetic ablation of this receptor reduces neurosphere generation after several passages in culture. *In vivo* administration of the CB2R selective agonist HU-308 significantly increased hippocampal progenitor proliferation, which depended on ERK and Akt phosphorylation (Palazuelos,J. *et al*., 2006).

Evidence for endo/cannabinoid impact on glio/neurogenesis is discordant, and the different actions may be ascribed to different pharmacological properties of endo- and exo-cannabinoids *in vivo*, to the intensity of cannabinoid stimulation (endogenous modulation *vs* pharmacological target), or the physiological context of neural stem/progenitor cell regulation (normal *vs* injured brain). Published evidence suggests that eCB signaling plays a role in promoting astroglial differentiation of neural progenitors. CB1 and CB2 receptors are present in the rat postnatal SVZ and administration of CBR agonists to newborn rats affects postnatal oligodendrogenesis. Some authors report that CB1R expression is developmentally regulated, with peak expression in the rat hippocampus coinciding with the beginning of gliogenesis *in vivo* (Harkany,T. *et al*., 2007). ACEA treatment increases proliferation of stem cells and increases the number of glial precursors. Aguado *et al*. reported a gliogenic action on neural stem cells in the SGZ through the activation of CB1R (Aguado,T. *et al*., 2006). CB1R and FAAH are expressed both *in vivo* and *in vitro* in postnatal radial glia and in adult neural progenitor cells. WIN 55,212-2 (a cannabinoid agonist that does not bind to TRPV1), AEA and 2-AG increase the number of $GFAP^+$, $GLAST\text{-}1^+$, and $S100\beta^+$ cells . The activation of CB2R increases the number of migratory neuroblasts that enter the rostral stream and oligodendrocyte precursors that migrate to the white matter in the rat postnatal SVZ .

Endogenous cannabinoids have been reported to inhibit adult hippocampal neurogenesis. *In vivo*, the non-hydrolyzable AEA analog methanandamide produces a significant decrease

in hippocampal neurogenesis, while SR141716A increases neuronal cell differentiation of neural progenitors, suggesting the existence of an eCB tone that actively modulates neural progenitor differentiation (Rueda,D. *et al*., 2002). These authors reported that AEA, acting through CB1R inhibits rat cortical neuron progenitor and human neural stem cell (HNSC.100) differentiation *in vitro*. AEA inhibits NGF-induced PC12 (pheochromocytoma) cell differentiation through the inhibition of the Rap1/B-Raf-mediated sustained ERK activation. During cortical neurogenesis, sustained mitogen-activated protein kinase ERK signaling is required for neuronal cell generation and inhibition of gliogenesis. In this context, AEA decreases NGF-induced TrkA tyrosine phosphorylation and Rap1 and B-Raf activation, resulting in attenuated ERK activation.

In rat postnatal cerebellar granule cells, CB1R antagonists inhibit axonal growth stimulated by the cell adhesion molecule N-cadherin and bFGF, but not by BDNF. N-cadherin activates an FGF receptor-signaling cascade in growth cones to promote motility. The FGF receptor, through activation of PLCγ generates DAG. The subsequent hydrolysis is coupled to a Ca^{2+} influx into growth cones through N-and L-type calcium channels. BDNF stimulates axonal growth by activating the TrkB receptor tyrosine kinase, and its response is independent of DAG hydrolysis. ACEA and WIN 55,212-2 stimulate neurite outgrowth and are not affected by the FGF inhibitor PD 173074, demonstrating that CB1R function is downstream of FGF receptor activation. L- and N-type calcium channel antagonists inhibit the CB1R response and do not affect that of BDNF. Moreover, calcium influx into cells by CBR agonists and their response are not inhibited by PTX (Williams,E.J. *et al*., 2003).

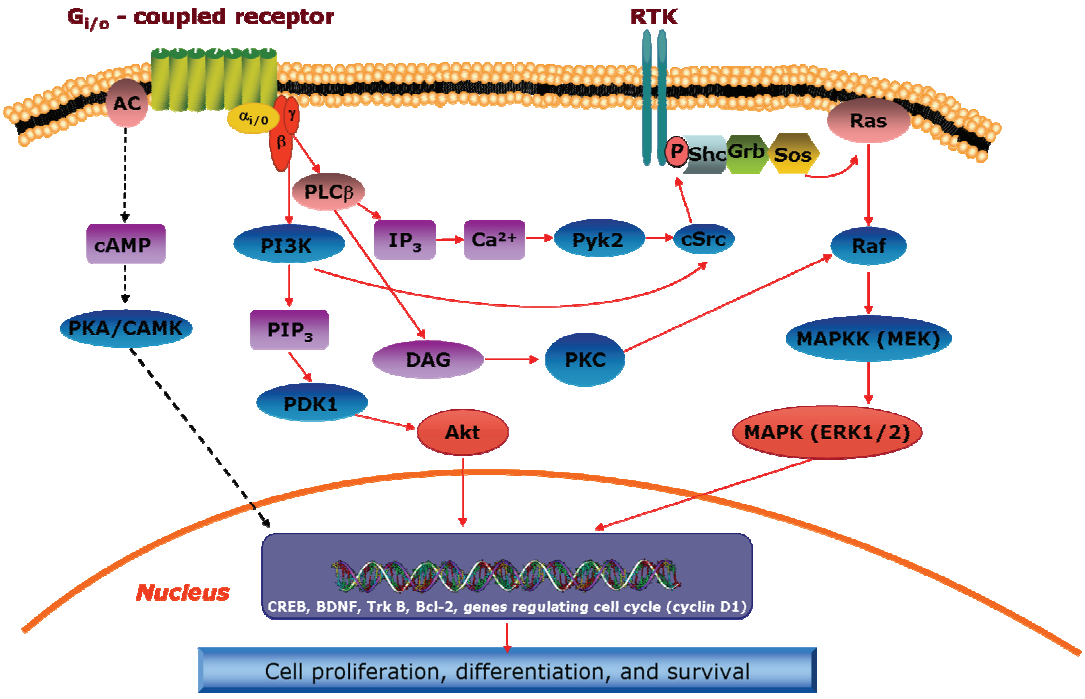

Figure 6. Neurotrophins and their receptors: a convergent point for many signaling pathways.

1.3 Cerebellar development.

Progenitor cells have been isolated and differentiated *in vitro* into neurons and macroglia from several, otherwise non-neurogenic, regions of the mammalian brain such as the isocortex, optic nerve, spinal cord, hypothalamus, and cerebellum (Lee,A. *et al*., 2005). These progenitors are thought to be responsible for the continuous low generation of astrocytes and oligodendrocytes in the mammalian brain (Dawson,M.R. *et al*., 2003; Levine,J.M. *et al*., 2001).

Cerebellum is one of the first brain areas to differentiate, although its cellular organization continues to change for many months after birth until a mature configuration is achieved. This brain structure originates from the mesencephalic and metencephalic dorsal regions of the posterior embryonic neural tube. The developing cerebellum contains two distinct germinal matrices that give rise to cerebellar cortical neurons. From the primary germinal matrix, the ependymal layer in the roof of the fourth ventricle, cells migrate radially late in gestation and evolve into the Purkinje cells that continue to mature after birth. During their final maturation, they develop synaptic connections with granule neurons that influence this developmental phase through their signals. Following Purkinje cell formation the ventricular zone gives rise to three other neuronal cell populations: stellate, basket, and Golgi interneurons of the molecular layer. Cerebellar granule neurons derive from dividing progenitors located in a second germinal matrix, the rhombic lip, between the fourth ventricle and the roof plate in the metencephalon (Fig. 7). The position of the rhombic lip results from incomplete closure of the dorsal neural tube and the subsequent formation of the pontine flexure that displaces the gapped edges laterally. Around embryonic day 13 (E13) in the mouse, granule cell precursors proliferate and then assume a unipolar morphology. At mid-gestation they migrate out from the rhombic lip to populate the external granular layer (EGL) at which time they still express nestin, a marker of undifferentiated precursors. Rhombic lip cells continue to migrate to the cerebellar anlage and settle on its periphery to form the EGL.

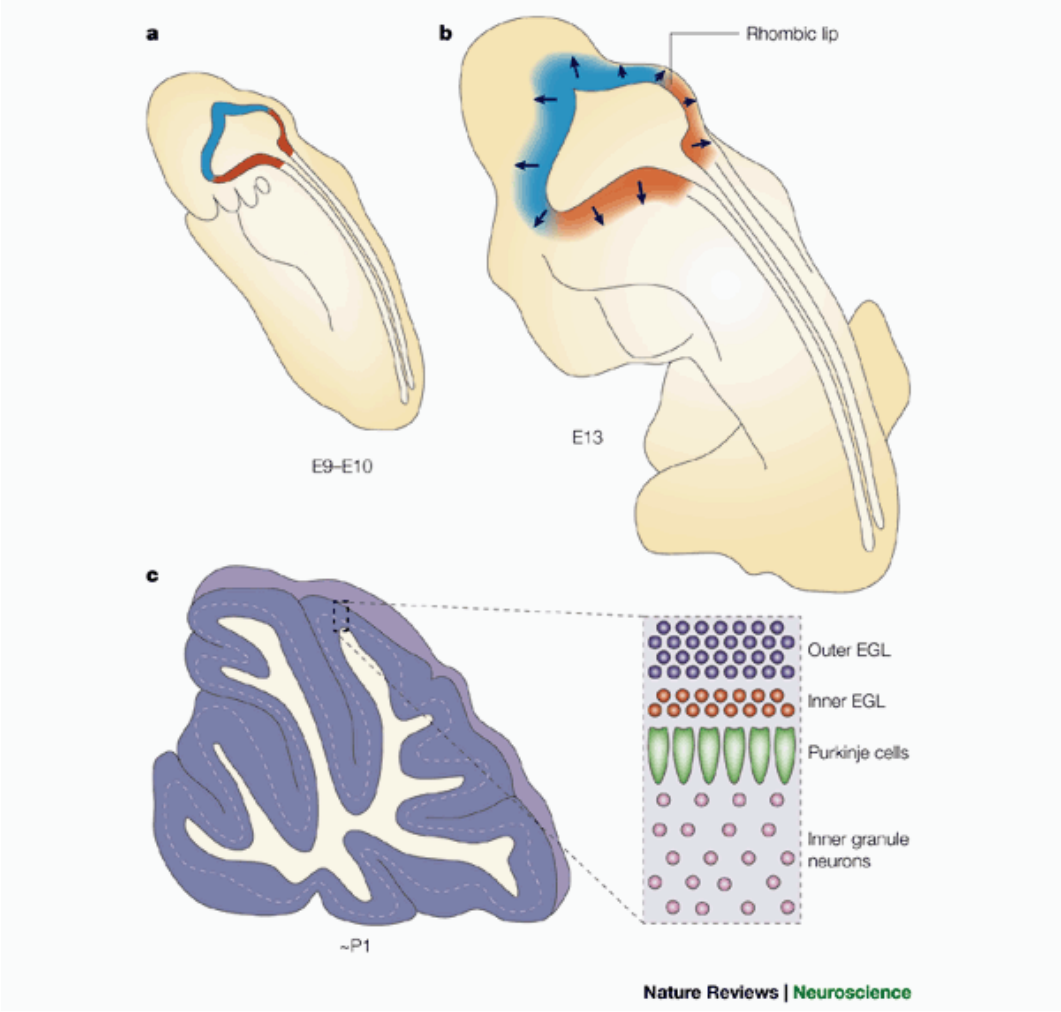

Figure 7. Granule neuron development in mice. a | At embryonic day (E) 9, the rhombic lip (blue and orange) is a zone of proliferation between the fourth ventricle and the neural tube. The cells in the blue region give rise to the cerebellar granule neurons and pontine nucleus, whereas cells in the red region yield other rhombic lip derivatives such as the inferior olivary nucleus. **b** | At about E13, cells from the rhombic lip migrate outwards to populate the cerebellar anlage. **c** | The granule neuron precursors continue to proliferate in the outer external granule layer (EGL; blue), then become postmitotic in the inner EGL (orange). The Purkinje cells control the proliferation of the granule neuron precursors through the release of neuron-diffusable factors such as sonic hedgehog. From the inner EGL, granule neuron precursors migrate into the inner granule layer and complete the final stage of differentiation. P1, postnatal day 1 (Wang,V.Y. and Zoghbi,H.Y. 2001).

By E16 the mouse EGL extends across the whole roof of the cerebellar anlage as a thin layer of proliferating cells. Once in the outer postnatal EGL, these precursors are specified to become granule neurons and respond to signals leading to differentiation into granule neurons. Rapid proliferation in the EGL expands the zone from a single cell layer to a layer about eight cells in thickness. Neuronal cell proliferation requires Purkinje cell interaction, as the latter control cell proliferation of the outer EGL precursors and release diffusable factors such as sonic hedgehog (Shh). During the second postnatal week, granule cell precursors migrate from the outer EGL to the inner EGL, where they exit the cell cycle and are found in a pre-migration state. This migration results in the disappearance of the EGL (Fig. 8). Several trophic factors, like BDNF and insulin-like growth factor 1 (IGF1) control cell number during development. During early postnatal life they undergo an inward migration through the molecular layer into the internal granular layer (IGL), under the guidance of interstitial junctional interactions with radial glial fibres. At this developmental stage cells express class 3 β-tubulin/Tuj1 and develop parallel fibres. While preparing for migration, granule neuron precursors undergo electrophysiological changes. NMDA receptor activation is involved and a class of inwardly-rectifying K^+ channels induces hyperpolarization to balance NMDA-receptor-induced depolarization. The final stage of maturation of granule neurons occurs in the IGL. Granule cells express mature markers such as GABA receptors and interact with Golgi cells and precerebellar nuclei mossy fibres (Fig. 9).

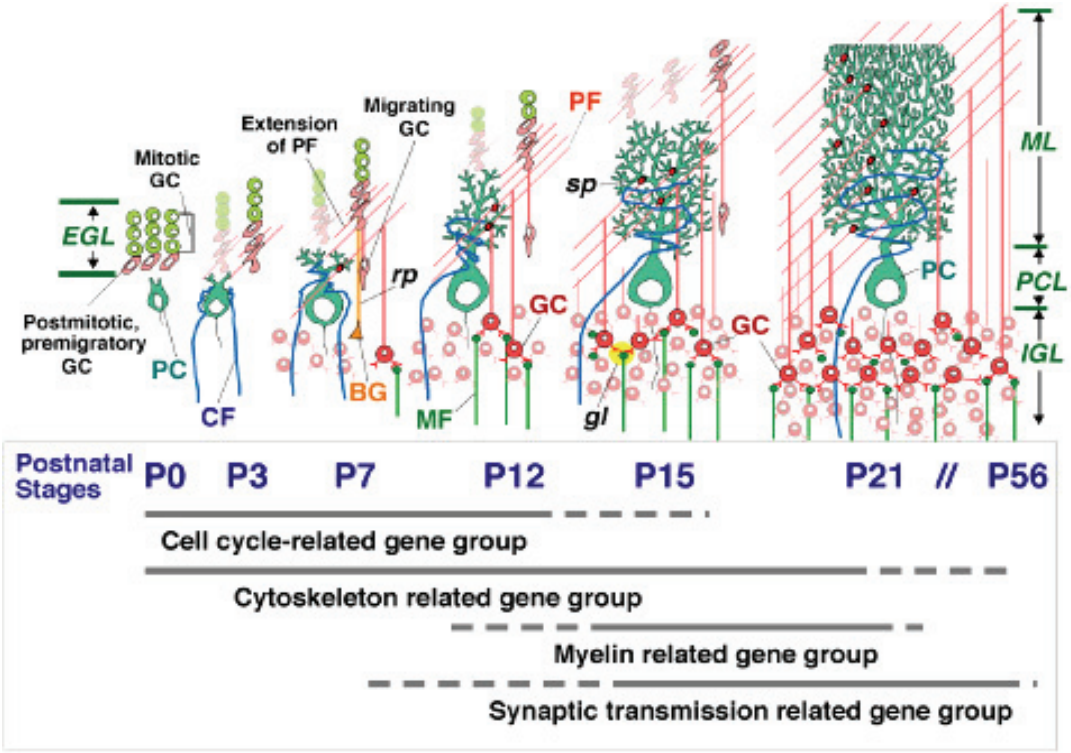

Figure 8. Postnatal developmental stages of mouse cerebellum. Granule neuroblasts proliferate massively in the external granular layer (EGL) shortly after birth, and undifferentiated Purkinje cells (PC) underneath the EGL. By postnatal day 3 (P3), formation of the PCL is followed by synapse (sp) formation between a climbing fibre (CF) and the proximal dendrites of PCs. Postmitotic granule cells (GC) begin their differentiation at P3, with the extension of a horizontal bifurcate axon called parallel fibre (PF), at the bottom of the EGL. From P7 to P21, molecular layer (ML) forms as the Purkinje dendrites extend and become arborescent. The inward and vertical migration of GCs, guided by Bergman glia (BG) fibres (also known as radial processes, rp) through the developing ML and the PCL to the inner granular layer (IGL), the takes place at P7-P15 and results in a T-shaped axonal projection from the PF. The PFs extending perpendicularly to the plane of Purkinje dendrites, and form synapses with the dendritic spines of Purkinje, basket, Golgi, and stellate cells as they mature. Two major afferent inputs to the cortex, the inferior olive's CF to PCs and the mossy fibre (MF) axons to the GC dendrites (forming glomeruli, gl) are formed at around P10. By P21, the architectures at the cellular, neural circuit, and lobular levels show almost no difference from those of the adult.

1.3.1 CB1 and CB2 receptor distribution and functions in the cerebellum.

The cerebellar cortex IGL contains the highest number of neurons in the brain. Imaging studies of granule cell somata, located in this lamina, suggest that cerebellum is a primary substrate for cannabinoid withdrawal. Several of the molecular and cellular adaptations involved in addiction are also implicated in learning and memory. Particularly relevant is activation of the cAMP-cAMP response element binding protein (CREB) pathway related to learning and LTP of synaptic transmission. Acute Δ^9-THC administration induces the expression of CREB and c-fos in the rat cerebellar glutamatergic granular layer, while chronic treatment prevents these effects. Cannabinoid effects on CREB might alter plasticity at the level of Purkinje cell synapses (Rubino,T. *et al*., 2004).

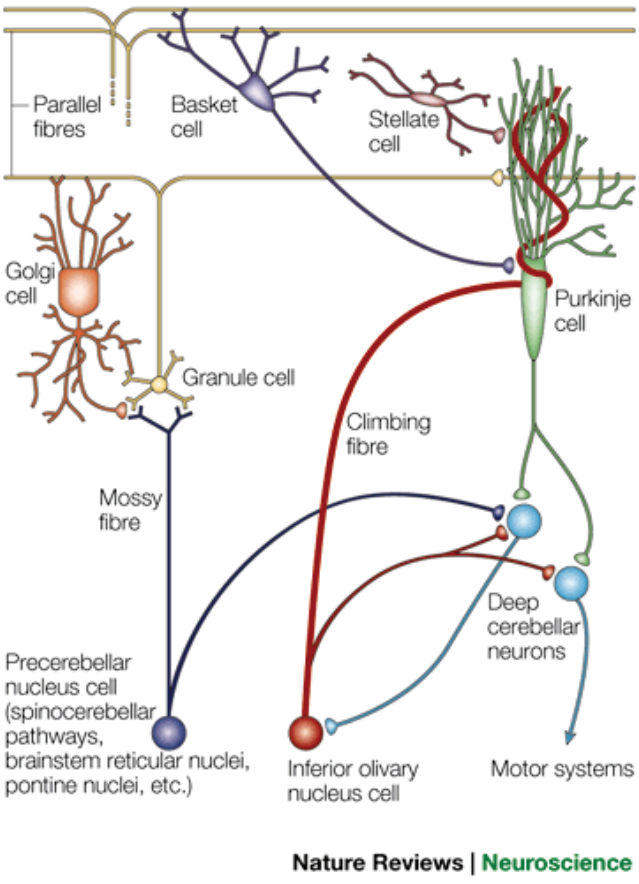

Figure 9. Neurons of the cerebellum and their connections. (Wang,V.Y. and Zoghbi,H.Y. 2001)

In a radioligand binding assay study, Belue *et al*. reported that CB1R binding capacity in cerebellum doubles at 7-day postnatal intervals until adulthood, while no differences in affinity are evident in the postnatal developmental period (Belue,R.C. *et al*., 1995). In P14 rat CB1R immunoreactivity is very intense in parallel fibre terminals in the molecular layer, and shows a superficial to deep gradient. CB1Rs are also present in the inhibitory fibres and terminals around Purkinje cell somata and around inhibitory terminals in contact with Purkinje cell dendrites. During cerebellar maturation CB1Rs accumulate in the perisynaptic region at parallel fibre axon terminals, as suggested by the higher extrasynaptic labeling at P14 than the adult. Kawamura *et al*. suggest the CB1R heterogeneous distribution along parallel fibres is functionally relevant, because eCB release triggered by parallel fibre activity requires activation of postsynaptic type I mGluRs in the perisynaptic site. This would allow perisynaptic CB1Rs to detect eCBs more effectively than extra/synaptic receptors (Kawamura,Y. *et al*., 2006). Adult cerebellum shows a similar immunoreactivity pattern, but differs in the loss of CB1R gradient in the molecular layer and appearance of an intense immunoreactivity in basket cell axons and axon terminals surrounding Purkinje cell somata. CB1Rs are mostly present in the molecular layer, at the level of axon terminals of cerebellar granule cell parallel fibres and climbing fibres of inferior olive neurons, the latter providing excitatory input on Purkinje cells (Fig. 9). Moreover, CB1Rs are located in axon terminals of basket and stellate cells that provide inhibitory input on Purkinje cells. Although similar, CB2R distribution differs because of a moderate presence in the granular layer, and a much more intense immunoreactivity in cerebellar and vestibular nuclei. In the cerebellar cortex, FAAH immunoreactivity is complementary to eCB receptor distribution and is reported in Purkinje cell bodies and the dendritic tree, in granule cells, and in climbing and parallel fibre terminals. MAGL immunoreactivity partially overlaps that of eCB receptors, and is found in basket and stellate cells, climbing fibres and parallel fibre terminals, Purkinje cell bodies, granule cells, mossy fibres, and Golgi cells. The presynaptic location of MAGL may be related to the retrograde messenger role of 2-AG that determines a basal eCB tone. In contrast, DAGL-α is largely present in Purkinje cell dendrites in the molecular layer, and correlates with CB1R and CB2R localization in climbing fibres. DAGL-α immunoreactivity is far more intense than that of DAGL-β, which is specifically expressed by Purkinje cell bodies. The postsynaptic location of DAGL-β in Purkinje and granule somata correlates with CBRs location in basket cell axons and CB2R presence in mossy fibres. This different

localization suggests that Purkinje cell dendrites postsynaptically release 2-AG by DAGL-α, and Purkinje somata and granule cell somata/dendrites by DAGL-β in mossy and parallel fibres. NAPE-PLD immunoreactivity is distributed in the molecular layer (Suarez,J. *et al*., 2008).

Regulation of Purkinje cell activity is important for motor behaviour and motor learning. These cells receive the excitatory inputs of ascending branches and parallel fibres of granule cell axons, and a climbing fibre synapse from neurons in the inferior olive. Purkinje cells receive inhibitory inputs from basket and stellate cells (Fig. 9). The regulation of this circuitry mediates short-term plasticity and learning (Zucker,R.S. and Regehr,W.G. 2002; Carey,M. and Lisberger,S. 2002). The cerebellum plays a role in higher cortical functions and is an important cognitive organ. Several studies describe cerebellar abnormalities and dysfunctions in psychiatric diseases. The eCB system plays a central role in the regulation of movement and neuroadaptations underlying motor control and motor learning. Pharmacological actions of cannabinoids include ataxia and catalepsy, and modulation of eye blink conditioning. Endogenous cannabinoid signaling through CB1R is essential for cerebellum-dependent discrete motor learning, expecially for its acquisition in mice. (Safo,P.K. *et al*., 2006)

In cerebellum, brief depolarization of Purkinje cells results in a calcium-dependent liberation of eCBs that decreases transmission from inhibitory stellate/basket cell synapses onto Purkinje cells for several seconds (DSI). DSE is found at parallel and climbing fibre inputs of Purkinje cells. Alternatively, local release of eCBs can be achieved via synaptic activation. High frequency parallel fibre stimulation can elevate dendritic calcium and lead to a mGluR1-dependent depression. This synaptically-evoked suppression of excitatory synapses requires calcium increases within Purkinje cell dendrites and is greatly reduced by inhibiting mGluR1 and eliminated when mGluR1 and ionotropic AMPA receptors (α-amino-3-hydroxyl-5-methyl-4-isoxazole-propionate receptors) are inhibited. Depolarization of one Purkinje cell not only inhibits its afferent inhibitory postsynaptic currents, but also those of other Purkinje cells sharing a common interneuron input. An important step during cerebellar motor learning involves the associative activation of climbing fibres and parallel fibres to induce LTD of parallel fibres to Purkinje cell synapses (Fig. 10).

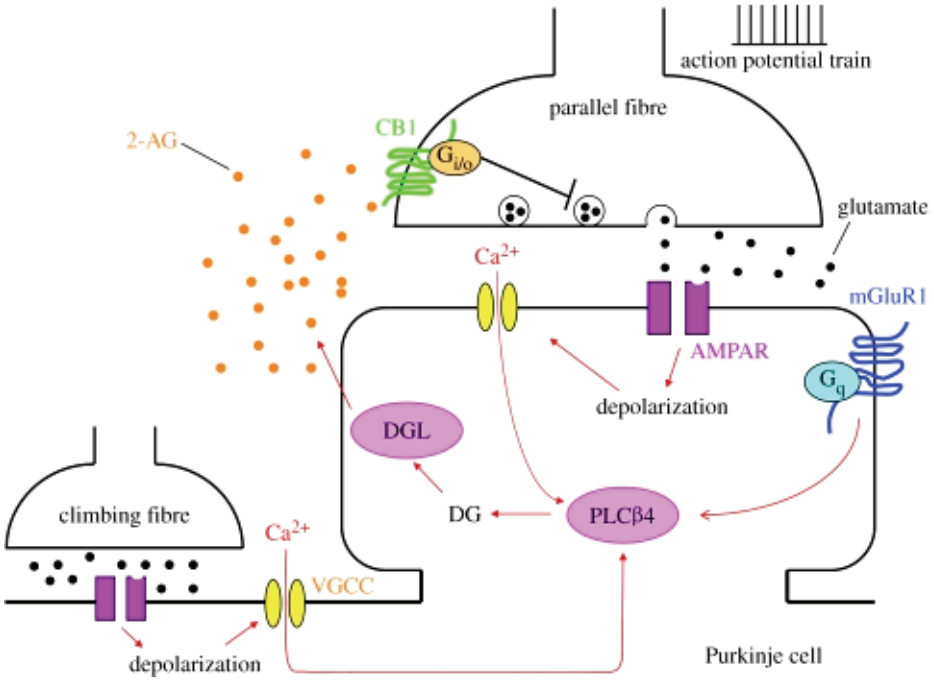

Figure 10. LTD of parallel fibres to Purkinje cell synapses.

In vitro studies report that although cerebellar cortex contains the highest level of CB1R in the brain, CB1R knockout mice are not ataxic and do not show profound motor deficits. This suggests that eCB-mediated synaptic modulation contributes to dynamic regulation of cerebellar output and motor learning without disrupting cerebellar function. CB1R knockout mice exhibit deficits in behaviours that rely on LTD. 2-AG stimulates cerebellar neuron neurite outgrowth through a mechanism dependent on DAGL activity within axonal growth cones, while CB1R antagonists abolish N-cadherin- and Fgf8-induced neurite extension (Williams,E.J. *et al*., 2003).

GABA is the major inhibitory neurotransmitter involved in cerebellar intrinsic and extrinsic nervous circuits, and cannabinoids are implicated in their modulation. Chronic treatment of pregnant rats with cannabinoids, at a dose devoid of effects on reproduction, development, and histomorphogenesis of cerebellar cortex, induces up-regulation of GABAergic neurotransmission in adult rats. In particular, GAD (glutamate decarboxylase) - 65/67 expression in GABA-synthesizing stellate and basket neurons of the molecular layer increases, along with GABA immunoreactivity. These authors concluded that prenatal exposures affect only the GABAergic stellate neurons and basket cells generated postnatally, because prenatal exposure manifests its effects mainly during the developmental period when

these cells are less differentiated and more susceptible to cannabinoid treatment (Benagiano,V. *et al*., 2007).

Cerebellar pathologies have been reported in neurodevelopmental neuropsychiatric disorders such as autism and schizophrenia. López-Gallardo *et al*. suggest that eCB system up-regulation can be an adaptive response to counteract the maternal deprivation-induced neuron degeneration and glial cell increase in postnatal male rats (Lopez-Gallardo,M. *et al*., 2008).

1.4 Chemical tools for studying CB receptor function.

CBR ligands are characterized by a wide chemical diversity. Among non-selective CBR agonists are CP 55,940 and the aminoalkylindole WIN 55,212-2. The latter is a chiral molecule, and the (S)-enantiomer displays micromolar activity at CBRs. It binds with similar affinity to native CB1 and CB2 receptors on cerebellar membranes, but has higher affinity for the cloned CB2R (Shim,J.Y. and Howlett,A.C. 2006). CP 55,940 potently inhibits cAMP accumulation in Chinese hamster ovary cells stably transfected with either the human CB1R and CB2R.

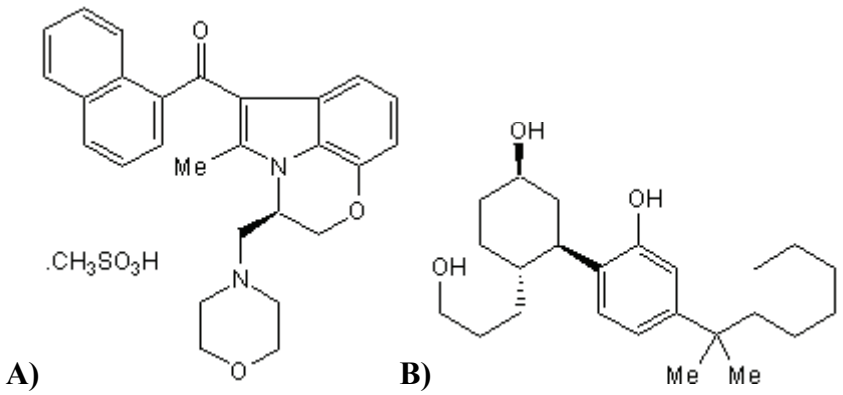

Figure 11. Structures of synthetic non-selective, high-affinity CBR agonists:
A) (R)-(+)-WIN 55,212-2, chemical name: (R)-(+)-[2,3-Dihydro-5-methyl-3-(4-morpholinylmethyl)pyrrolo[1,2,3-de]-1,4-benzoxazin-6-yl]-1-naphthalenylmethanone mesylate. **B) CP 55,940**, chemical name: (-)-*cis*-3-[2-Hydroxy-4-(1,1-dimethylheptyl)phenyl]-trans-4-(3-hydroxypropyl)cyclohexanol.

AEA analogs with a more hydrophobic amide head group bind to CB1R with greater affinity than the endogenous compound. ACEA is an AEA analog with improved CB1R selectivity

over the parent compound. The K_I value for ACEA is not significantly different from that for WIN 55,212-2 (Table 1), but both K_Is differ significantly from that of AEA. AEA and WIN 55,212-2 compete for [^{3}H]-CP 55,940 binding to CB2R in spleen, with WIN 55,212-2 having a higher affinity for CB2R than CB1R *vs* AEA. ACEA competes for [^{3}H]-CP 55,940 binding in rat spleen, but with low affinity relative to both AEA and its affinity for CB1R. ACEA at low nanomolar concentrations inhibits forskolin-stimulated AC activity in chinese hamster ovary cells stably transfected with human CB1R, but not with human CB2R. ACEA inhibits electrically induced contractions of mouse *vas deferens* at picomolar concentrations via activation of inhibitory CB1Rs on sympathetic nerve terminals. It induces the exchange GDP for GTP via CB1R activation, increasing the binding of the non-hydrolyzable GTP analog, [^{35}S]-GTPγS, with a potency similar to WIN 55,212-2 and greater than AEA. ACEA reduces rectal temperature in mice in a dose-dependent manner following intravenous administration (Hillard,C.J. *et al*., 1999).

JWH 133 is a potent CB2R-selective agonist (K_I = 3.4 nM), with approximatively 200-fold selective over CB1R.

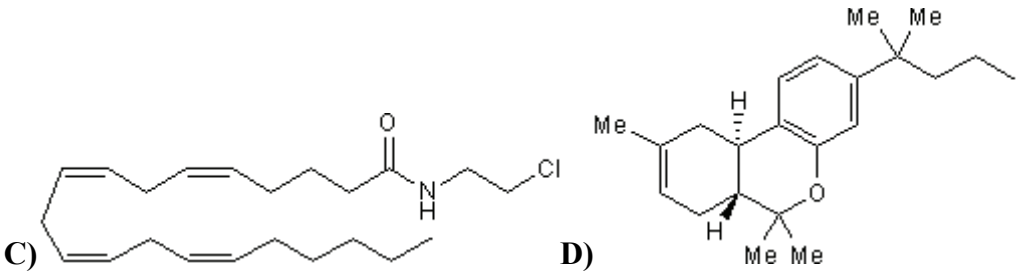

Figure 12. Structures of synthetic CBR selective agonists:
C) ACEA, alternative name: Arachidonyl-2'-chloroethylamide, chemical name N-(2-Chloroethyl)-5Z,8Z,11Z,14Z-eicosatetraenamide. **D) JWH 133**, chemical name: (6aR,10aR)-3-(1,1-Dimethylbutyl)-6a,7,10,10a-tetrahydro-6,6,9-trimethyl-6H-dibenzo[b,d]pyran.

Table 1. Affinities for CB1 and CB2 receptors:

Ligand	$K_{D/I}$, **CB1R**1-a	$K_{D/I}$, **CB2R**1-b	**Potency Ratio (CB2/CB1)**
	nM	nM	
CP 55,940	0.5 ± 0.1 (4)	2.8 ± 0.4 (4)	5.6
WIN 55,212-2	4.4 ± 1.3 (3)1-c	1.2 ± 0.25 (3)	0.27
AEA	71.7 ± 7.3 (4)1-d	279 ± 58 (3)1-d	3.9
ACEA	1.4 ± 0.3 (4)	> 2000 (2)	> 1400

1-a Affinities for the CB1R were determined either from saturation isotherms (CP 55,940) or from competition isotherms using [^{3}H]-CP 55,940 in rat cerebellar membranes. Membranes (10 μg of protein) were incubated with 0.5 to 1 nM [^{3}H]-CP 55,940 for 60 min at room temperature. **1-b** Affinities for the CB2R were determined either from saturation isotherms (CP 55,940) or from competition isotherms using [^{3}H]-CP 55,940 in rat spleen membranes. Membranes (10 μg of protein) were incubated with 0.5 to 1 nM [^{3}H]-CP 55,940 for 60 min at 30°C. **1-c** Data are shown as mean ± S.E.M. Numbers in parentheses, indicate number of replicate experiments. **1-d** Significantly different from KD for CP 55,940 at $p < 0.05$ using Tukey's test (Hillard,C.J. *et al*., 1999).

AM 251 is representative of CB1R-selective antagonists/inverse agonists (IC_{50} = 8 nM, K_I = 7.49 nM), and displays 306-fold selectivity over CB2R.

AM 630 is a CB2R-selective antagonist/inverse agonist (K_I = 31.2 nM) that displays 165-fold selectivity over CB1R. It behaves as a weak partial/inverse agonist at CB1R.

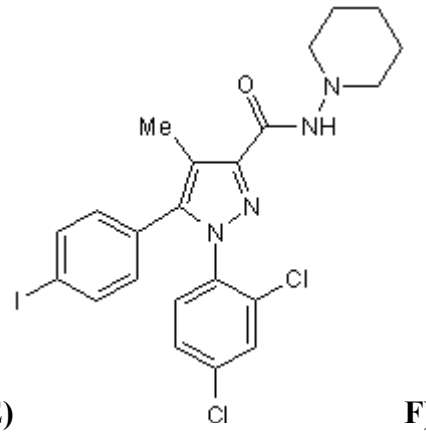

E)

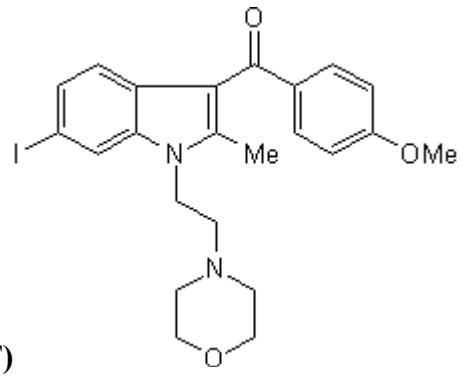

F)

Figure 13. Structures of synthetic selective CBR antagonists.
E) AM 251, chemical name: N-(Piperidin-1-yl)-5-(4-iodophenyl)-1-(2,4-dichlorophenyl)-4-methyl-1H-pyrazole-3-carboxamide. **F) AM 630**, chemical name: 6-Iodo-2-methyl-1-[2-(4-morpholinyl)ethyl]-1H-indol-3-yl](4-methoxyphenyl)methanone.

In some CBR-containing systems AM 251 was found to produce "inverse cannabimimetic effects", that is, opposite from those produced by CBR agonists. AM 251 is reported to induce inhibition of basal G-ptotein activity in rat cerebellar membranes, to enhance electrically-evoked glutamate release from rat cerebellar neurons and electrically-evoked GABA release from rat hippocampal neurons, and to increase Ca^{2+} currents and decrease inward rectifier potassium currents in human embryonic kidney 293 cells. Many authors have found that AM 251 exhibits greater potency in opposing effects induced by CB1R agonists than in producing inverse effects at CB1R. Pertwee has suggested two possible explanations for this: first, AM 251 may be a neutral CB1R antagonist at low concentrations and behave as an inverse agonist only at higher concentrations; second, there may be two different sites of action at CB1R, one at which it displaces agonists to produce antagonism, and another at which it induces inverse agonism, through an allosteric mechanism (Pertwee,R.G. 2005).

1.5 An *in vitro* model of multipotent neural progenitor cells isolated from early postnatal rat cerebellum.

Given the existence of a protracted postnatal neurogenesis in the cerebellum, Zusso *et al.* (Zusso,M. *et al*., 2004) sought to establish a procedure to isolate and culture neural progenitors from cerebellum. Primary cultures of neural progenitors were obtained by culturing cerebellar granule cells (CGC) in gelatin-coated dishes in a serum-free medium with bFGF and EGF to maintain a mitotic and undifferentiated state. Under these conditions, glial cells attach to the gelatin substratum, while neurons remain suspended in the medium and die after several days. At 2-3 days *in vitro* (DIV) neural progenitors, initially attached to the substratum, became hypertrophic, phase-bright, proliferated (5-6 DIV) and, upon formation of small clusters, lifted off the substratum and floated in suspension (10-12 DIV). These cerebellar neural progenitors display the cardinal features of stem/precursor cells. Immunocytochemical analysis at 10 DIV demonstrates immunoreactivity for the neural markers nestin, Tuj1, and PSA-NCAM. They partially possess a self-renewal property, being unable to proliferate in the long-term: the number of these neural precursor cells increases for a few passages when subcultured at 10 DIV. Cerebellar neural progenitors cultured in a differentiating medium (Eagle's Basal Medium + 10% fetal bovine serum), without bFGF and EGF on a poly-D-lysine substratum can differentiate into neurons, astrocytes, and oligodendrocyte

AIM OF THE THESIS

The cannabinoid system has recently been shown to increase proliferation of neural precursor cells in the subventricular zone and subgranular layer. Although the molecular mechanisms underlying this effect are not fully understood, it is becoming evident that endogenous cannabinoid lipid mediators (endocannabinoids) are involved in the regulation of neural progenitor proliferation and neurosphere generation acting through the metabotropic cannabinoid receptor CB1. The CB1R is highly expressed in the CNS (neocortex, hippocampus, basal ganglia, cerebellum, and brainstem), where cannabinoids act as neuromodulators at presynaptic CB1R to elicit changes in the synaptic efficacy of neuronal circuits. The presence and function of cannabinoid CB2 receptors in the CNS have been demonstrated in the brainstem and cortex.

Neural progenitors isolated from rat postnatal cerebellum will be used as an *in vitro* model of neural cell proliferation to test whether a proliferative response can be induced by synthetic CBR agonist treatment. The neural progenitors will be characterized for the presence of CBRs, utilizing real time RT-PCR and Western blotting. Subsequently, a [^{3}H]-thymidine incorporation assay will be used to assess a proliferative response mediated by CB1R activation. Finally, immunoblotting using phospho-specific antibodies for two major signaling pathway kinases, Akt and ERK, will be carried with the aim of elucidating the cellular and molecular mechanisms underlying the cannabinoid neurogenic action.

CHAPTER 2

MATERIALS AND METHODS

2.1 MATERIALS

2.1.1 Reagents and culture supplies.

General chemicals were obtained from Sigma Aldrich (St. Louis, MO, USA) except where indicated. CBR agonists and antagonists, growth factors, and kinase inhibitors were purchased from Tocris Bioscience (Ellisville, Missouri, USA), unless indicated otherwise. Cell culture media and supplements were purchased from Invitrogen Life Technologies (Milan, Italy). Tissue culture plastic ware was obtained from Falcon (San Jose, CA, USA). Glass tips and pipettes were sterilized by autoclaving (30 minutes at 121°C under 101.325 kPascal (Pa) (=standard atmosphere).

2.1.2 Cell culture media and reagents.

2.1.2.1 Cell culture solutions.

Solution A:

12 mM NaCl
0.5 mM KCl
0.12 mM KH_2PO_4
1.4 mM glucose
2.5 mM $NaHCO_3$
0.5 % (v/v) phenol red
0.05 mM $MgSO_4$
0.3 % (w/v) bovine serum albumin (BSA)
distilled water to a final volume of 250 ml

Solution B:

0.25 mg/ml Trypsin in Solution A

Solution C:

2.4 mg DNase I (Roche Diagnostics, Germany)
15.6 mg trypsin inhibitor
11.1 mg $MgSO_4$
30 ml Solution A

Solution D:

4 ml Solution A
21 ml Solution C

Solution E:

$1.2x10^{-3}$ M $MgSO_4 \cdot 7H_2O$
$9.6x10^{-5}$ M $CaCl_2 \cdot 2H_2O$
25 ml Solution A

Solutions were filter sterilised through a Millipore filter (Millipore Corporation, Bedford, MA), 0.22 μm pore size, and stored at 4°C.

Borate Buffer (0.15 M, pH 8.4):

4.635 g H_3BO_3
3.0 g NaOH
500 ml distilled water
The pH was adjusted to 8.4 with 1 M HCl

Poly-D-Lysine (100X):

Poly-D-Lysine (MW 30-70 kDa) was dissolved in 0.15 M borate buffer, pH 8.4, at 2 mg/ml final concentration and filter sterilised through a Millipore filter, 0.22 μm pore size, and stored at 4°C.

2% Gelatin:

2 g of gelatin (type B: from bovine skin) were dissolved in 100 ml of distilled water. The solution was autoclaved and stored at 4°C.

2.1.2.2 Cell culture media.

Growth medium (100 ml):

95.8 ml Neurobasal medium

25 mM KCl

2 mM L-glutamine

2 ml B27 supplement

50 μg/ml gentamicin

20 ng/ml basic fibroblast growth factor (bFGF; Sigma Aldrich, St. Louis, MO, USA)

20 ng/ml epidermal growth factor (EGF; Sigma Aldrich, St. Louis, MO, USA)

Differentiation medium (100 ml) (According to Skaper *et al*., 1990) (Skaper, S.D. *et al*., 1990)**:**

87.9 ml eagle's basal medium (BME; Sigma Aldrich, St. Louis, MO, USA)

25 mM KCl

2 mM L-glutamine

50 μg/ml gentamicin

10 ml heat-inactivated fetal calf serum

2.1.2.3 [^{3}H]-thymidine solution (50X).

$3.7x10^5$ Becquerel (Bq)/ml [^{3}H]-thymidine (GE Healthcare Life Sciences, Milan, Italy; TRK120) was diluted to $0.185x10^5$ Bq/ml in sterile phosphate-buffered saline (PBS).

2.1.2.4 Chemical compounds.

5 mM ACEA:

ACEA (N-(2-Chloroethyl)-5Z,8Z,11Z,14Z-eicosatetraenamide) supplied pre-dissolved in ethanol at a concentration of 5 mg/ml, was diluted in anhydrous ethanol at a final concentration of 5 mM. Stock solutions were aliquoted in tightly sealed vials and stored at -20°C. To be used within 1 month.

5 mM AM 251:

2.7762 mg of AM 251 (N-(Piperidin-1-yl)-5-(4-iodophenyl)-1-(2,4-dichlorophenyl)-4-methyl-1H-pyrazole-3-carboxamide) were dissolved in 1 ml anhydrous ethanol at a final concentration of 5 mM. Stock solutions were aliquoted in tightly sealed vials and stored at -20°C. To be used within 1 month.

5 mM AM 630:

2.52185 mg of AM 630 (6-Iodo-2-methyl-1-[2-(4-morpholinyl)ethyl]-1H-indol-3-yl](4-methoxyphenyl)methanone) were dissolved in 1 ml DMSO at the final concentration of 5 mM. Stock solutions were aliquoted in tightly sealed vials and stored at -20°C. To be used within 1 month.

100 µg/ml Brain-Derived Neurotrophic Factor (BDNF):

10 µg of BDNF (PeproTech EC, UK) were dissolved in 100 µl PBS containing 1% w/v BSA and stored as working aliquots at -20°C for 3 months.

5 mM CP 55,940:

1.92795 mg of CP 55,940 ((-)-cis-3-[2-Hydroxy-4-(1,1-dimethylheptyl)phenyl]-trans-4-(3-hydroxypropyl)cyclohexanol) was dissolved in 1 ml anhydrous ethanol to a final concentration of 5 mM. Stock solutions were aliquoted in tightly sealed vials and stored at -20°C. To be used within 1 month.

5 mM JWH 133:

1.56245 mg of JWH 133 ((6aR,10aR)-3-(1,1-Dimethylbutyl)-6a,7,10,10a-tetrahydro-6,6,9-trimethyl-6H-dibenzo[b,d]pyran) was dissolved in 1 ml DMSO to a final concentration of 5 mM. Stock solutions were aliquoted in tightly sealed vials and stored at -20°C. To be used within 1 month.

10 mM LY294002:

1.5 mg of LY294002 (Methyl N-[(2-hydroxynaphthalen-1-yl)-(phenyl)methyl]carbamate, Cell Signaling Technology, Inc., MA, USA) was reconstituted in 488 µl DMSO to a final concentration of 10 mM, and aliquots stored at -20°C.

25 mM U0126:

9.512 mg of U0126 (1,4-Diamino-2,3-dicyano-1,4-bis[2-aminophenylthio]butadiene) were dissolved in 1 ml DMSO to a final concentration of 25 mM. Aliquots were stored at -20°C and used within one month.

5 mM WIN 55,212-2 mesylate:

2.6581 mg of WIN 55,212-2 mesylate ((R)-(+)-[2,3-Dihydro-5-methyl-3-(4-morpholinylmethyl)pyrrolo[1,2,3-de]-1,4-benzoxazin-6-yl]-1-naphthalenylmethanone mesylate) were dissolved in 1 ml ethanol to a final concentration of 5 mM. Aliquots were stored at -20°C and used within one month.

2.1.3 Immunofluorescence solutions.

Phosphate Buffered Saline with Triton (PBS-T) (100 ml):

0.1 ml Triton X100 (Sigma Aldrich, St.Louis, MO, USA)

99.9 ml PBS

(3%) BSA:

3 g BSA (Sigma Aldrich, St.Louis, MO, USA)

100 ml PBS-T

2.1.4 SDS-PAGE (Sodium Dodecyl Sulphate-Polyacrylamide Gel Electrophoresis) **solutions.**

Cell lysis buffer:

Solution I:

1% (v/v) Triton X100

0.5% (w/v) SDS

0.75% (w/v) deoxycholic acid

10 mM Trizma base, pH 7.4

75 mM NaCl

10 mM EDTA

Solution II (prepared fresh and kept on ice)**:**

5 ml solution I

0.5 mM PMSF (phenylmethylsulfonyl fluoride)

2 mM Na_3VO_4

10 µg/ml leupeptin

25 µg/ml aprotinin

1.25 mM NaF

1 mM Na-pyrophosphate ($Na_2H_2P_2O_7$)

4 ml distilled water

5X Laemmli sample buffer: 16ml:

6.8 ml distilled water

2 ml 0.5 M Tris pH 6.8

3.2 ml glycerol

1.6 ml 20% (w/v) SDS

0.8 ml β-mercaptoethanol

1.6 ml 1% (w/v) bromophenol blue

10% Resolving gel (5 ml):

2.3 ml distilled water

1.3 ml 40% (w/v) acrylamide-N,N'-methylenebisacrylamide

1.3 ml 1.5 M Tris pH 8.8

50 µl 10% (w/v) SDS

50 µl 10% (w/v) ammonium persulfate ($(NH_4)_2S_2O_8$)

5 µl N,N,N',N'-Tetramethylethylenediamine (TEMED)

5% Stacking gel (4 ml):

2.87 ml distilled water

0.5 ml 40% (w/v) acrylamide- N,N'-methylenebisacrylamide

0.5 ml 1 M Tris pH 6.8

40 µl 10% (w/v) SDS

40 µl 10% (w/v) ammonium persulfate

5 µl TEMED

2.1.5 Western blotting solutions.

SDS-PAGE reservoir buffer: 1 liter (1X):

3 g Trizma base (25 mM)
18.8 g glycine (250 mM)
0.1% (w/v) SDS
distilled water to make 1 liter

Electroblotting transfer buffer: 1 liter (1X):

3 g Trizma base (25 mM)
14.4 g glycine (192 mM), pH 8.3
distilled water to make 1 liter

Tris buffered saline with Tween-20 (TBS-T) (1X):

1.21 g Trizma base (50 mM), pH 7.6
8.75 g NaCl (150 mM)
0.1% (v/v) Tween-20
distilled water to make 1 liter

Blocking solution:

3 g BSA
100 ml TBS-T

Stripping solution (50 ml):

0.905 ml β-mercaptoethanol
10 ml 10% (w/v) SDS
3.125 ml 1 M Tris, pH 6.7
46.875 ml distilled water

2.1.6 Immunocytochemistry solutions.

Paraformaldehyde: 4% (w/v) paraformaldehyde in PBS, pH 7.4

2.1.7 Solutions for total RNA extraction.

TRIzol® Reagent (Invitrogen, Milan, Italy)
Chloroform
Isopropyl alcohol
Ethanol

RNase-free water:

0.01% (v/v) diethylpyrocarbonate (DEPC)
Autoclaved distilled water in RNase-free glass bottles

2.1.8 Agarose gel electrophoresis of nucleic acids.

Tris-acetate-EDTA (TAE) (50X):

40 mM Tris-acetate
1 mM EDTA (pH 8.0)

Running buffer:

0.8 mM Trizma base
20 mM Glacial acetic acid
0.02 mM EDTA (pH 8.0)
0.1 mg/ml Ethidium bromide

Ethidium bromide is an intercalating fluorescent compound used as nucleic acid stain for both double-stranded DNA and single-stranded RNA. When excited at 260 nm wavelength it emits fluorescence at 590 nm.

2.1.9 Enzymes and buffers for reverse transcription reaction.

75 ng/µl Random examers

10 mM deoxyribonucleotide triphosphates (dNTP) Mix (10 mM each dATP, dGTP, dCTP and dTTP at neutral pH)

5X First-Strand Buffer (250 mM Tris-HCl, pH 8.3, 375 mM KCl, 15 mM $MgCl_2$)

0.1 M Dithiothreitol (DTT)

RNase OUT Recombinant Ribonuclease Inhibitor (40 units/µl); storage buffer: 20 mM Tris-HCl (pH 8.0), 50 mM KCl, 0.5 mM EDTA, 8 mM DTT, and 50% (v/v) glycerol.

SuperScript™ III Reverse Transcriptase (200 units/µl); storage buffer: 20 mM Tris-HCl (pH 7.5), 100 mM NaCl, 0.1 mM EDTA, 1 mM DTT, 0.01% (v/v) NP-40, 50% (v/v) glycerol.

sterile distilled water to 20 µl

All the reagents were supplied by Invitrogen, Milan, Italy.

SuperScript™ III Reverse Transcriptase is an engineered version of M-MLV (Moloney Murine Leukemia Virus) RT (Reverse Transcriptase) with reduced RNase H activity and increased thermal stability. The enzyme is purified to near homogeneity from *E. coli* (*Escherichia coli*) containing the modified *pol* gene of M-MLV. The enzyme can be used to synthesize first-strand complementary DNA (cDNA) at temperatures up to 55°C, providing increased specificity, higher yields of cDNA, and more full-length products than other reverse transcriptases. It can generate cDNA from 100 bp to >12 kb.

2.1.10 Polymerase chain reaction (PCR) reagents.

10X PCR Buffer (Tris-Cl, KCl, $(NH_4)_2SO_4$, 15 mM $MgCl_2$; pH 8.7 (20°C))

25 mM $MgCl_2$

dNTP mix (10 mM of each)

HotStarTaq DNA Polymerase (5 units/µl)* (Qiagen, Milan, Italy); storage and dilution buffer containing: 20 mM Tris-Cl, 100 mM KCl, 1 mM DTT, 0.1 mM EDTA, 0.5% (v/v) Nonidet® P-40, 0.5% (v/v) Tween® 20, 50% glycerol (v/v), stabilizer; pH 9.0 (20°C).

*One unit of HotStarTaq Polymerase corresponds to the amount of enzyme that will incorporate 10 nmol of dNTP into acid-insoluble material within 30 min at 72°C.

All reagents were supplied by Invitrogen (Milan, Italy).

2.1.11 Real Time quantitative PCR (qPCR) reagents.

SYBRGreen JumpStart Taq ReadyMix (Sigma-Aldrich, St. Louis, MO, USA): 20 mM Tris-HCl, pH 8.3, 100 mM KCl, 7 mM $MgCl_2$, 0.4 mM each dNTP (dATP, dCTP, dGTP, TTP), stabilizers, 0.05 unit/ml Taq DNA Polymerase, JumpStart Taq

antibody, and SYBR Green I.

ROX (6-carboxy-X-rhodamine)

RNase-free water

The JumpStart Taq antibody inactivates the DNA polymerase at room temperature; heating at 70°C in the first denaturation step of the cycling process dissociates the complex and the polymerase becomes fully active. Internal Reference Dye ROX is provided for reaction normalization. Maximum excitation of this dye is 586 nm and maximum emission is 605 nm.

2.2 METHODS

2.2.1 PRIMARY CULTURES OF RAT POSTNATAL CEREBELLAR GRANULE CELLS.

2.2.1.1 Coverslip coating.

12 mm diameter glass coverslips were flamed with absolute ethanol and then transferred to sterile 24-well plates, and coated with 500 µl of 20 µg/ml Poly-D-Lysine solution for 45 min at room temperature. The coating solution was then removed and the plates maintained in the 37°C incubator until used.

2.2.1.2 Preparation of rat cerebellar granule cell (CGC) cultures.

CGC cultures were prepared from 7-day-old Sprague-Dawley rats (P7) as described previously (Skaper, S.D. *et al*., 1990). Cerebella were removed under aseptic conditions, following decapitation. The tissue was placed in a sterile 60 mm-dish with solution A to prevent the tissue from drying out. The cerebellum was freed of associated meninges with the aid of a dissecting microscope. Following solution A removal, the tissue was minced with a flamed razor blade and collected with solution A into a 15 ml tube and centrifuged at 200 g for 1 min.

The supernatant was removed with a pasteur pipette and 1 ml/cerebellum of 0.25% trypsin in solution B was added. After 15 min incubation at 37°C with gentle shaking, trypsin action was stopped by adding 1 ml/cerebellum of 0.25% trypsin inhibitor in solution D. The tissue was collected by centrifugation at 800 g for 3 min and the supernatant removed. The cerebellar tissue was dissociated 25 times with a flamed pasteur pipette, in the presence of 2 ml of solution C, after which time 3 ml of the same solution were added and an additional 15 trituration strokes performed. To the cell suspension were then added 6 ml of solution E and this centrifuged at 200 g for 7 min. The supernatant was then removed and the cells suspended in 14 ml of culture medium. To assess the number of viable cells obtained, 90 µl of cell suspension was added to an equal volume of 0.4% trypan blue and cells counted using a hemacytometer.

$7x10^5$ trypan blue-excluding cells, in a volume of 0.5 ml of culture medium/well, were plated in poly-D-lysine coated 24-well plates with 12 mm glass coverslips. Cultures were incubated at 37°C in a humidified atmosphere with 5% CO_2. Experiments were performed on granule cells at 8 days in vitro (DIV).

2.2.2 PRIMARY CULTURES OF RAT POSTNATAL CEREBELLAR NEURAL PROGENITOR CELLS.

2.2.2.1 Preparation of coverslip coating.

12 mm glass coverslips were flamed with absolute ethanol and transferred to sterile 24-well plates. Multi-well plates were coated with 2% gelatin solution for 2 h at 37°C. Afterwards the solution was aspirated and the 24-well plates were left to dry under a laminar air flow hood, and kept in the 37°C incubator until taken for cell plating.

2.2.2.2 Isolation of cerebellar neural progenitor cells.

CGC were plated in gelatin-coated dishes in a serum-free medium with bFGF and EGF to maintain a mitotic and undifferentiated state (growth medium). Under these conditions, glial cells attach to the gelatin substratum, while neurons remain suspended in the medium and die after several days. At 2-3 DIV neural progenitors, initially attached to the substratum, become hypertrophic, phase-bright, proliferate (5-6 DIV) and, upon formation of small clusters, lift off the substratum and float in suspension (10-12 DIV).

2.2.3 CELLULAR PROLIFERATION ASSAY.

2.2.3.1 Cellular proliferation assay: [^{3}H]-thymidine incorporation.

Cerebellar neural progenitor cells at 10 DIV were incubated at 37°C with $3.7x10^2$ Bq/ml [^{3}H]-thymidine (Zusso,M. *et al*., 2004) for increasing periods of time (24-72 h). Subsequently, the cell suspension contained in each well was collected in distinct vials and centrifuged at 200 g for 5 min to remove excess radionuclide. Cells were washed with PBS and processed on a cell harvester equipped with Whatman® glass microfiber filters, Grade GF/C (Sigma Aldrich, St.

Louis, MO, USA). Samples were washed six times with PBS. Filters were allowed to dry and the radioactivity was counted in a liquid scintillation β counter (Fiszman,M.L. *et al*., 1999), and expressed as a percentage of the corresponding vehicle control (PBS, ethanol, DMSO).

2.2.4 Cerebellar neural progenitor differentiation

Cerebellar neural progenitors at 10 DIV were collected, mechanically dissociated to a single-cell suspension, and then plated on poly-D-lysine-coated glass coversplips (12 mm), and cultured in differentiation medium. Cultures were fixed (4% paraformaldehyde) 2, 4, and 6 days after plating and processed for immunocytochemistry (see below).

2.2.5 IMMUNOCYTOCHEMICAL ANALYSIS.

Cerebellar neural progenitors at 10 DIV were harvested, mechanically dissociated to obtain a single cell suspension and centrifuged at 200 g for 5 min. Following supernatant removal, cells were resuspended in few µl of PBS and the suspension divided among multiple cover glasses to obtain single spots. Cerebellar neural progenitors were fixed with 4% paraformaldehyde for 15 min at room temperature, washed 3x5 min in PBS and processed for immunocytochemistry according to the same protocol used for CGC grown on poly-D-lysine-coated glass coverslips. Following fixation and washing in PBS, CGC and neural progenitor cells were permeabilized with PBS-T at room temperature for 15 min and incubated with PBS-T containing 3% (w/v) BSA for 1 h, to avoid antibodies bind aspecific sytes. Cell samples were incubated at room temperature for 1 h in the presence of one or more primary antibodies (Table 2). Following washing in PBS 3x5 min, cells were incubated at room temperature for 1 h, in the presence of the appropriate secondary antibody-fluorophore conjugate, diluted in blocking solution: goat anti-rabbit (1:1000, AlexaFluor488, Molecular Probes, USA), or goat anti-mouse (1:1000, AlexaFluor594, Molecular Probes, USA). Following washing in PBS 3x5 min, all samples were incubated at 37°C for 3 min with a 100 ng/ml 4'-6'-diamidino-2-phenylindole (DAPI) (Boehringer, Mannheim, Germany) methanol solution, a nuclear fluorescence stain. Cells were then washed twice in methanol and twice in distilled water. Cover glasses were mounted onto glass slides using "Mowiol mounting media" (VWR International, Milan, Italy), and were imaged using a digital camera (DC 200; Leica

Imaging Systems, Cambridge, UK) connected to a fluorescence microscope (DMR, Leica), or by confocal microscopy.

Table 2. Primary antibodies for immunocytochemistry

Protein	**Antibody**	**Dilution**
microtubule-associated protein 2 (MAP2) (Millipore Corporation, Bedford, MA)	rabbit polyclonal	1:1000
glial fibrillar acidic protein (GFAP) (Millipore Corporation, Bedford, MA)	rabbit polyclonal	1:1000
caveolin (610059, BD Transduction Laboratories)	rabbit policlonal	1:100
β-tubulin type III (Tuj1) (Millipore Corporation, Bedford, MA)	mouse monoclonal	1:500
β-COP (β-coatomer protein) (Sigma Aldrich St. Louis, MO, USA)	mouse monoclonal	1:100
neurofilament (NF) (Millipore Corporation, Bedford, MA)	rabbit polyclonal	1:300
CB1R (H-150) (Santa Cruz Biotechnology, Inc., USA)	rabbit polyclonal	1:100
CB2R (H-60) (Santa Cruz Biotechnology, Inc., USA)	rabbit polyclonal	1:100

2.2.6 PROTEIN ANALYSIS.

2.2.6.1 Protein extraction and quantification.

Cell extracts were prepared by lysing cells on ice in an appropriate volume of solution II, for 30 min at 4°C. Lysates were then centrifuged at 12,000 g for 15 min at 4°C. The Bradford method (Bradford,M.M. 1976) was used to determine sample protein concentration: protein binding to Coomassie Brilliant Blue G-250 under acidic conditions shifts the dye's absorbance peak from 465 nm to 595 nm. A calibration curve is made for each assay with serial dilutions of a 1 mg/ml BSA solution.

2.2.6.2 SDS-polyacrylamide gel electrophoresis.

Protein lysates were resuspended in Laemmli buffer (1:5) and denaturated at 100°C for 5 min. Equal amounts of protein (15 µg/lane) were size fractionated by SDS-PAGE (10%) according to Laemmli (Laemmli,U.K. 1970). In the same gel a molecular weight marker was loaded (Full Range Rainbow Molecular Weight Markers, GE Healthcare Life Sciences, Milan, Italy), and run in 1X running buffer at a constant current of 15 mA (Bio-Rad 200, power supply).

2.2.6.3 Western blotting.

Resolved proteins were transferred from SDS-PAGE gels to polyvinylidene difluoride membranes (PVDF) (Amersham Biosciences), previously activated by soaking in methanol. The gel was sandwiched together with the membrane between Whatman paper, two porous pads (all equilibrated in transfer buffer for few minutes), and two plastic supports. The blot "sandwich" was placed into the Mini-Transblot electrophoresis system (Bio-Rad Laboratories Ltd.) filled with 1X transfer buffer and the membrane facing the anode. A constant current of 200 mA was applied at 4°C for a time necessary to complete the blot transfer, and depended on protein molecular weight and gel thickness. Membranes were blocked in TBS-T buffer containing 3% (w/v) BSA at room temperature for 45 min. Membranes were gently agitated overnight at 4 °C with primary antibodies diluted in 3% (w/v) BSA in TBS-T. Primary antibodies used are listed in Table 3. Membranes were next washed 3x5 min in TBS-T at room temperature and incubated for 1 h with a goat anti-mouse horseradish peroxidase

(HRP)-conjugated or goat anti-rabbit HRP-conjugated secondary antibody (Millipore Corporation, Bedford, MA) diluted in TBS-T with 3% (w/v) BSA. Membranes were then washed 3x5 min in TBS-T, and immunoreactivity detected using enhanced chemiluminescence (ECL) (GE Healthcare Europe GmbH, Milan, Italy). Chemiluminescence was detected using Hyperfilm-ECL (GE Healthcare Europe GmbH, Milan, Italy). The film was developed in GBX developer (Sigma Aldrich, St. Louis, MO, USA), and then transferred to GBX fixer fixing solution (Sigma Aldrich, St. Louis, MO, USA).

To detect total protein for loading control, stripping was carried out as follows: membranes used for phospho-kinase analysis were stripped of antibody signal using a stripping solution, for 5 min at 50°C, then washed with 1X TBS-T (3x10 min) and incubated for 30 min at room temperature in blocking solution. The membranes were then incubated for 1 h at room temperature with the primary antibodies against total proteins diluted in blocking solution (Table 3). After 3x10 min wash in 1X TBS-T membranes were incubated for 1 h at room temperature with secondary antibody. Visualization was carried out as described above. Band densities were semi-quantified using the Image-J software program (freely downloaded from the National Institutes of Health website). The optical densities of the phospho-protein bands were corrected relative to the density of the corresponding total protein band.

Table 3. Primary antibodies for Western blotting.

Protein	**Antibody**	**Dilution**
CB1R (H-150) (Santa Cruz Biotechnology, Inc., USA)	rabbit polyclonal	1:100
CB2R (H-60) (Santa Cruz Biotechnology, Inc., USA)	rabbit polyclonal	1:100
Akt1/2/3 phosphorylated (Ser473) (Santa Cruz Biotechnology, Inc., USA)	rabbit polyclonal	1:1000
Akt1/2/3 (H-136) (Santa Cruz Biotechnology, Inc., USA)	rabbit polyclonal	1:1000
ERK1/2 phosphorylated (E-4) (Santa Cruz Biotechnology, Inc., USA)	mouse monoclonal	1:1000
ERK1 (K-23) (Santa Cruz Biotechnology, Inc., USA)	rabbit polyclonal	1:1000

2.2.7 RNA methodology.

2.2.7.1 Total RNA extraction.

TRIZOL® Reagent was used for total RNA isolation from cells grown in monolayer or in suspension, according to the manufacturer's instructions. The reagent is a mono-phasic solution of phenol and guanidine isothiocyanate, which maintains RNA integrity during sample homogenization while disrupting cells and dissolving cell components. Cells were pelleted by centrifugation (200 g for 5 min), and lysed in TRIZOL® Reagent by repetitive pipetting. After homogenization, samples were incubated for 5 min at room temperature to permit the complete dissociation of nucleoprotein complexes. Two hundred microlitres of chloroform per 1 ml of TRIZOL® were added, the samples shaken manually for 15 seconds, and re-incubated at room temperature for few min. Samples were then centrifuged at 11,000 g for 15 min at 4°C to separate the mixture into 3 phases: a lower red, phenol-chloroform organic phase containing proteins, an interphase containing DNA, and a colorless upper aqueous phase containing RNA. The aqueous phase was transferred to fresh vials and RNA precipitated by mixing with an equal volume of isopropyl alcohol (0.5 ml of isopropyl alcohol per 1 ml of TRIZOL® Reagent, approximately). Samples were incubated at 4°C for 15 min and centrifuged at 12,000 g for 15 min at 4°C. RNA appeared as a gel-like pellet, and the supernatant was removed. RNA was washed with 75% ethanol in RNAse-free water (1 ml ethanol per 1 ml TRIZOL®) and centrifuged at 11,000 g for 15 min at 4°C. Afterwards, RNA was briefly air-dried, then dissolved in RNAse-free water and stored at -80°C.

2.2.7.2 Preparation of RNA sample prior to RT-PCR.

Duplicate tubes were prepared, as positive and negative reverse transcriptase (RNA) samples were to be used in the amplification reaction. To avoid DNA contamination all samples were treated for 15 min at room temperature with Deoxyribonuclease I, Amplification Grade (Invitrogen, Milan, Italy). To a RNase-free, 0.5-ml microcentrifuge tube were added the following:

17 µl RNA sample

2 µl 10X DNase I Reaction Buffer (200 mM Tris-HCl pH 8.4, 20 mM $MgCl_2$, 500 mM KCl)

1 µl DNase I, Amp Grade, 1U/µl

DEPC-treated water to 10 µl

DNase I was inactivated by the addition of 2 µl of 25 mM EDTA solution (pH 8.0) (Invitrogen, Milan, Italy) to the reaction mixture. DNase was completely denatured by heating at 70°C for 15 min.

2.2.7.3 Agarose gel electrophoresis of RNA for quality determination.

Agarose (Ultra pure, electrophoresis grade, Invitrogen, Milan, Italy) was dissolved in boiling 1X TAE buffer. The gel was than cast on a gel bed with a suitable comb using a horizontal gel apparatus. Gel was placed in an electrophoresis tank containing 1X TAE buffer to a level just above the gel surface. For gel electrophoresis, to each RNA sample was added 0.62 mM Ficoll 400 (Sigma Aldrich, St.Louis, MO), a highly branched sucrose and epichlorohydrin copolymer that acts as a stabilizer in the electrolyte, and 4µg/ml Orange G sodium salt (Sigma Aldrich, St.Louis, MO), as tracking dye for nucleic acid gel electrophoresis. During electrophoresis an electrical potential difference of 6 V/cm was applied to the gel. Gel was then placed on a 3UV transilluminator for viewing. A single fluorescent band near the loading lane is assigned to high molecular weight RNA, while a fluorescent smear directed to the anode suggests partial or total RNA degradation.

2.2.7.4 RNA spectrophotometric quantification.

The yield of total RNA was determined by measuring the spectrophotometric absorption at 260 nm. The absorbance of RNA samples at 260 nm and 280 nm, diluted in sterile distilled water, was used to evaluate protein contamination (A_{260}/A_{280} ratio). A_{260} should be higher than 0.15, with an absorbance of 1 unit at 260 nm corresponding to 40 µg RNA per ml. This relation is valid only for measurements at neutral pH. The A_{260}/A_{280} ratio was determined and used to assess the purity of the sample.

The concentration of RNA purified was calculated by the following equation:

[RNA] in µg/µl=(A_{260} x D)/1000

Where 1 optical density unit is equivalent to 40 µg/ml single-stranded RNA, and D is the dilution factor.

2.2.8 RT-PCR.

2.2.8.1 First-Strand cDNA Synthesis.

Retrotranscription reaction mixture was prepared in a final volume of 20 µl.

The following components were added to a nuclease-free microcentrifuge tube:

2 µl 75 ng/µl Random examers

1 µl 10 mM dNTP Mix

10 µl total RNA

The mixture was heated to 65°C for 6 min for primer annealing and incubated on ice for at least 1 min. To the tubes was then added:

4 µl 5X First-Strand Buffer

1 µl 0.1 M DTT

1 µl RNase OUT

1 µl SuperScript™ III Reverse Transcriptase

Retrotranscription reaction was performed at 50°C for 70 min and inactivated by heating at 75°C for 15 min. cDNA was used as a template for amplification in PCR.

2.2.8.2 PCR Reaction.

cDNA samples were amplified using HotStarTaq® DNA Polymerase in a MX 3000P Thermal Cycler (Stratagene, La Jolla, USA). All reaction mixtures were prepared in an area separate from that used for DNA preparation, and disposable tips containing hydrophobic filters were used to minimize cross-contamination.

PCR mix composition:

1.25 µl 10X PCR Buffer

0.25 µl 25 mM $MgCl_2$

0.25 µl dNTP mix

500 nM Forward Primer

500 nM Reverse Primer

2.5 units/reaction HotStarTaq DNA Polymerase

1 µl cDNA

DEPC water to 11.5 µl

A negative control (without template DNA) was always included to evaluate accidental reagent contamination.

Each PCR program started with an initial heat activation step at 95°C for 15 min and a final extension step at 72°C for 7 min. The cycling program was optimized for each template target and primer pair.

Table 4. RT-PCR primer pairs.

Gene	Primer sequence (5′-3')	Melting temperature (Tm) and PCR extension time (seconds)	PCR cycle number
AUF1	F: CGACGCCAGTAAGAATGAGG R: TGATGACCACCTCGTCTGGA	58°C, 30 s	30

PCR products were identified loading them into the wells in a 3% agar gel for electrophoresis.

2.2.8.3 DNA amplification efficiency assessment.

Many substances are known RT-PCR inhibitors and may compromise DNA amplificability: haemoglobin, urea, humic acid, citric acid, polysaccharides, bilirubin, heparin, DNA extraction reagent residues, chelants, Triton X-100, and sodium dodecyl sulfate (Wilson,I.G. 1997). Amplification of a fragment of glyceraldehyde 3-phosphate dehydrogenase (GAPDH) was used as a control for DNA quality and amplificability. Non-amplificable sample DNA was re-extracted and the amplification of the GAPDH house-keeping gene was repeated. To specifically amplify a 165 base pair (bp), the GAPDH fragment primers reported in Table 5 were used. The PCR mix composition and program are described belove.

2.2.9 REAL TIME QUANTITATIVE PCR.

Real Time PCR allows one to measure the amount of PCR product after each round of amplification, making use of a fluorescent label that binds to the accumulating DNA molecules. Fluorescence values are recorded during each cycle of the amplification process. The fluorescent signal is directly proportional to the DNA concentration. The linear correlation between PCR products and fluorescence intensity is used to calculate the amount of template present at the beginning of the reaction. Within the exponential increase phase, the point upon the amplification baseline at which the detected fluorescence is significant higher than the background signal is called the threshold cycle or Ct Value; it is inversely correlated to the logarithm of the initial DNA copy number. At the threshold level it is assumed that all reactions contain an equal number of specific amplicons.

As a qPCR detection method the fluorescent binding dye SYBR® Green I was used: it binds all double-stranded DNA (dsDNA). After excitation at 497 nm, an increase in emission fluorescence at 520 nm results during the polymerization step followed by a decrease as DNA is denatured. Fluorescent measurements are taken at the end of the elongation step of each PCR cycle. SYBR® Green I binds non-specifically to any dsDNA, which results in non-specific fluorescence. Non-specific binding yields fluorescence readings in the "no template control" (NTC) due to dye molecules binding to primer dimers and misprimed products. The specificity of qRT-PCR was tested in reaction without reverse transcriptase (no-RT control) to evaluate the specificity of DNA amplification, with DNase-digested RNA.

qPCR was performed in a final volume of 12.5 µl.

Reaction mix composition:

6.25 µl SYBRGreen JumpStart Taq ReadyMix
0.125 µl ROX
200 nM Forward Primer
200 nM Reverse Primer
1 µl cDNA
DEPC water to 12.5 12.5 µl

Typical thermal profile: initial denaturation (94°C, 2 min), 45 cycle denaturation (95°C, 30 s), primer annealing (55°C, 30 s), and elongation (72°C, 40s) steps, followed by a final denaturation step (72°C, 7 min).

To test reaction efficiency, a standard curve was generated performing qPCR with a serial dilution of template containing the PCR target, and extending past both the highest and lowest levels of target expected in test samples.

Table 5. Real Time RT-PCR primer pairs.

Gene	Primer sequence (5′-3')	Tm and PCR extension time (seconds)	PCR cycle number
GAPDH	F: CAAGGTCATCCATGACAACTTTG R: GGGCCATCCACAGTCTTCTG	55°C, 30 s	45
CB1R	F: CATCATCATCCACACGTCAG R: ATGCTGTTGTCTAGAGGCTG	58°C, 60 s	45
CB2R	F: CCTCCTGGGCTGGCTTCT R: AGCAGCCTGGTGTTCTGGA	58°C, 60 s	45

2.2.10 STATISTICAL ANALYSIS

Results are given as means ± standard deviation (SD). For statistical analysis of variance (ANOVA) was followed by the Bonferroni's *post-hoc* test for multiple comparisons. The probability level chosen was $p < 0.05$.

CHAPTER 3

RESULTS

3.1 Rat postnatal cerebellum and cerebellar neural progenitors express CBR gene transcripts.

The expression of cannabinoid CB1 and CB2 receptors both in rat postnatal cerebellum (P7) and cerebellar progenitor cells at 10 DIV was investigated (Fig. 14). Sample total RNA was extracted and real-time RT-PCR reaction was performed using specific CBR primer pairs as described in Table 5. The expression levels of CB1 and CB2 receptors were compared.

CB1R/CB2R ratio is 1.91 ± 0.09 and 1.33 ± 0.14 in rat postnatal cerebellum and cerebellar neural progenitor cells, respectively.

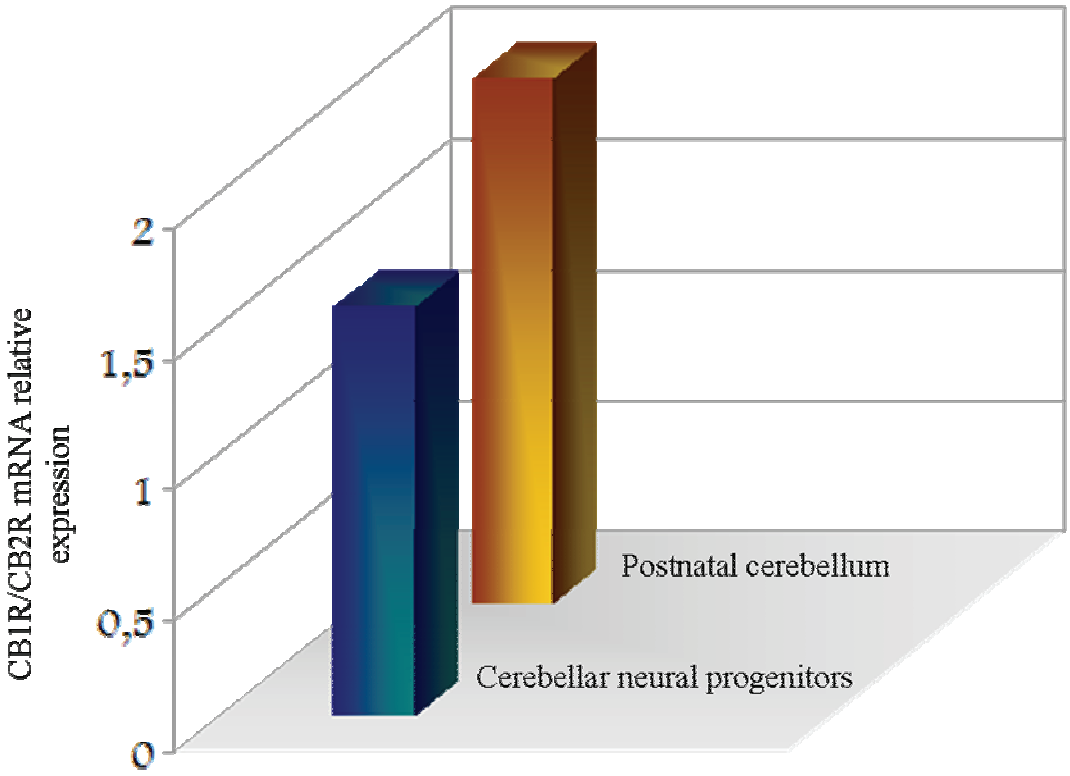

Figure 14. Rat postnatal cerebellum and cerebellar neural progenitor cultures express CBR gene transcripts. Total RNA was extracted and real time RT-PCR was performed with specific CBR primer pairs. CB1R and CB2R mRNA levels were evaluated. Data are expressed as CB1R/CB2R ratio.

3.2 Cerebellar neural progenitors express CBR proteins.

The expression of CB1 and CB2 receptor proteins in cerebellar neural progenitors was detected by Western blot analysis (Fig. 15) and immunocytochemistry (Fig. 16). Cell protein lysates were separated by SDS-PAGE (10%) and transferred to PVDF membranes. Membranes were incubated with rabbit polyclonal antibody anti-CB1R or –CB2R. Following incubation with a goat anti-rabbit HRP-conjugated secondary antibody, immunoreactivity was detected using the ECL development method. The presence of CB1R was shown by two immunostained bands with molecular masses of ~ 55 and ~ 60 kDa (Fig. 15A), respectively, consistent with Song and Howlett (Song,C. and Howlett,A.C. 1995). The antibody anti-CB1R (H-150) maps at the N-terminus of the receptor which is reported to have three potential N-

glycosylation sites. The 64 kDa band is suggested to correspond to the mature glycosylated protein, while the 53 kDa band corresponds to the non-glycosylated form. The antibody anti-CB2R (H-60) maps at the C-terminus of the receptor. Three major bands at 45, 55, and 60kDa were detected (Fig. 15B), in agreement with Van Sickle *et al*. (Van Sickle,M.D. *et al*., 2005).

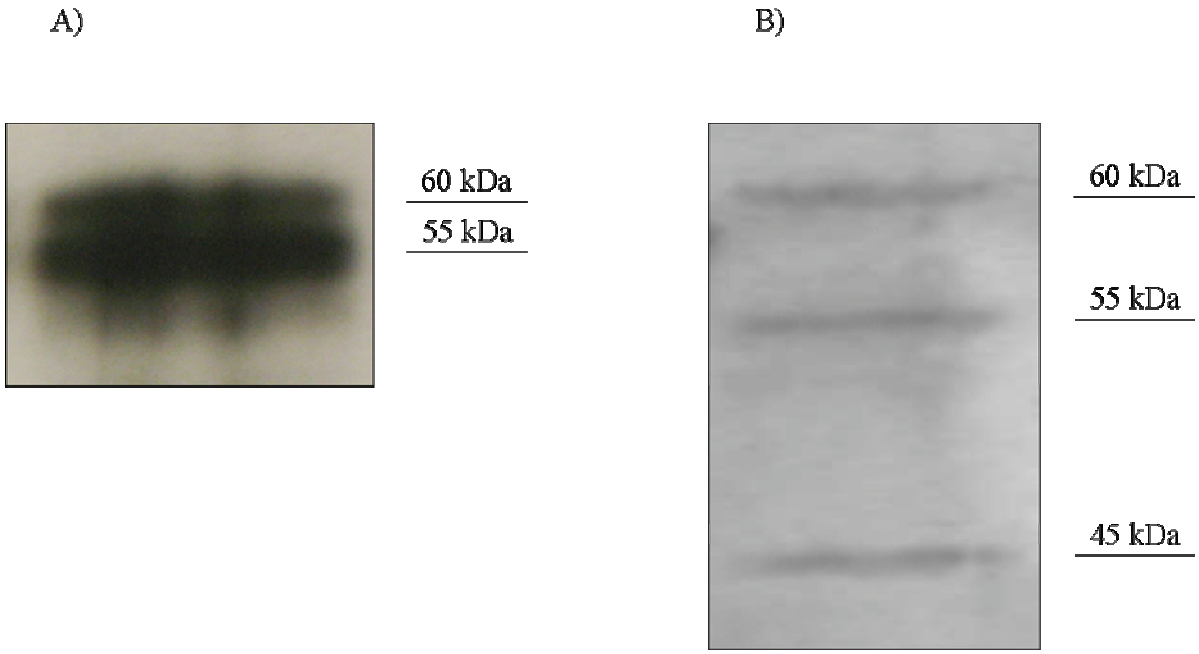

Figure 15. Cerebellar neural progenitors express CBR proteins. Cerebellar neural progenitor cells at 10 DIV were processed by SDS-PAGE and Western blotting: A) CB1R bands at 64 and 53 kDa; B) CB2R bands at 60, 55, and 45 kDa.

Similarly, confocal microscopy revealed cerebellar neural progenitor expression of both CBRs (Fig. 16). Cerebellar neural precursor cells at 10 DIV were fixed with 4% paraformaldehyde and stained with antibody against Tuj1 (Fig. 16I) and CB1 (Fig. 16II) or CB2 (Fig. 16III) receptor. Following incubation with a secondary antibody-fluorophore conjugate, images of different planes of a single Z-stack were acquired by a confocal microscope. CB2R punctate immunolabeling distribution *vs* CB1R prompted an investigation of the existence of a functionally distinct localization. First, the presence of CB1R at the caveolae lipid raft level was assessed, as suggested by recent literature reports. Caveolae are specialized microdomains implicated in numerous cellular processes including signal transduction, membrane trafficking, and molecular sorting, and provide additional significance for CBRs. Double immunostaining of cerebellar neural progenitors with the polyclonal antibody anti-caveolin (Fig. 17I) and anti-CB1R (Fig. 17II) mapping the N-terminus of the protein was performed and images were acquired by confocal microscopy. Images corresponding to the same distinct optical sections of a single Z-stack highlight the expression of caveolin 1 in cerebellar neural progenitors and a partial co-localization with CB1R (Fig. 17III). Double immunostaining with anti-caveolin (Fig. 18I) and anti-CB2R (Fig. 18II) does not permit one to assign with certainty a localization of the latter in lipid rafts because of an aspecific overlapping of the two immunolabelings (Fig. 18III), attributable to the polyclonal anti-CB2R antibody. This problem could not be avoided either by inverting the order of staining or by using the mouse monoclonal antibody anti-flotillin 1, raised against another protein enriched in detergent-resistant domains of the plasma membrane rich in sphingolipids and cholesterol. The immunocytochemical method applied (see paragraph 2.2.5) demonstrates this cellular system is not immunoreactive for flotillin 1 (data not shown).

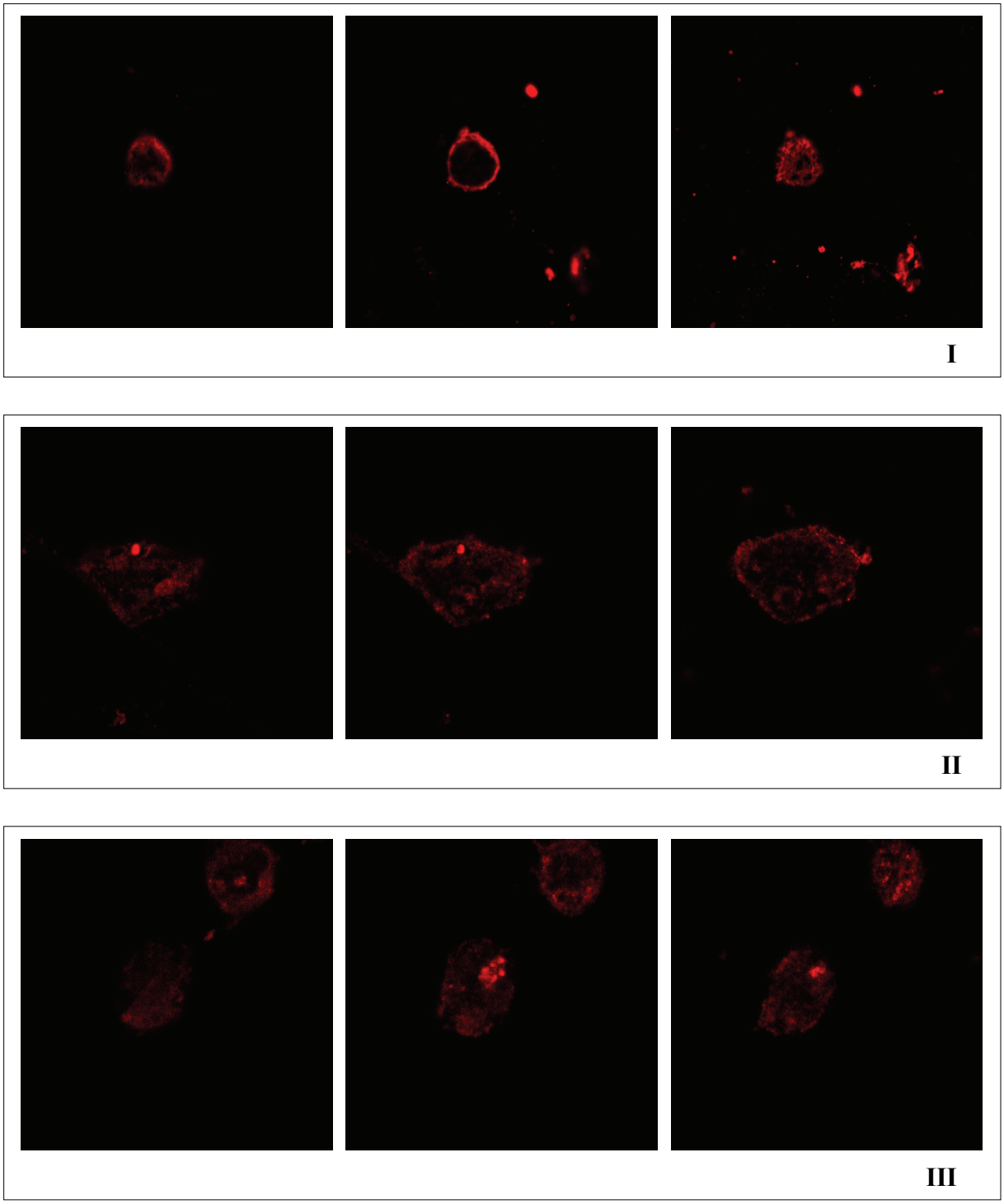

Figure 16. Confocal microscopy showing CBR expression in rat cerebellar neural progenitor cell cultures at 10 DIV. Images of each panel correspond to three different planes of a Z-stack. Cerebellar neural progenitors were fixed with 4% paraformaldehyde and stained with antibodies against Tuj1 (panel I), CB1R (panel II), and CB2R (panel III).

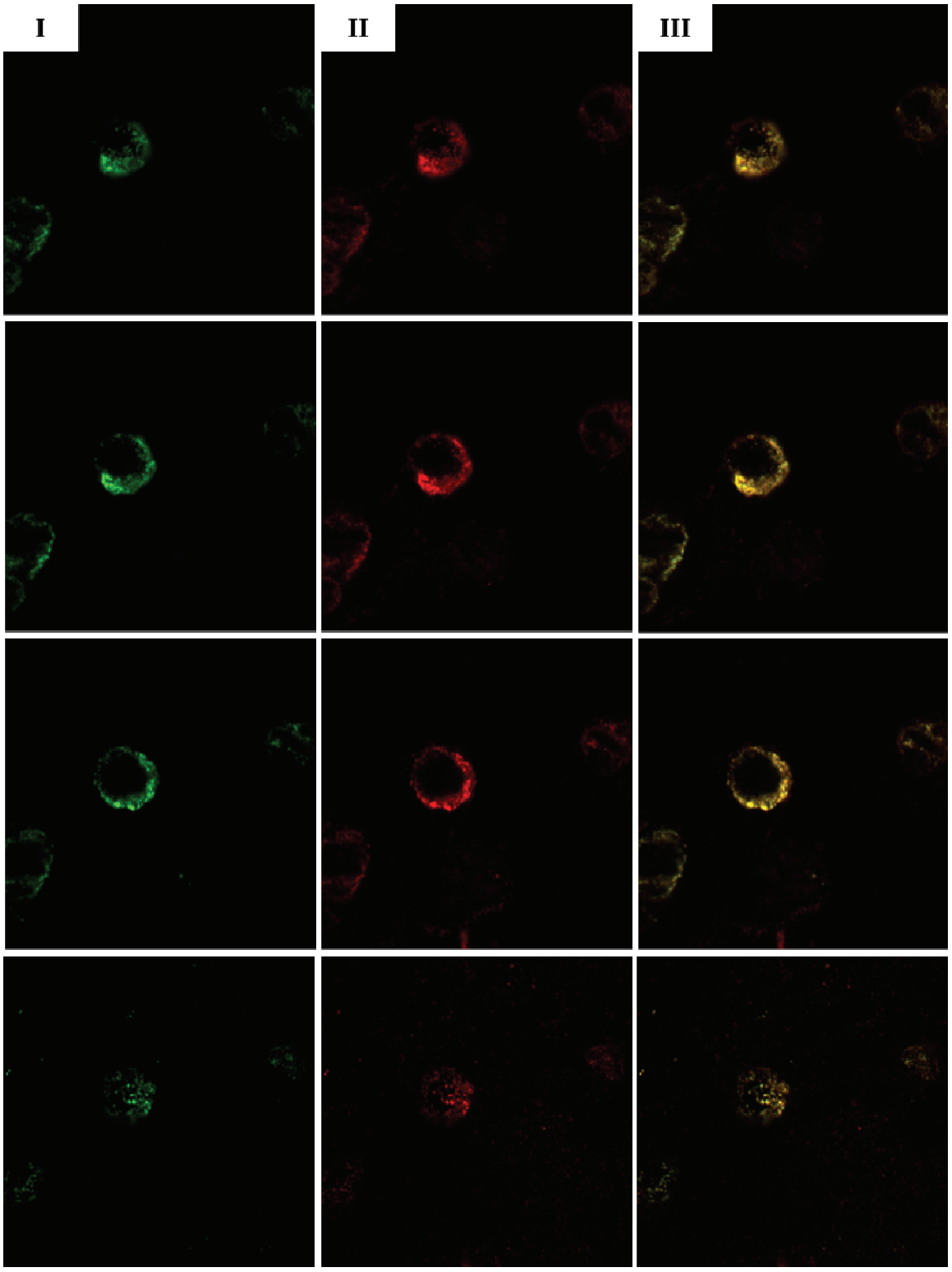

Figure 17. Confocal microscopy showing caveolin-1 and CB1R expression in rat cerebellar neural progenitor cell cultures at 10 DIV. Images of each panel correspond to three different planes of a single Z-stack. Cerebellar neural progenitors were fixed with 4% paraformaldehyde and stained with antibodies anti-caveolin (panel I) and CB1R (panel II). Panel III: merge.

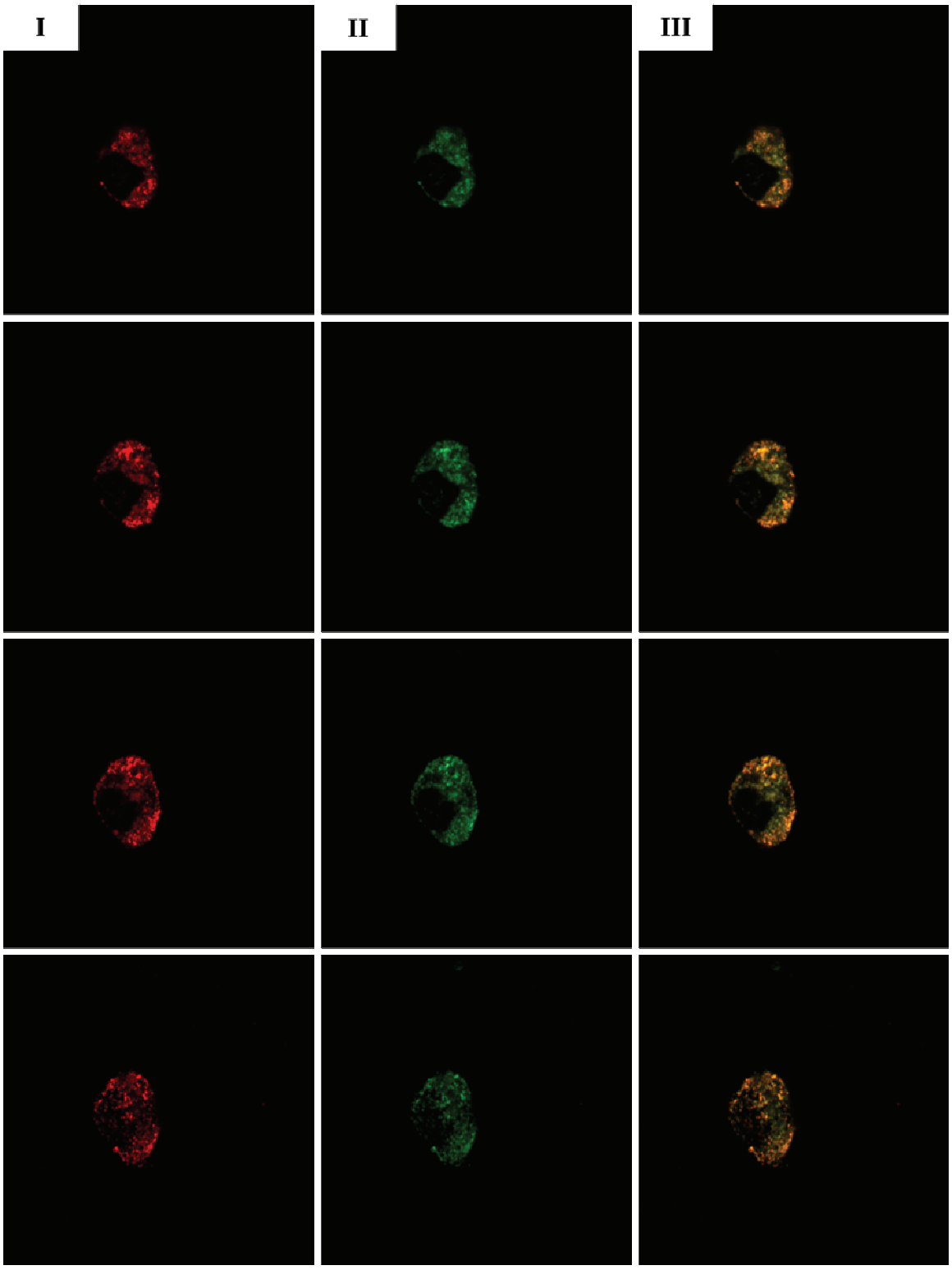

Figure 18. Confocal microscopy showing caveolin-1 and CB2R expression in rat cerebellar neural progenitor cell cultures at 10 DIV. Images of each panel correspond to three different planes of a single Z-stack. Cerebellar neural progenitors were fixed with 4% paraformaldehyde and stained with antibodies anti-caveolin (panel I) and CB2R (panel II). Panel III: merge.

To assess whether CB2R could have a neosynthetic origin being localized, at least in part, at the Golgi or secretory pathway level, cerebellar granule cells were stained with the antibody directed against β-COP (Fig. 19); β-COP is a 110 kDa non-clathrin-coated vesicle-associated coat protein that stains the periphery of the Golgi complex, being involved in vesicle transport between the endoplasmic reticulum and the Golgi apparatus. The morphological structure of cerebellar neural progenitors and particularly the spread Golgi distribution (Fig. 19) did not permit further analysis of co-localization of this structure with CB2R.

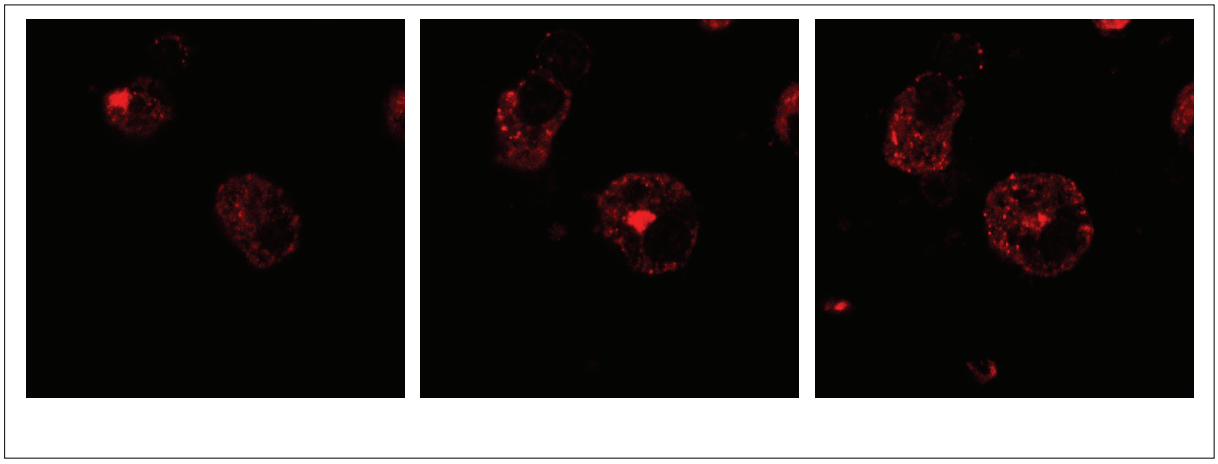

Figure 19. Confocal microscopy showing Golgi expression in rat cerebellar neural progenitor cell cultures at 10 DIV. Panel images correspond to three different planes of a Z-stack. Cerebellar neural progenitors were fixed with 4% paraformaldehyde and stained with antibodies anti-β-COP.

3.3 Cerebellar neural progenitors under differentiation conditions still retain CB1 and CB2 receptor expression.

Many authors focused on the presence of the eCB system from the earliest stages of embryonic development and throughout pre- and postnatal development, and its involvement in the control of neurogenesis, neural progenitor proliferation, lineage segregation, and the migration, and phenotypic specification of immature neurons.

To assess if multipotent cerebellar neural progenitor cells retain the expression of CBR protein in differentiation conditions, they were collected at 10 DIV and induced to differentiate by culturing them on a Poly-D-Lysine substratum, in eagle's basal medium + 10% fetal calf serum, according to Skaper *et al*. (Skaper,S.D. *et al*., 1990). After 2, 4, and 6 days cells were fixed with 4% paraformaldehyde and double-stained with specific antibodies

against CB1 or CB2 receptor and the neuronal protein MAP2 or the glial protein GFAP (Fig. 20-23); DAPI blue fluorescent dye was used to stain nuclei.

Immunocytochemical anlysis of CB1 and CB2 receptors in P7 rat cerebellar granule cell cultures was used as positive control (Fig. 24); CGC at 8 DIV were fixed with 4% paraformaldehyde and stained with antibodies against β-COP (Fig. 24IA, II, and III), CB1R (Fig. 24IB, II) and CB2R (Fig. 24IC, III), MAP2 (Fig. 24IID, IIID) or NF (Fig. 24IIE, IIIE) as neuronal markers, and GFAP (Fig. 24IIF, IIIF) as glial marker. Nuclei were stained with propidium iodide (red) (Fig. 24I). Fluorescent photographs show CGC express both CBRs (Fig. 24IB, IC) which partially co-localize with the Golgi region, in both neurons and glial cells (Fig. 24II, III). Cerebellar neural progenitors induced to differentiate for 2 days express the neuronal protein MAP2 (Fig. 20IB, 21IB) and both CB1 (Fig. 20IC) and CB2 (Fig. 21IC) receptors. Following 4 (Fig. 20II; Fig. 21II) and 6 (Fig. 20III; Fig 21III) days of differentiation an increase in neuronal phenotype (Fig. 20IIB, IIIB; Fig. 21IB, IIIB) and presence of the cannabinoid proteins (Fig. 20IIC, IIIC; Fig. 21IIC, IIIC) is detectable, whilst CB1R immunostaining fluorescence (Fig.20IIC, IIIC) is more intense than the CB2R immunolabeling (Fig. 21IIC, IIIC). From the 2^{nd} to the 6^{th} differentiation day (Fig. 22B; Fig. 23B) immunofluorescence images show a progressive maturation of $GFAP^{+}$ cells. This labeling signal is strong from the beginning, because these neural cerebellar progenitors spontaneously tend to differentiate first to a glial phenotype. The photographs show that CB1R (Fig. 22C) and CB2R (Fig. 23C) staining in glial cells is much less intense than in $MAP2^{+}$ cells.

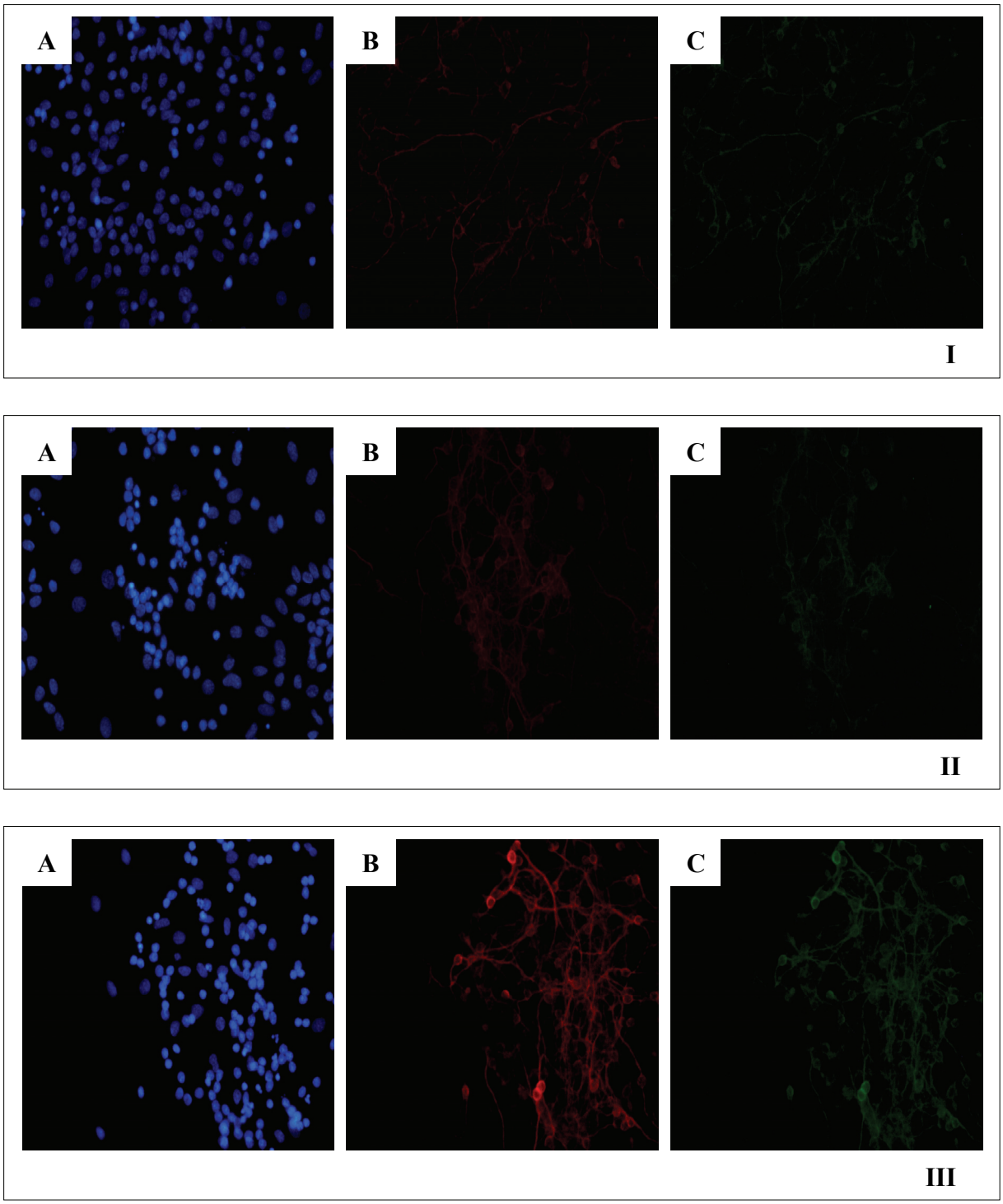

Figure 20. Immunocytochemical analysis of MAP2 and CB1R expression in rat cerebellar progenitors cultured under conditions which lead to their differentiation (Skaper *et al*., 1990), and using a poly-D-lysine coating. Following 2 (panel I), 4 (panel II), and 6 (panel III) differentiation days, cells were fixed with 4% paraformaldehyde and stained with antibodies anti-MAP2 (B), and anti-CB1R (C).

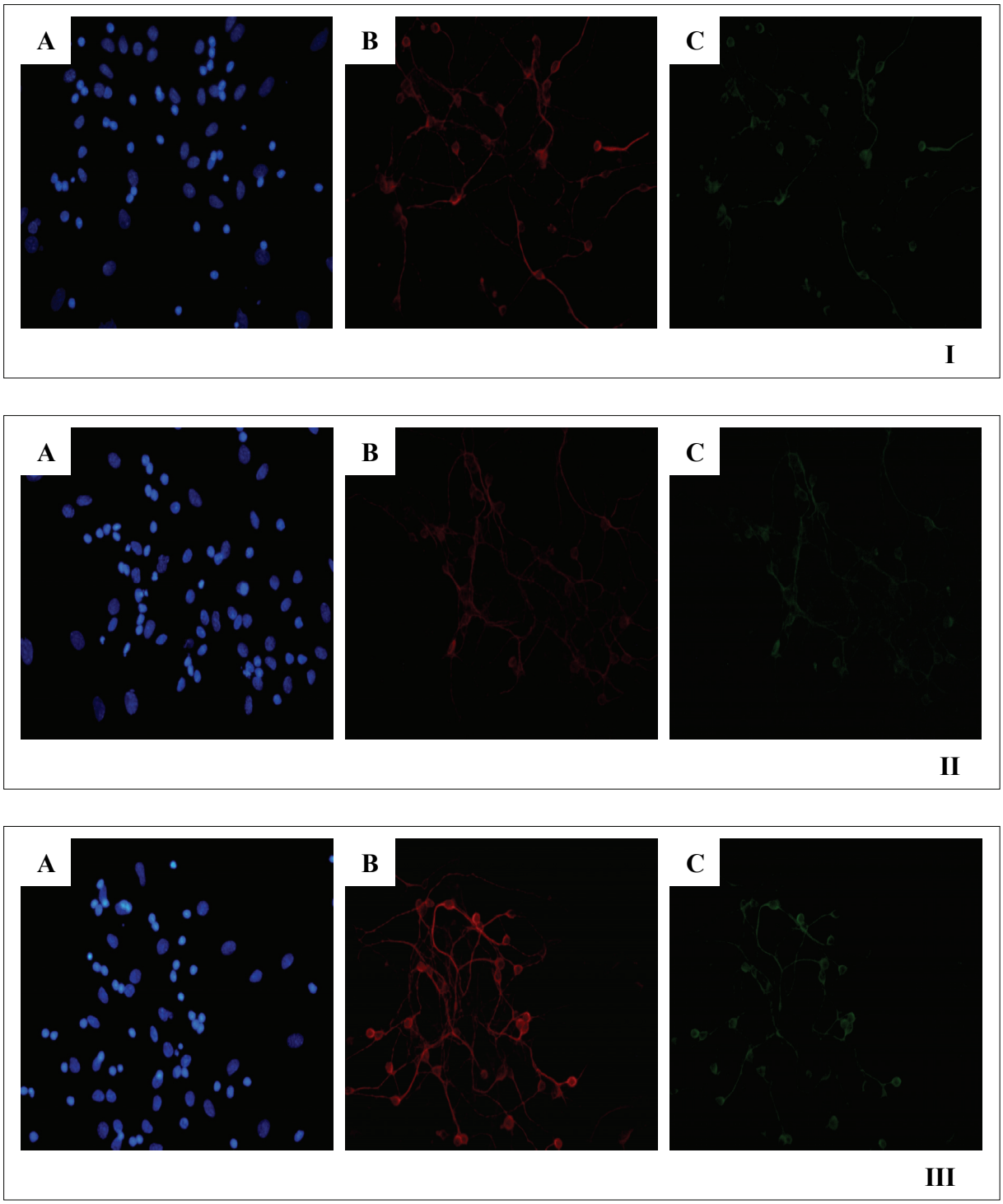

Figure 21. Immunocytochemical analysis of MAP2 and CB2R expression in rat cerebellar progenitors cultured under conditions which lead to their differentiation (Skaper *et al*., 1990), and using a poly-D-lysine coating. Following 2 (panel I), 4 (panel II), and 6 (panel III) differentiation days, cells were fixed with 4% paraformaldehyde and stained with antibodies anti-MAP2 (B), and anti-CB2R (C)

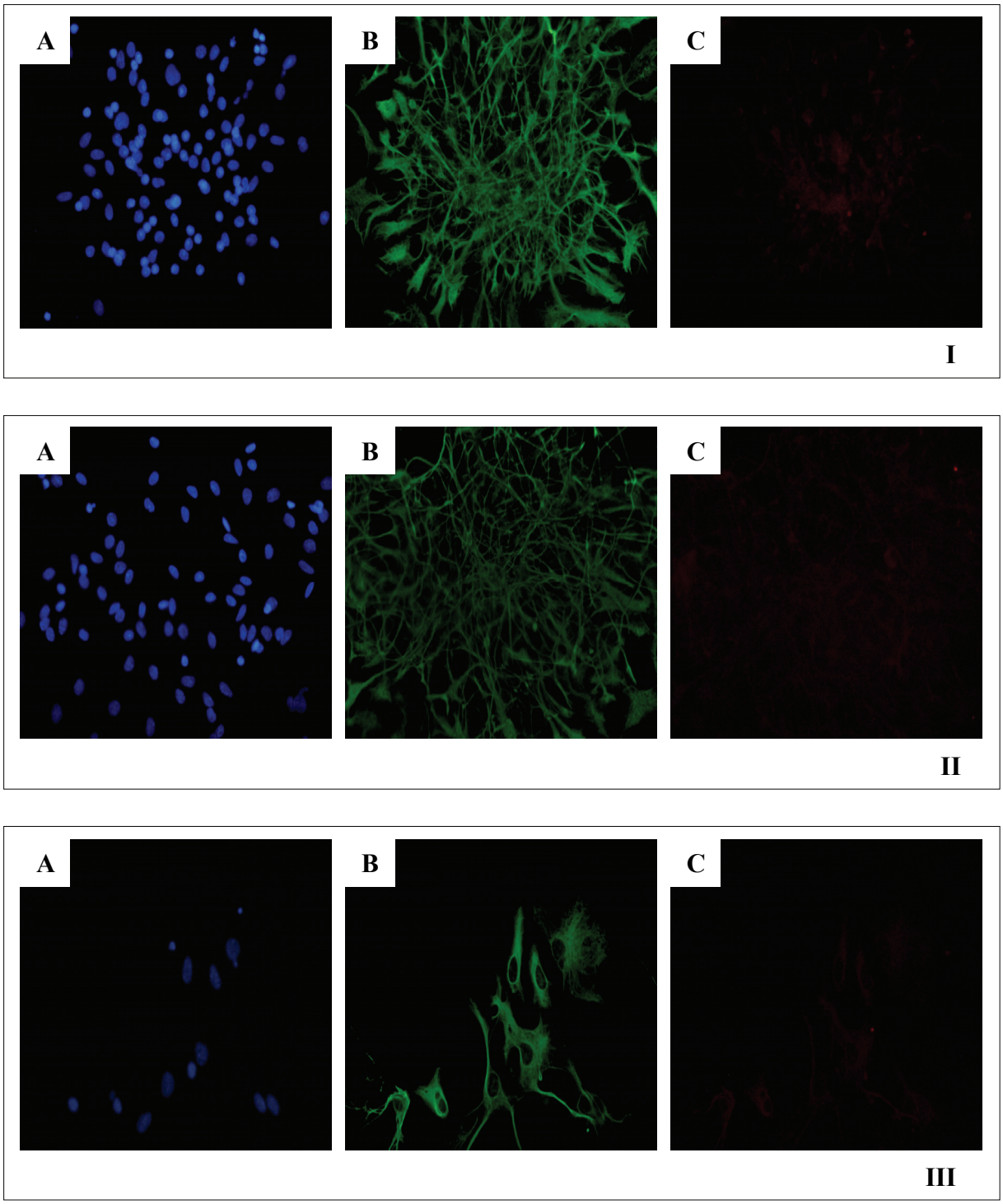

Figure 22. Immunocytochemical analysis of GFAP and CB1R expression in rat cerebellar progenitors cultured under conditions which lead to their differentiation (Skaper *et al*., 1990), and using a poly-D-lysine coating. Following 2 (panel I), 4 (panel II), and 6 (panel III) differentiation days, cells were fixed with 4% paraformaldehyde and stained with antibodies anti-GFAP (B), and anti-CB1R (C).

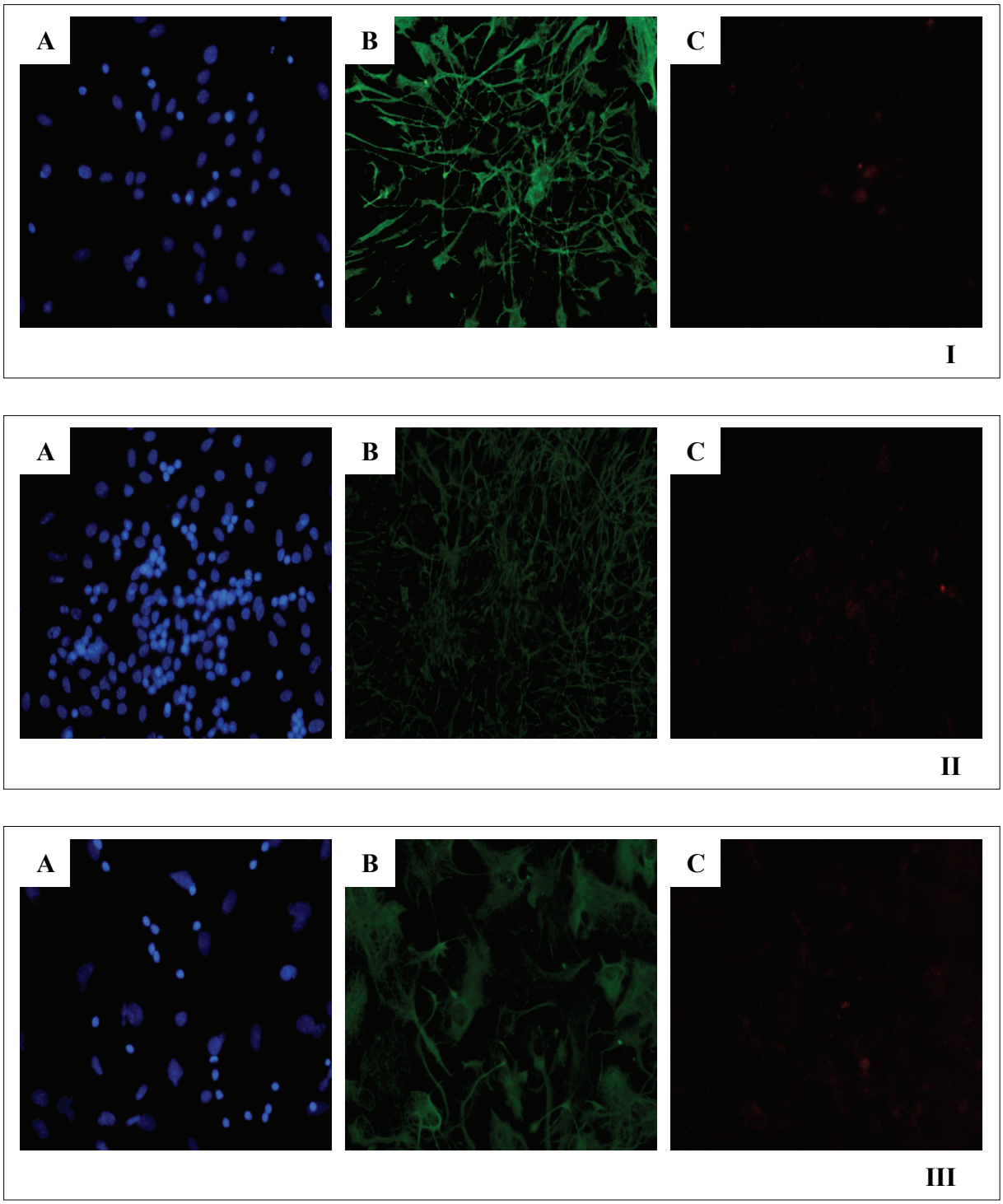

Figure 23. Immunocytochemical analysis of GFAP and CB2R expression in rat cerebellar progenitors cultured under conditions which lead to their differentiation (Skaper *et al*., 1990), and using a poly-D-lysine coating. Following 2 (panel I), 4 (panel II), and 6 (panel III) differentiation days, cells were fixed with 4% paraformaldehyde and stained with antibodies anti-GFAP (B), and anti-CB2R (C).

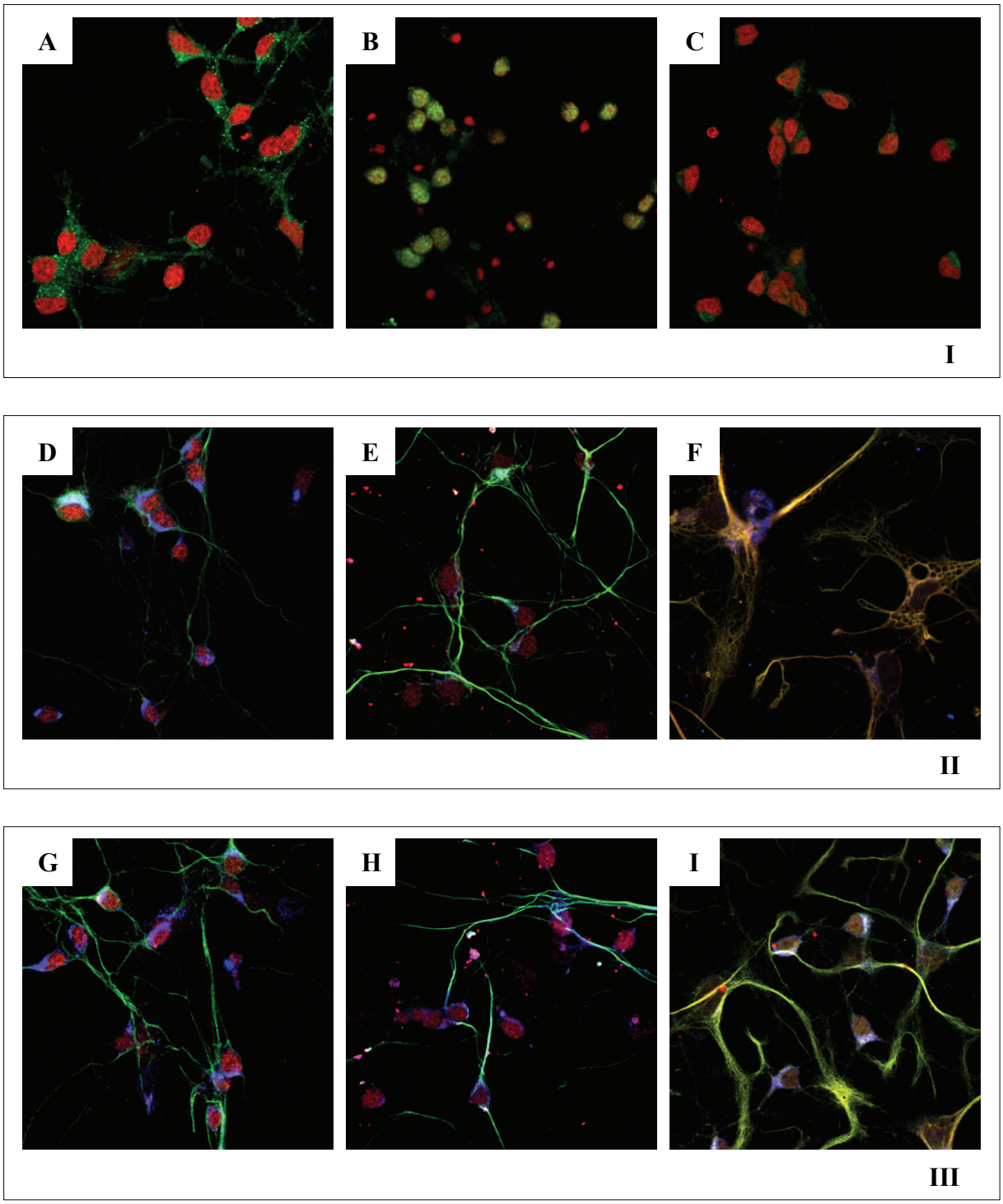

Figure 24. Immunocytochemical analysis of CBR expression in rat cerebellar granule cell (CGC) cultures at 8 DIV. CGC at 8 DIV were fixed with 4% paraformaldehyde and stained with antibodies against:

Panel I: β-COP (A), CB1 and CB2 receptors (B and C, respectively). Nuclei were stained with propidium iodide (red). Panel II: β-COP (blue), CB1R (red), MAP2 (D, green), NF (E, green), and GFAP (F, green). Panel III: β-COP (blue), CB2R (red), MAP2 (D, green), NF (E, green), and GFAP (F, green).

3.4 24-h treatment with synthetic non-selective, high-affinity CBR agonists increases cerebellar neural progenitor cell proliferation.

To examine the impact of CBR modulation on cerebellar neural progenitor cell proliferation, cerebellar precursors at 10 DIV were incubated for 24, 48, and 72 h with different concentrations (1-1000 nM) of the synthetic non-selective, high-affinity CBR agonists WIN 55,212-2 or CP 55,940. Twenty-four hours before the end of treatment to the cells were added $3.7x10^2$ Bq/ml [^{3}H]-thymidine. Proliferation was evaluated as [^{3}H]-thymidine incorporation. Twenty-four hours incubation with 100 nM WIN 55,212-2 or 1000 nM CP 55,940 induces a significant increase in neural proliferation of 43 ± 22 % and 37 ± 8 %, respectively, *vs* the corresponding vehicle control (Fig. 25). All other concentrations tested fail to promote neural proliferation and no significant [^{3}H]-thymidine incorporation changes are detected at later times (Fig. 25).

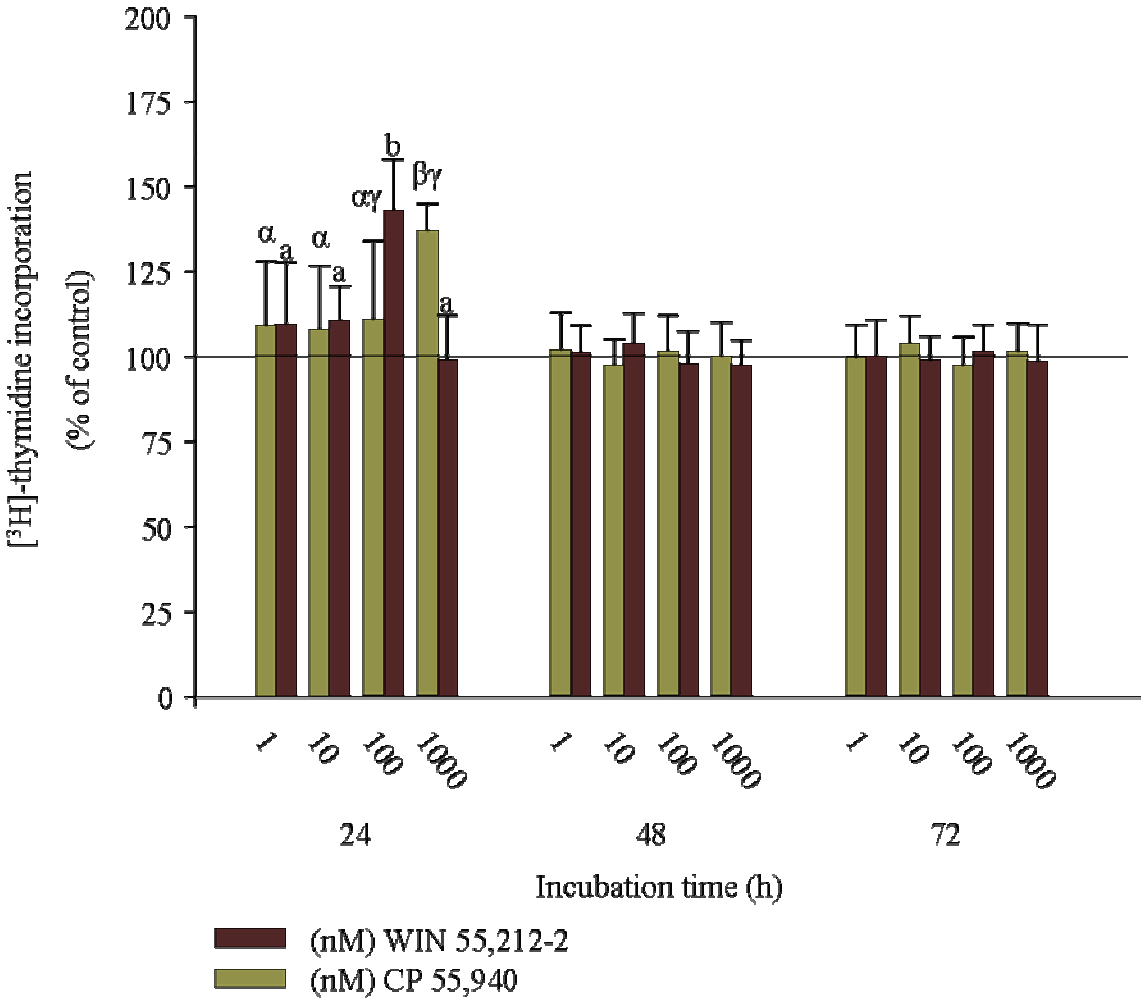

Figure 25. Twenty-four hours treatment with synthetic non-selective, high-affinity CBR agonists increases cerebellar neural progenitor cell proliferation. Cerebellar neural progenitor cells at 10 DIV were incubated for 24-48, and -72 hours (h) with increasing concentrations (1-1000 nM) of WIN 55,212-2 or CP 55,940. The proliferative effect was evaluated by [^{3}H]-thymidine incorporation. Results are expressed as percentage of the corresponding vehicle control values (mean ± SD of at least 5 independent experiments). Different letters indicate statistical differences ($p < 0.05$; ANOVA followed by Bonferroni *post hoc* multiple comparison test): letters in Italics and Greek correspond to WIN 55,212-2 and CP 55,940 treatment conditions, respectively.

3.5 Synthetic non-selective, high-affinity CBR agonists increase cerebellar neural progenitor proliferation upon 24-h incubation via CB1R.

To investigate whether the non selective CBR agonist-induced cell proliferation is mediated by CB1R and/or CB2R, cerebellar neural progenitor cells were incubated for 24 h with 100 nM WIN 55,212-2 or 1000 nM CP 55,940 in the presence of increasing concentrations (10-1000, 1 h pre-incubation) of AM 251 (Fig. 26) or AM 630 (Fig. 27), selective CB1R and CB2R antagonists, respectively. Proliferation was evaluated with [^{3}H]-thymidine incorporation. Incubation with either CB1R or CB2R antagonists did not significantly influence cerebellar neural proliferation *vs* the corresponding vehicle control, indicating the absence of an active endogenous cannabinoid tone.

AM 251 (1000 nM, 1 h pre-incubation) completely reverts to control level neural progenitor proliferation promoted by 24 h treatment with 100 nM WIN 55,212-2 and 1000 nM CP 55,940 (Fig. 26). AM 630 does not affect [^{3}H]-thymidine incorporation values obtained following 24 h incubation with the non-selective CBR agonists, at any of the concentrations used (10-1000 nM) (Fig. 27).

It can be concluded that the synthetic non-selective CBR agonist proliferative response is entirely mediated by CB1R activation.

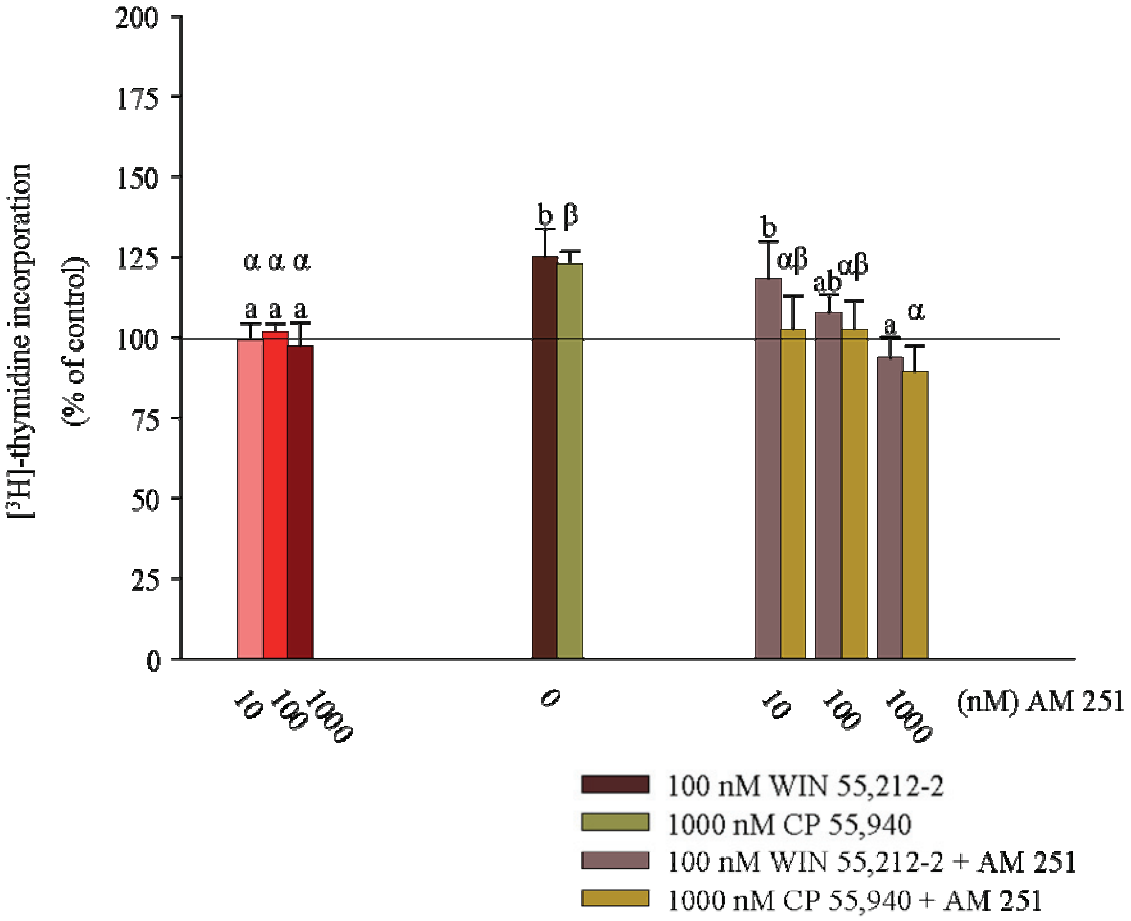

Figure 26. Synthetic non-selective, high-affinity CBR agonists increase cerebellar neural progenitor proliferation upon 24-h incubation via CB1R. Cerebellar neural progenitor cells at 10 DIV were incubated for 24 h with 100 nM WIN 55,212-2 or 1000 nM CP 55,940 in the absence or presence of the selective CB1R antagonist AM 251 (10-1000 nM; 1 h pre-incubation). The proliferative effect was evaluated by [^{3}H]-thymidine incorporation. Results are expressed as percentage of the corresponding vehicle control values (mean ± SD of at least 5 independent experiments). Different letters indicate statistical differences ($p < 0.05$; ANOVA followed by Bonferroni *post hoc* multiple comparison test): letters in Italics and Greek correspond to WIN 55,212-2 and CP 55,940 ± AM 251 treatment conditions, respectively.

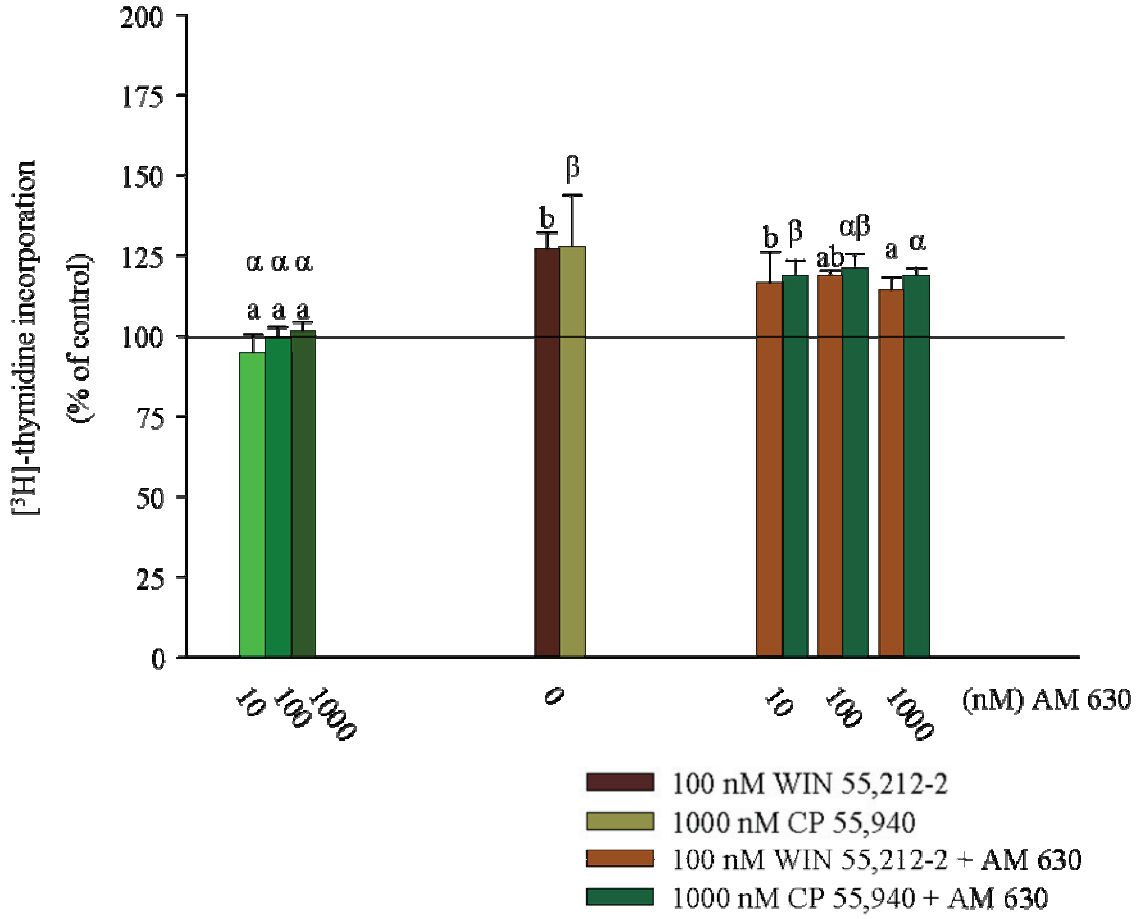

Figure 27. CB2R is not involved in cerebellar neural progenitor proliferation induced by 24 h treatment with synthetic non-selective, high-affinity CBR agonists. Cerebellar neural progenitor cells at 10 DIV were incubated for 24 h with 100 nM WIN 55,212-2 or 1000 nM CP 55,940 in the absence or presence of the selective CB2R antagonist AM 630 (10-1000 nM; 1 h pre-incubation). The proliferative effect was evaluated by [^{3}H]-thymidine incorporation. Results are expressed as percentage of the corresponding vehicle control values (mean ± SD of at least 4 independent experiments). Different letters indicate statistical differences ($p < 0.05$; ANOVA followed by Bonferroni *post hoc* multiple comparison test): letters in Italics and Greek correspond to WIN 55,212-2 and CP 55,940 ± AM 630 treatment conditions, respectively.

3.6 The synthetic highly selective CB1R agonist ACEA increases cerebellar neural progenitor proliferation upon 24 h incubation.

To confirm the involvement of CB1R in cannabinoid regulation of cerebellar neural progenitor proliferation, the cells were incubated with increasing concentrations (1-1000 nM) of the potent and highly selective CB1R agonist ACEA for 24, 48 and 72 h. Proliferation was evaluated as [^{3}H]-thymidine incorporation.

Twenty-four hours treatment with 1 nM and 10 nM ACEA significantly increased neural progenitor proliferation by 50.59 ± 6.72 % and 35.77 ± 4.48 %, respectively, *vs* the corresponding vehicle control. No significant differences in [^{3}H]-thymidine incorporation were obtained with longer incubation periods (Fig. 28). On the basis of these results, all the following experiments were performed by treating cells with the lowest effective concentration (1 nM).

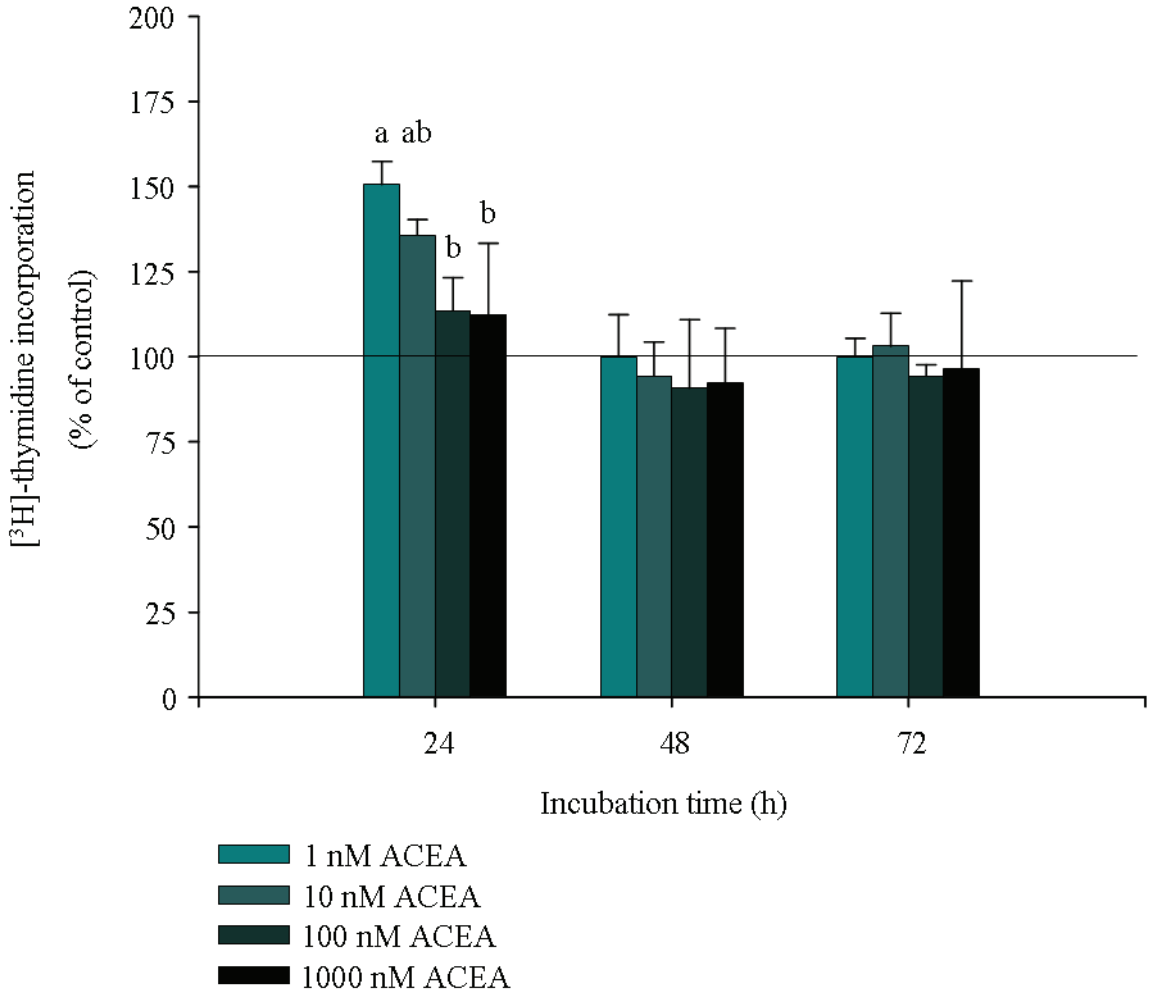

Figure 28. The synthetic highly selective CB1R agonist ACEA increases cerebellar neural progenitor proliferation upon 24 h incubation. Cerebellar neural progenitor cells at 10 DIV were incubated for 24 h with increasing concentrations (1-1000 nM) of ACEA. The proliferative effect was evaluated by [^{3}H]-thymidine incorporation. Data are expressed as percentage of the corresponding vehicle control values (mean ± SD of at least 3 independent experiments). Different letters indicate statistical differences ($p < 0.05$; ANOVA followed by Bonferroni *post hoc* multiple comparison test).

Selectivity of the proliferative response was assessed by measuring [^{3}H]-thymidine incorporation following 24 h incubation of neural progenitor cells with the selective CB1R antagonist AM 251 (10-1000 nM, 1 h pre-incubation) in the presence of 1 nM ACEA (Fig. 29). AM 251, at all concentrations tested reverts to control level radionuclide incorporation induced by 1 nM ACEA (Fig. 29).

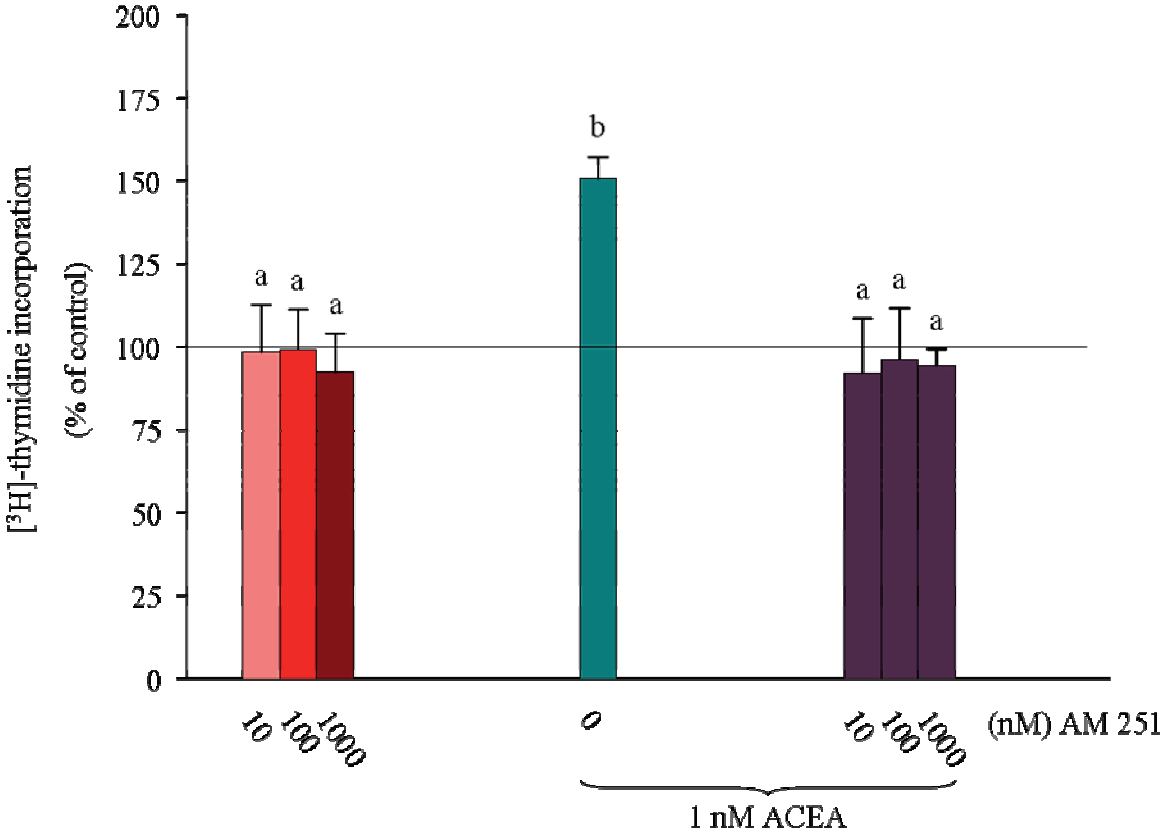

Figure 29. ACEA increases cerebellar neural progenitor proliferation upon 24 h incubation via CB1R. Cerebellar neural progenitor cells at 10 DIV were incubated for 24 h with 1 nM ACEA in the absence or presence of the selective CB1R antagonist AM 251 (10-1000 nM; 1 h pre-incubation). The proliferative effect was evaluated by [^{3}H]-thymidine incorporation. Results are expressed as percentage of the corresponding vehicle control values (mean ± SD of 5 independent experiments). Different letters indicate statistical differences ($p < 0.05$; ANOVA followed by Bonferroni *post hoc* multiple comparison test).

3.7 The synthetic CB2R selective agonist JWH 133 does not affect cerebellar neural progenitor cell proliferation.

CB2R involvement in the cannabinoid-mediated proliferative response of cerebellar neural progenitors was further excluded by incubating cells with the synthetic CB2R selective agonist JWH 133 (10-1000 nM) for 24, 48, and 72 h. Proliferation was measured by [^{3}H]-thymidine incorporation. No significant variation in radionuclide incorporation *vs* the corresponding vehicle control was observed under any of these treatment conditions (Fig. 30).

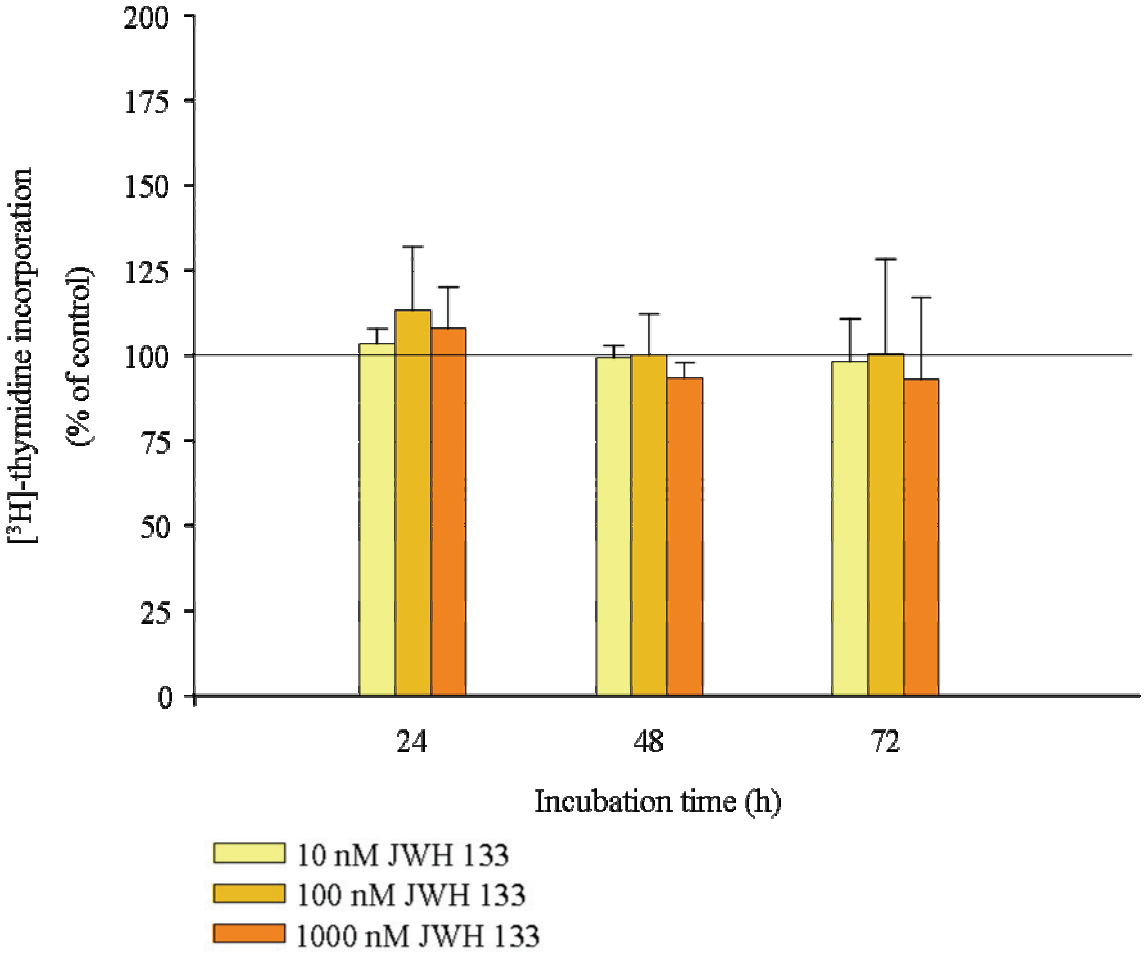

Figure 30. The synthetic CB2R selective agonist JWH 133 does not affect cerebellar neural progenitor cell proliferation. Cerebellar neural progenitor cells at 10 DIV were incubated for 24 h with increasing concentrations (10-1000 nM) of JWH 133. The proliferative effect was evaluated by [^{3}H]-thymidine incorporation. Data are expressed as percentage of the corresponding vehicle control values (mean ± SD of 5 independent experiments).

3.8 Intracellular signaling involved in ACEA-induced cerebellar neural progenitor proliferation.

3.8.1 CB1R is coupled to MAPK ERK1/2-MEK activation.

To investigate the mechanisms underlying the action of the selective CB1R agonist ACEA on cerebellar neural progenitor cell proliferation, several major intracellular signaling pathways were examined (see Fig. 6). Since the $G_{i/o}$ CB1R protein is reported to activate ERK signaling, phospho-ERK levels were assessed by Western blotting following 5-60 min incubation with 1 nM ACEA, in the presence or absence of the selective CB1R antagonist AM 251 (10 nM, 1 h pre-incubation). A 30-min treatment with 1 nM ACEA induced a significant increase in phospho-ERK1/2 levels *vs* the corresponding vehicle control (32 ± 4 %). AM 251 *per se* does not affect MAPK phosphorylation but does inhibit the ACEA agonistic effect (Fig. 31).

The involvement of ERK1/2 signaling in cerebellar neural progenitor proliferation induced by 1 nM ACEA was supported by using the specific MEK1 inhibitor U0126. A concentration of 10 μM U0126 was chosen, as *in vitro* assays demonstrate a reduction in MEK1 activity to 56 ±1 % of that in control incubations (Davies,S.P. *et al*., 2000).

U0126 influence on cerebellar neural progenitor proliferation was first evaluated by [^{3}H]-thymidine incorporation. Cerebellar neural progenitors were incubated for 24 h with 10 μM U0126 (1 h pre-incubation) in the presence or absence of 1 nM ACEA. Ten micromolar U0126 *per se* inhibits cerebellar neural progenitor proliferation to 67.38 ± 3.84 % of the corresponding vehicle control. ACEA-induced neural progenitor proliferation is reverted to the level with inhibitor alone following 1 h pre-incubation with U0126 (Fig. 32). Next, U0126 influence on ERK1/2 activation in cerebellar neural progenitor cells was evaluated by Western blotting. Treatment of cerebellar neural progenitors with 10 μM U0126 (1 h pre-incubation) completely blocks basal and ACEA-induced MAPK activation at 30 min (Fig. 33).

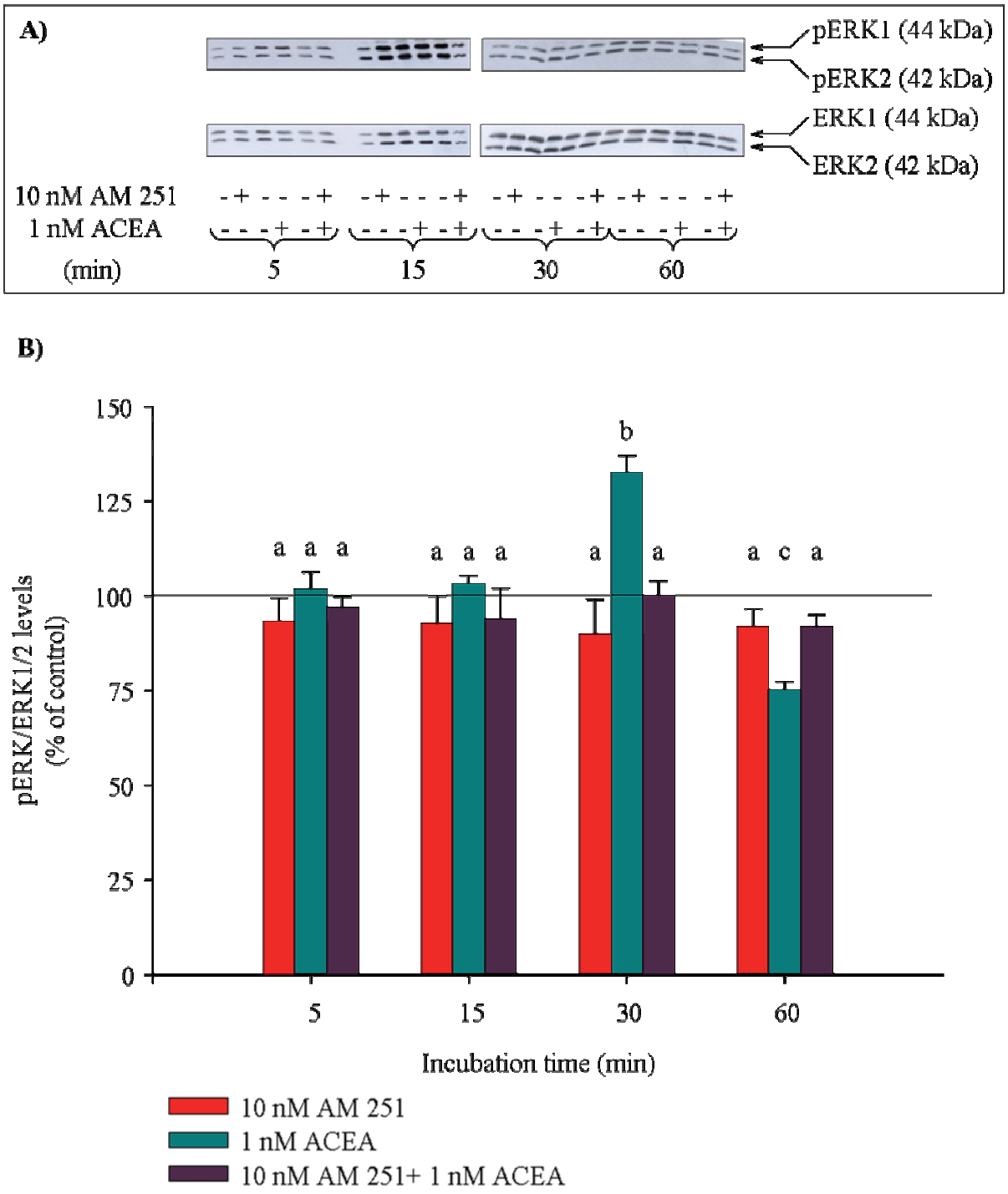

Figure 31. CB1R is coupled to ERK1/2 activation. Western blot analysis of cerebellar neural progenitor total and phosphorylated ERK1/2 levels, upon 5-60 min incubation with 1 nM ACEA and/or 10 nM AM 251 (1 h pre-incubation). **A)** A representative blot of phosphorylated and total ERK, determined by using anti-phospho-ERK or anti-total ERK antibodies (Table 3). **B)** Bar graphs depict densitometric quantification from blots of amounts of phospho-protein normalized to the total ERK1/2 protein, expressed as percentage of the corresponding control values (mean ± SD of at least 3 independent experiments). Different

letters indicate significant differences among groups ($p < 0.05$; ANOVA followed by Bonferroni *post hoc* multiple comparison test).

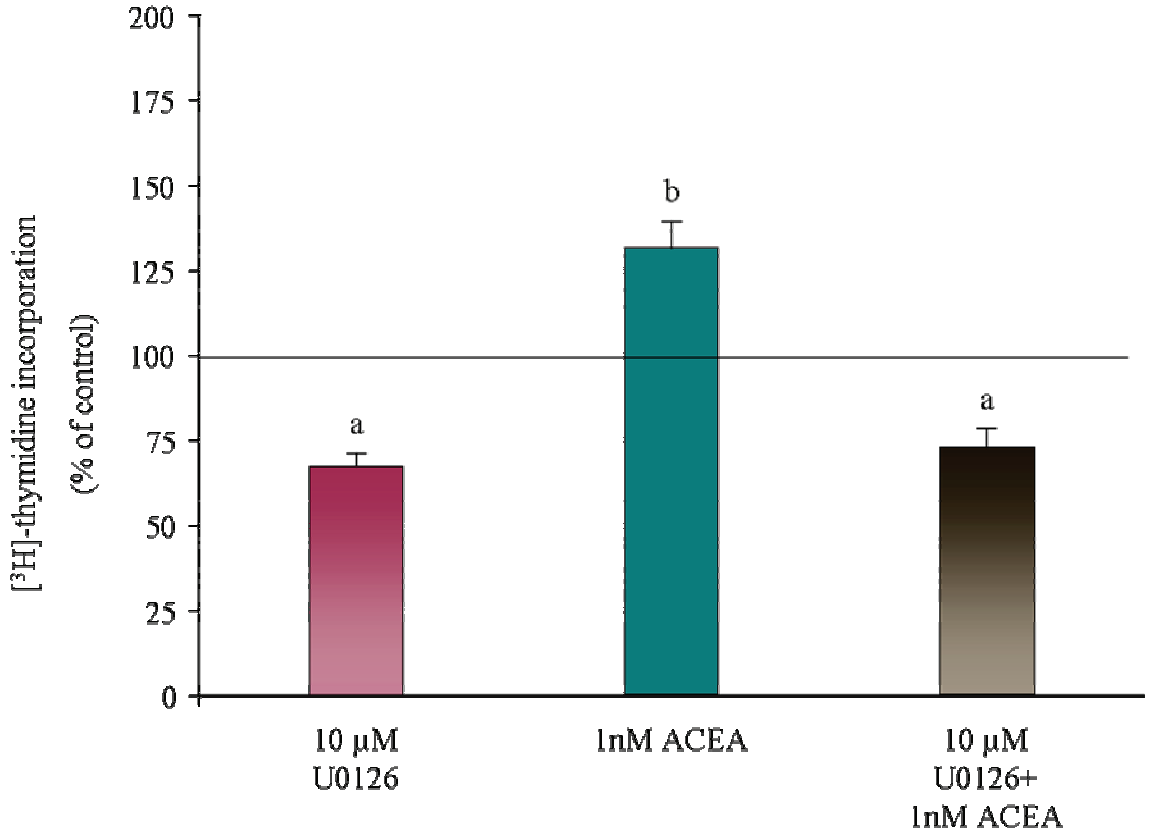

Figure 32. U0126 prevents the increase in cerebellar neural progenitor cell proliferation induced by 24 h ACEA treatment. Cerebellar neural progenitor cells at 10 DIV were incubated for 24 h with 1 nM ACEA in the absence or presence of 10 µM U0126 (1 h pre-incubation). The proliferative effect was evaluated by [^{3}H]-thymidine incorporation. Results are expressed as percentage of the corresponding vehicle control values (mean ± SD of 5 independent experiments). Different letters indicate statistical differences ($p < 0.05$; ANOVA followed by Bonferroni *post hoc* multiple comparison test).

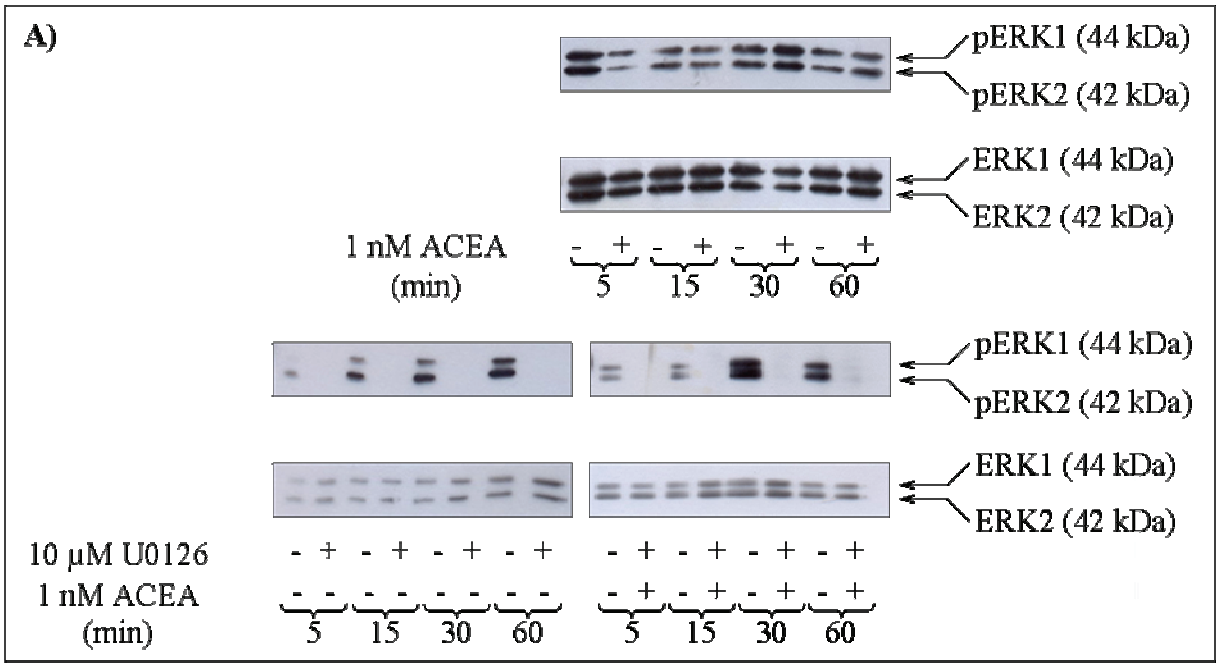
A)
pERK1 (44 kDa)
pERK2 (42 kDa)
ERK1 (44 kDa)
ERK2 (42 kDa)
1 nM ACEA
(min)
- + - + - + - +
5 15 30 60
pERK1 (44 kDa)
pERK2 (42 kDa)
ERK1 (44 kDa)
ERK2 (42 kDa)
10 µM U0126
1 nM ACEA
(min)
- + - + - + - + - + - + - +
- - - - - - - - - + - + - + - +
5 15 30 60 5 15 30 60

B)

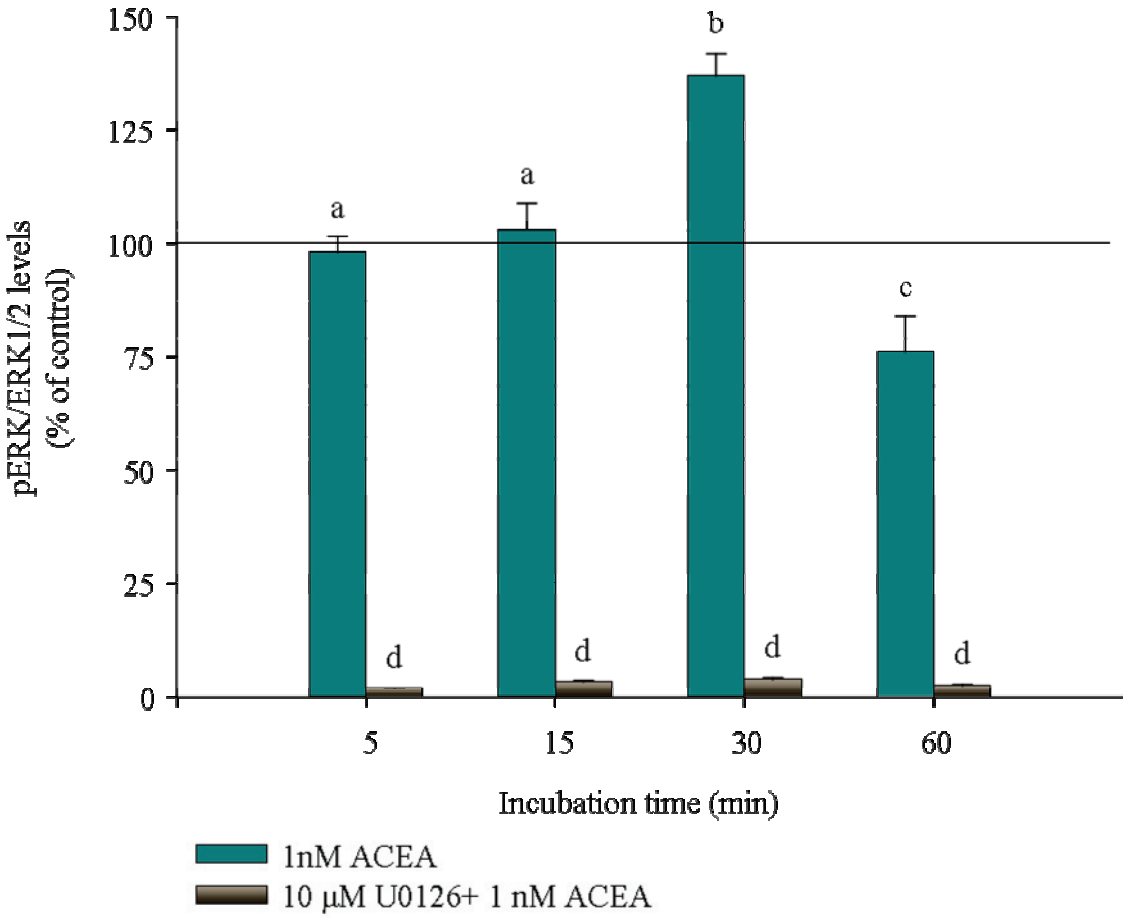
150
125
100
75
50
25
0
pERK/ERK1/2 levels
(% of control)
a
a
b
c
d
d
d
d
5
15
30
60
Incubation time (min)
1nM ACEA
10 µM U0126+ 1 nM ACEA

Figure 33. CB1R is coupled to MEK activation. Western blot analysis of cerebellar neural progenitor cell total and phosphorylated ERK1/2 levels, upon 5-60 min incubation with 1 nM ACEA and/or 10 μM U0126 (1 h pre-incubation). **A)** A representative blot of phosphorylated and total ERK, determined by using anti-phospho-ERK or anti-total ERK antibodies (Table 3). **B)** Bar graphs depict densitometric quantification from blots of amounts of phospho-protein normalized to the total ERK1/2 protein, expressed as percentage of the corresponding control values (mean ± SD of at least 3 independent experiments). Different letters indicate significant differences among groups ($p < 0.05$; ANOVA followed by Bonferroni *post hoc* multiple comparison test).

3.8.2 CB1R is coupled to PI3K-Akt activation.

Since CB1R is reported to activate PI3K/Akt/GSK-3β, phospho-Akt (Ser473) levels were assayed by Western blotting following 5-60 min incubation with 1 nM ACEA, in the presence or in the absence of the selective CB1R antagonist AM 251 (10 nM, 1 h pre-incubation). Treatment with 1 nM ACEA induces a significant increase in phospho-Akt (Ser473) levels *vs* the corresponding vehicle control at 15 and 30 min (36.54 ± 7.21 and 21 ± 5 %, respectively). AM 251 *per se* does not affect PKB phosphorylation but does inhibit the ACEA agonistic effect (Fig. 34). The involvement of PKB signaling in cerebellar neural progenitor proliferation induced by 1 nM ACEA was supported by using LY294002, a specific and reversible inhibitor of PI3K. LY294002 was used at 75 μM final concentration and 3 h pre-incubation, according to Facci *et al*. (Facci,L. *et al*., 2003). Western blot analysis of cerebellar neural progenitors was performed under these conditions: Akt and GSK-3β phosphorylation levels were reduced 69% and 38%, respectively, *vs* the corresponding vehicle control (data not shown). Davies *et al*. report PKBα and GSK-3β activity values of 60 ± 2 and 53 ± 1 %, respectively, of that in control incubations *in vitro* in the presence of 50 μM LY294002; PI3K activity is reduced to 13 ± 0 *vs* the control. (Davies,S.P. *et al*., 2000).

LY294002 influence on cerebellar neural progenitor proliferation was first evaluated by [^{3}H]-thymidine incorporation. Cerebellar neural progenitors were incubated for 24 h with 75 μM LY294002 (3 h pre-incubation) in the presence or absence of 1 nM ACEA. LY294002 *per se* inhibits cerebellar neural progenitor proliferation to 41.28 ± 3.21 % of the corresponding vehicle control. ACEA-induced neural proliferation is reverted to the inhibitor level following 3 h pre-incubation with 75 μM LY294002 (Fig. 35). Second, LY294002 influence on Akt activation in cerebellar neural progenitor cells was evaluated by Western blotting. LY294002 counteracts Akt phosphorylation induced by ACEA, while *per se* it reduces the kinase activation state of untreated progenitors (Fig. 36).

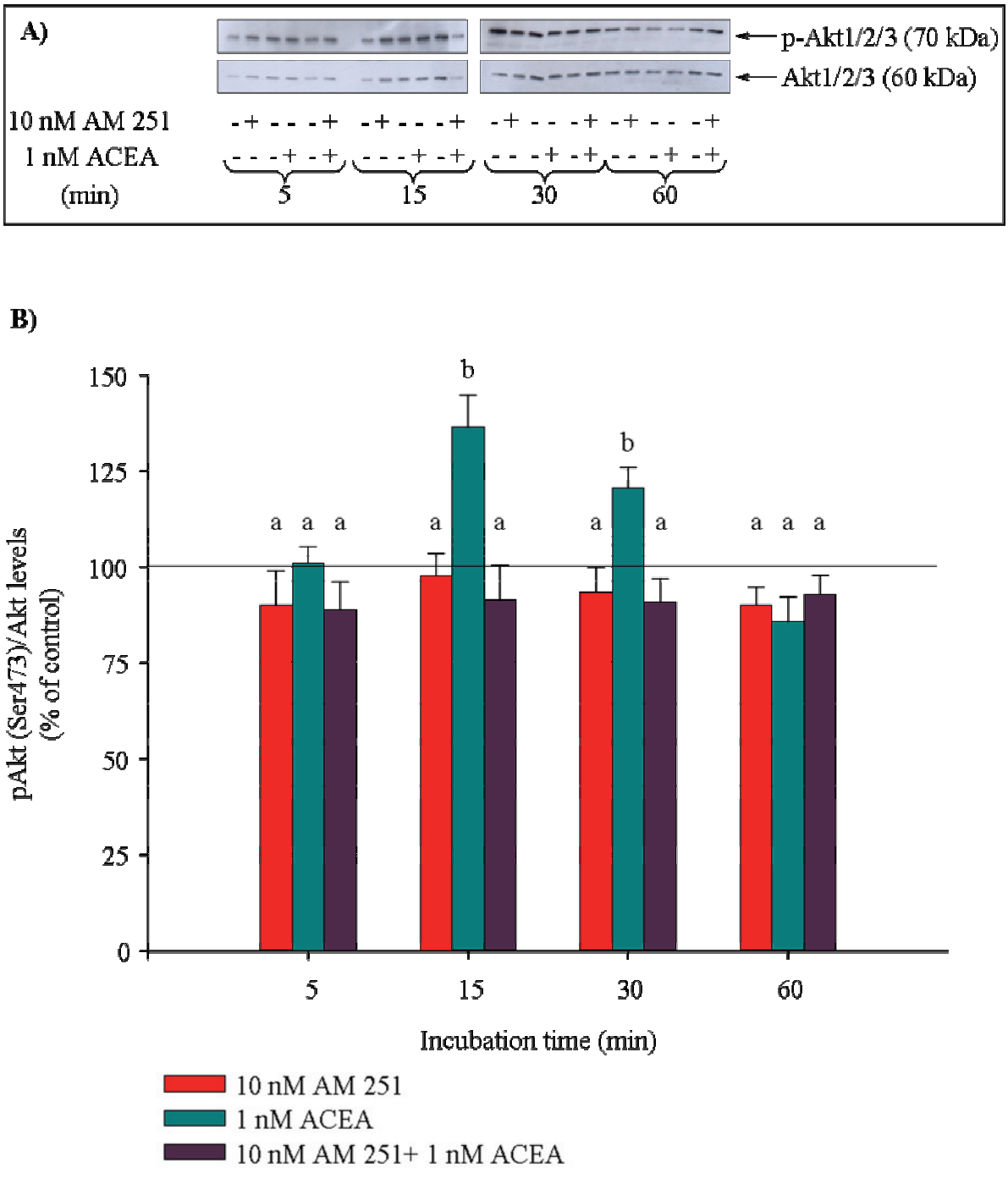

Figure 34. CB1R is coupled to Akt activation. Western blot analysis of cerebellar neural progenitor cell total and phosphorylated Akt levels, upon 5-60 min incubation with 1 nM ACEA and/or 10 nM AM 251 (1 h pre-incubation). **A)** A representative blot of phosphorylated and total Akt, determined using anti-phospho-Akt (Ser473) or anti-total Akt antibodies (Table 3). **B)** Bar graphs depict densitometric quantification from blots of amounts of phospho-protein normalized to the total Akt protein, expressed as percentage of the corresponding control values (mean ± SD of at least 3 independent experiments). Different letters indicate significant differences among groups ($p < 0.05$; ANOVA followed by Bonferroni *post hoc* multiple comparison test).

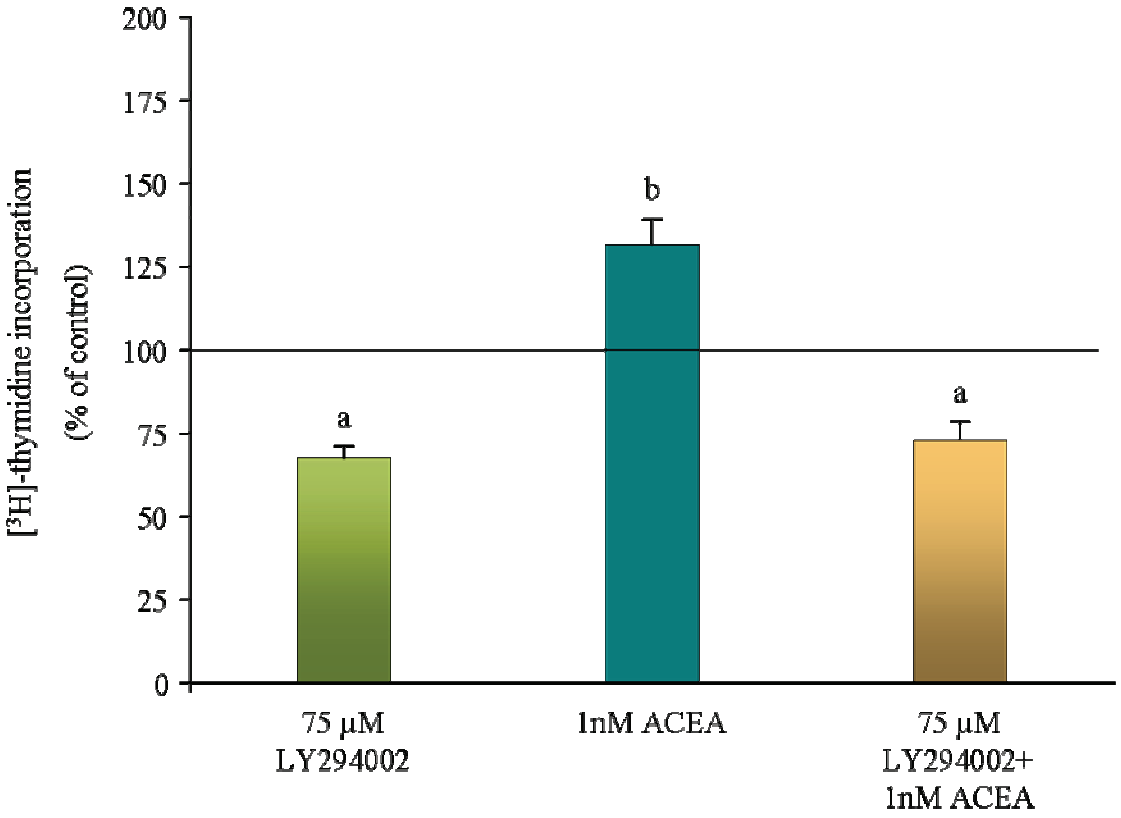

Figure 35. LY294002 prevents the increase in cerebellar neural progenitor induced by 24 h ACEA treatment. Cerebellar neural progenitor cells at 10 DIV were incubated for 24 h with 1 nM ACEA in the absence or presence of 75 µM LY294002 (3 h pre-incubation). The proliferative effect was evaluated by [^{3}H]-thymidine incorporation. Results are expressed as percentage of the corresponding vehicle control values (mean ± SD of 5 independent experiments). Different letters indicate statistical differences ($p < 0.05$; ANOVA followed by Bonferroni *post hoc* multiple comparison test).

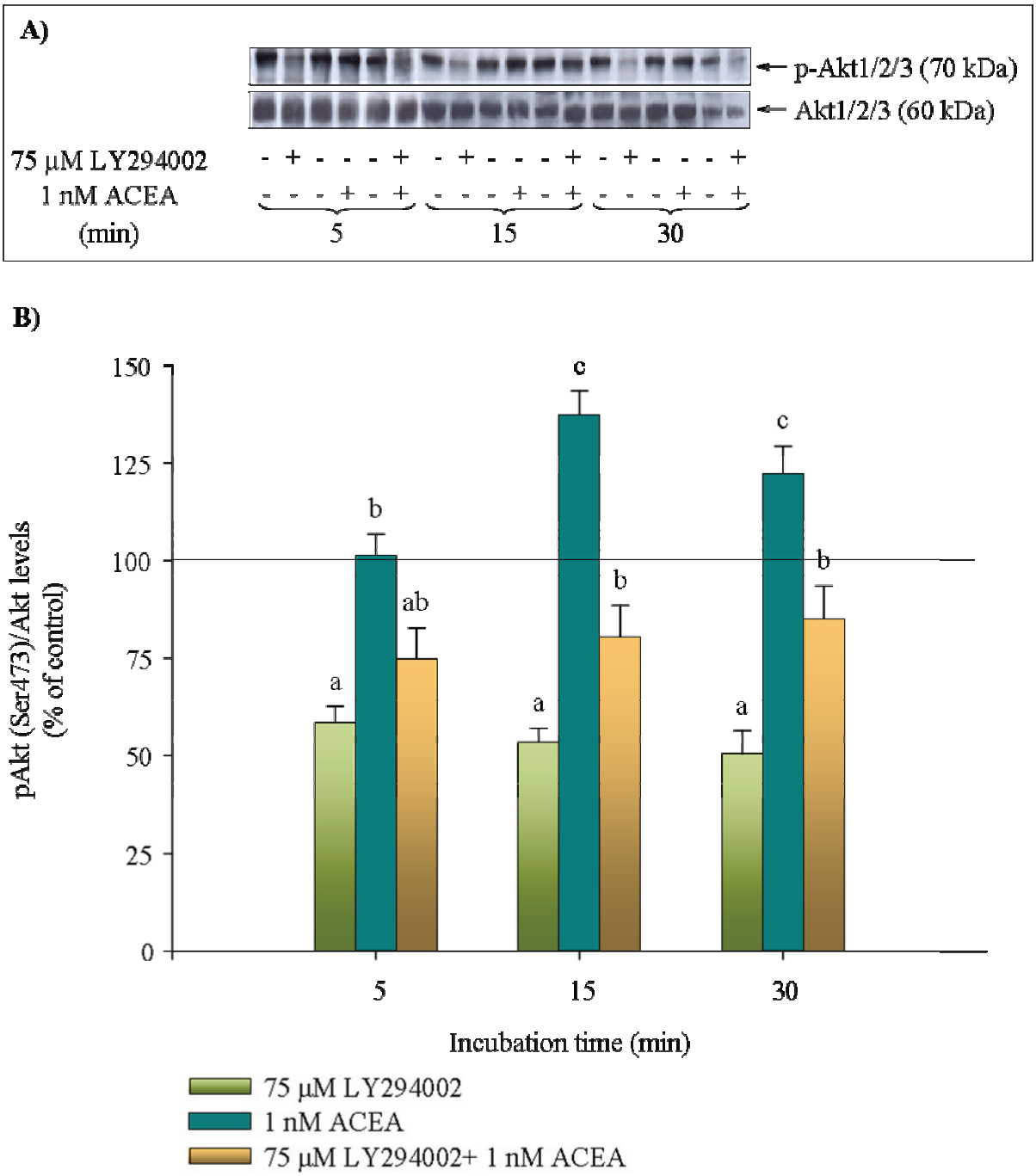

Figure 36. CB1R is coupled to PI3K activation. Western blot analysis of cerebellar neural progenitor cell total and phosphorylated Akt levels, upon 5-30 min incubation with 1 nM ACEA and/or 75 µM LY294002 (3 h pre-incubation). **A)** A representative blot of phosphorylated and total Akt, determined using anti-phospho-Akt (Ser473) or anti-total Akt antibodies (Table 3). **B)** Bar graphs depict densitometric quantification from blots of amounts of phospho-protein normalized to total Akt protein, expressed as percentage of the corresponding control values (mean ± SD of at least 3 independent experiments). Different letters indicate significant differences among groups ($p < 0.05$; ANOVA followed by Bonferroni *post hoc* multiple comparison test).

3.8.3 ACEA–induced cerebellar neural progenitor proliferation involves PI3K/ ERK1/2 pathway cross-talk.

Subsequently, the existence of a cross-talk between these two pathways in mediating CB1R-induced neural proliferation, and a possible contribution of the Akt cascade to the MAPK ERK one, was investigated. First, phosphorylation levels of ERK1/2 were evaluated following 1 nM ACEA treatment (5-30 min) in the presence of 75 μM LY294002 (3 h pre-incubation). The PI3K inhibitor reverts to the control level the p-ERK increase induced by ACEA, and *per se* reduces p-ERK basal levels (Fig. 37).

Second, Akt activation was evaluated following 1 nM ACEA treatment in the presence of 10 μM U0126 (1 h pre-incubation). The MEK inhibitor does not affect PKB activation, both in untreated and ACEA-treated neural progenitor cells (Fig. 38).

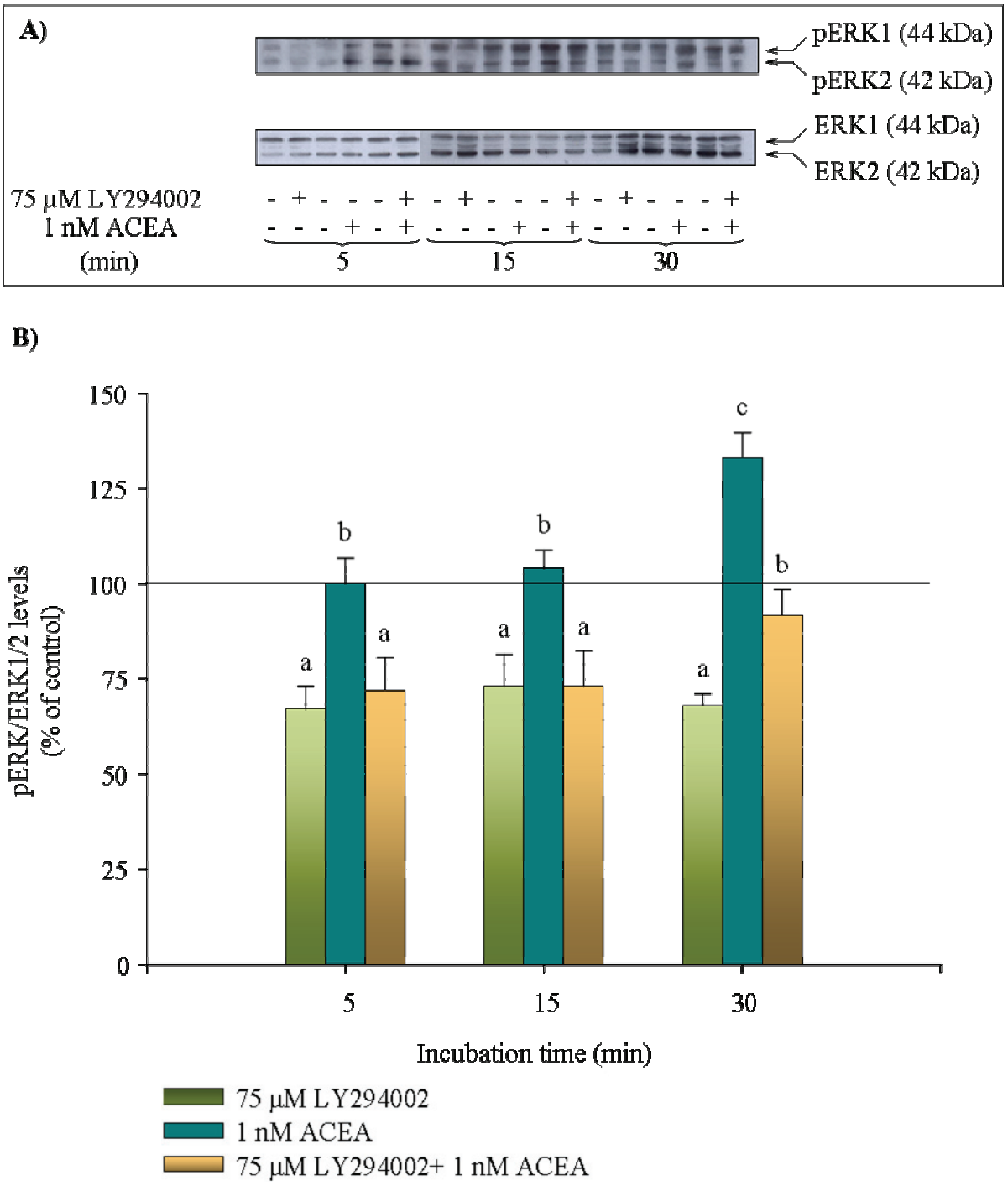

Figure 37. The PI3K inhibitor LY294002 affects ERK1/2 activation. Western blot analysis of cerebellar neural progenitor cell total and phosphorylated ERK1/2 levels, upon 5-30 min incubation with 1 nM ACEA and/or 75 µM LY294002 (3 h pre-incubation). **A)** A representative blot of phosphorylated and total ERK1/2, determined using anti-phospho-ERK or anti-total ERK1/2 antibodies (Table 3). **B)** Bar graphs depict densitometric quantification from blots of amounts of phospho-protein normalized to total ERK1/2 protein, expressed as percentage of the corresponding control values (mean ± SD of at least 3 independent experiments). Different letters indicate significant differences among groups ($p < 0.05$; ANOVA followed by Bonferroni *post hoc* multiple comparison test).

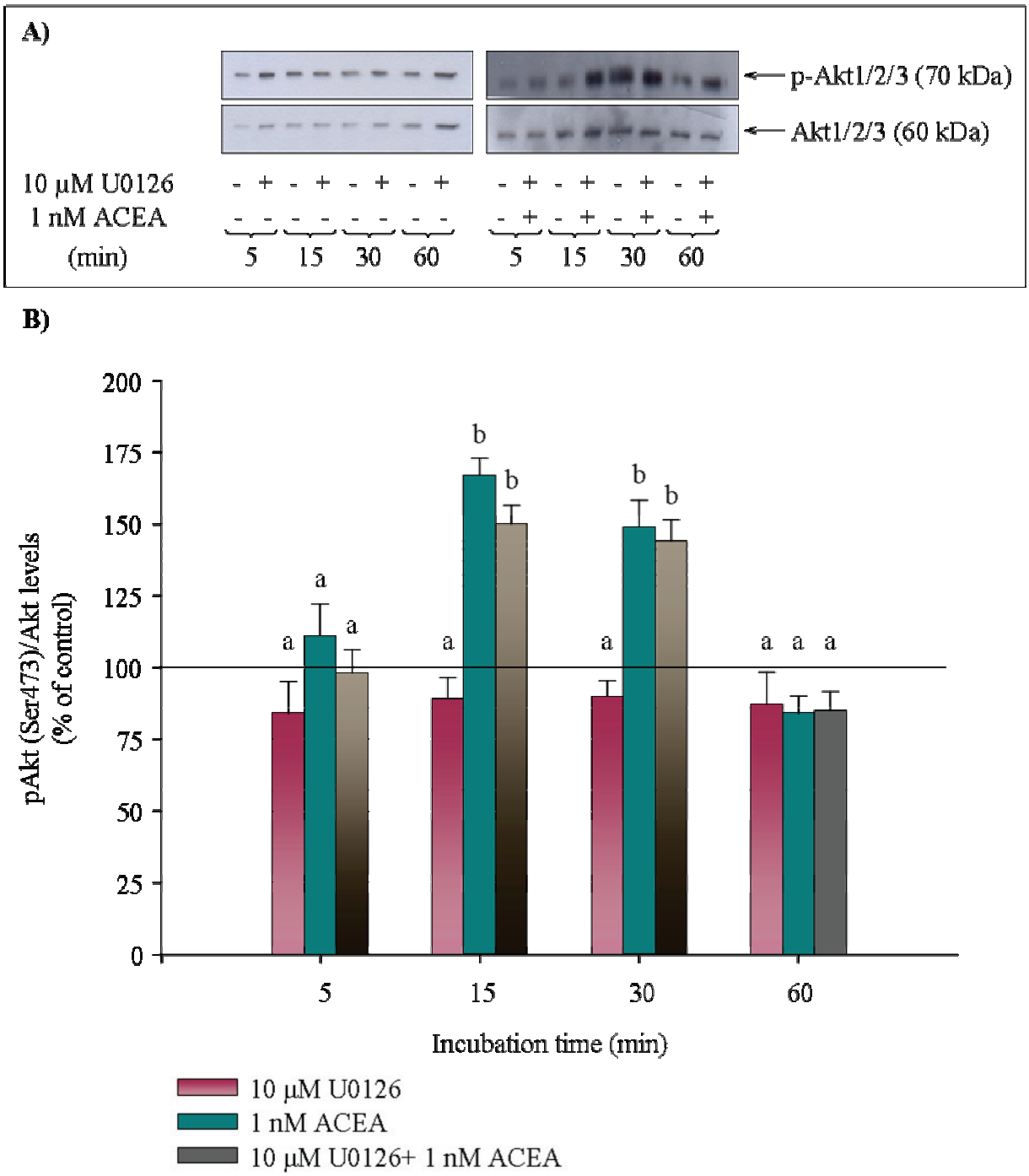

Figure 38. The MEK inhibitor U0126 does not affect PKB activation. Western blot analysis of cerebellar neural progenitor cell total and phosphorylated Akt levels, upon 5-60 min incubation with 1 nM ACEA and/or 10 µM U0126 (1 h pre-incubation). **A)** A representative blot of phosphorylated and total Akt, determined by using anti-phospho-Akt (Ser473) or anti-total Akt antibodies (Table 3). **B)** Bar graphs depict densitometric quantification from blots of amounts of phospho-protein normalized to the total Akt protein, expressed as percentage of the corresponding control values (mean ± SD of at least 3 independent experiments). Different letters indicate significant differences among groups ($p < 0.05$; ANOVA followed by Bonferroni *post hoc* multiple comparison test).

3.9 The synthetic selective CB1R agonist ACEA affects cerebellar neural progenitor differentiation.

Given cerebellar neural progenitor cell multipotency (Zusso,M. *et al*., 2008) and eCB modulation of neural progenitor differentiation in the developing and adult brain (Jiang,W. *et al*., 2005), the influence of ACEA treatment on cerebellar neural progenitor differentiation was investigated.

Chromatin structure remodeling during cell cycle S phase and post-transcriptional events, such as mRNA splicing, transport, transduction, and cytoplasmic RNA stabilization, control gene expression during neuronal differentiation. Given the emerging role of ARE (AU rich element)-binding proteins in this regulatory process, it may be possible to use these proteins as neuronal markers. Among this family, AUF1 (AU-rich element/poly(U)-binding/degradation factor 1/heterogeneous nuclear ribonucleoprotein D, hnRPD) (NW_047422.1 NCBI Reference Sequence) exists as 4 alternative mRNA splice variants in *Rattus Norvegicus* ("taxon: 10116"), corresponding to p37, p40, p42, and p45 proteins. Transcript expression is regulated in the brain from the embryonic stage through adulthood (Hambardzumyan,D. *et al*., 2009).

To investigate ACEA influence on cerebellar neural progenitor differentiation, cerebellar neural progenitor cells at 10 DIV were replated on a poly-D-lysine substratum, and cultured in differentiation medium for 2, 4, and 6 days, in the presence of increasing concentrations of ACEA (1-100 nM) (Fig. 40) or 100 ng/ml BDNF (Fig. 39). This neurotrophin was taken as positive control, as it stimulates neuronal cell differentiation (Zhou,P. *et al*., 2007). For comparison, cerebellar neural progenitors at 10 DIV and cerebellar granule cells at 8 DIV were utilized. Total RNA was extracted and RT-PCR performed. To compare relative levels of AUF1 mRNA splice variants, transcripts coding for AUF1 were detected by agarose gel electrophoresis of PCR products and quantified by ethidium bromide staining under UV light. The band optical density was normalized to the corresponding GAPDH value, quantified by real time RT-PCR.

AUF1 mRNA splice variant relative quantities are reported as ratio of p37 transcript expression, (taken as reference) (Tables 6 and 7).

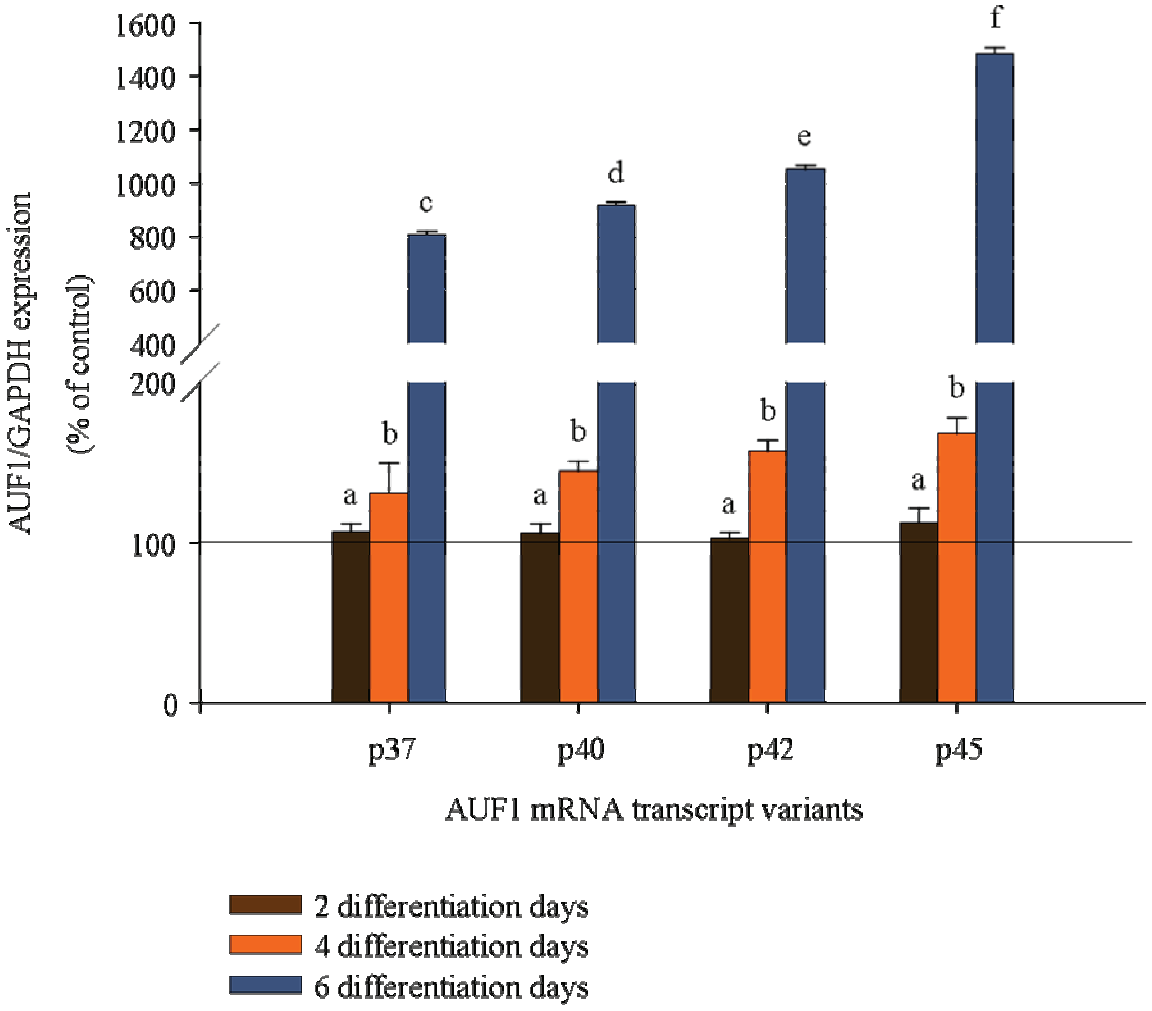

Figure 39. Expression of AUF1 mRNA splice variants in cerebellar neural progenitors induced to differentiate in the presence of BDNF. Cerebellar progenitors cultured under conditions which lead to their differentiation (Skaper *et al*., 1990), and using a poly-D-lysine coating, were exposed to 100 ng/ml BDNF for 2, 4, and 6 days. Total RNA was extracted and the relative levels of AUF1 transcripts analyzed. Bar graphs depict densitometric quantification from agarose gel electrophoresis of PCR products normalized to the corresponding GAPDH value quantified by real time RT-PCR. Values are expressed as percentage of the corresponding control (mean ± SD of 2 independent experiments). Different letters indicate significant differences among groups ($p < 0.05$; ANOVA followed by Bonferroni *post hoc* multiple comparison test).

Table 6. AUF1 mRNA splice variant/p37 ratio in cerebellar neural progenitors induced to differentiate by 100 ng/ml BDNF.

Differentiation days	AUF1 p40/p37 ratio	AUF1 p42/p37 ratio	AUF1 p45/p37 ratio
2	98.99 ± 1.96	96 ± 3	105.4 ± 4.9
4	110.52 ± 6.55	119.70 ± 2.63*	128.2 ± 1.8$^{\#}$
6	113.3 ± 4.7	130.19 ± 3.89**	183.97 ± 4.75$^{\#\#}$

Culture conditions and treatments are as described in Figure 39.

Differentiation in the presence of 100 ng/ml BDNF did not produce a change in the p40/p37 ratio at any time, while the p42/p37 ratio at 4 and 6 days differed significantly from the ratio at 2 days (*$p < 0.05$ and **$p < 0.001$, respectively; ANOVA followed by Bonferroni *post hoc* multiple comparison test). The greatest change was seen for AUF1 mRNA splice variant p45 at 6 days ($^{\#\#}p < 0.001$ *vs* 2 and 4 days), and for p45 at 4 days (#$p < 0.05$ *vs* 2 days). At 6 differentiation days p45 is the most expressed transcript variant, as it is significantly different from p42 ($p < 0.001$).

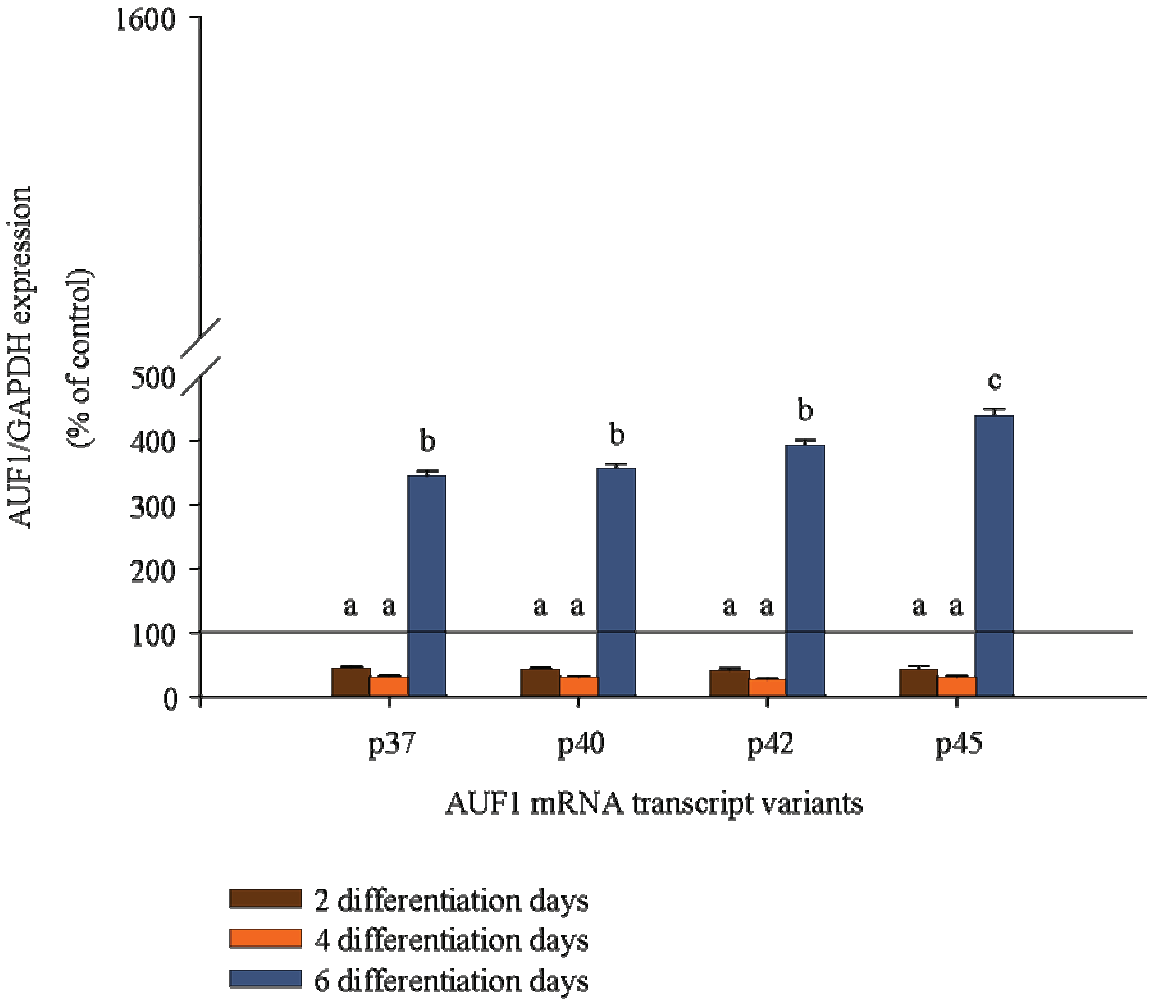

Figure 40. Expression of AUF1 mRNA splice variants in cerebellar neural progenitors induced to differentiate in the presence of 1 nM ACEA. Cerebellar progenitors cultured under conditions which lead to their differentiation (Skaper *et al*., 1990), and using a poly-D-lysine coating, exposed to 1 nM ACEA for 2, 4, and 6 days. Total RNA was extracted and the relative levels of AUF1 transcripts analyzed. Bar graphs depict densitometric quantification from agarose gel electrophoresis of PCR products normalized to the corresponding GAPDH value quantified by real time RT-PCR. Values are expressed as percentage of the corresponding control (mean ± SD of 2 independent experiments). Different letters indicate significant differences among groups ($p < 0.05$; ANOVA followed by Bonferroni *post hoc* multiple comparison test).

Table 7. AUF1 mRNA splice variant/p37 ratio in cerebellar neural progenitors induced to differentiate by 1 nM ACEA.

Differentiation days	AUF1 p40/p37 ratio	AUF1 p42/p37 ratio	AUF1 p45/p37 ratio
2	97.98 ± 2.88	91.17 ± 5.53	96.78 ± 2.94
4	97.14 ± 2.38	84.67 ± 11.39	96.67 ± 2.55
6	103.3 ± 1.7	114.37 ± 7.67*	127.67 ± 1.62$^{\#}$

Culture conditions and treatments are as described in Figure 40.

Differentiation in the presence of 1 nM ACEA did not produce a change in the p40/p37 ratio at any time, as seen for BDNF. The p42/p37 ratio at 6 days differed significantly from this ratio at 2 and 4 days (*$p < 0.05$; ANOVA followed by Bonferroni *post hoc* multiple comparison test). The AUF1 mRNA splice variant p45 changes more than the others at 6 differentiation days, and differs significantly from the p45/p37 ratio at 2 and 4 days ($^{\#}p < 0.05$).

These preliminary results are in agreement with the study conducted by Hambardzumyan *et al*. (Hambardzumyan,D. *et al*., 2009) on rat postnatal cerebellum, where p42 and p45 splice variants are the most abundantly expressed during cerebellar development adulthood.

CHAPTER 4

DISCUSSION

Cannabinoid CB1 and CB2 receptors are the primary targets of endogenous cannabinoids (endocannabinoids, eCBs). The eCBs, together with the enzymes responsible for their biosynthesis, degradation, and transport define the endocannabinoid system. The eCBs comprise a family of eicosanoids (Devane,W.A. *et al*., 1992), present in the brain and in peripheral tissues, that mediates retrograde synaptic signaling, which inhibits other neurotransmitter release. eCBs are released after a triggering signal as needed to maintain homeostasis. The G protein–coupled cannabinoid receptors play an important role in many cellular processes, including energy metabolism and appetite control, emesis, motor behaviour, sensory, autonomic, and neuroendocrine responses. CBRs modulate immune and inflammatory responses, pain perception, memory cognition, and emotions (anxiety) (Mackie,K. 2006).

The involvement of eCB system in regulating nervous system structural and functional maturation is an emerging concept. The eCB system is actively present from the earliest stages of ontogenetic development, during fertilisation, and in the preimplantation embryo. CB1 and CB2 receptor mRNA can be first identified in rat embryo brain at day 11 of gestation. During fetal life CB1R plays a major role in brain development, regulating neural progenitor proliferation, differentiation, and guiding axonal migration and synaptogenesis (Buckley,N.E. *et al*., 1998). There is a gradual increase in CB1R postnatally within the whole brain (Rodriguez de Fonseca,F. *et al*., 1993). In addition, CB1Rs seem to be already functionally coupled to $G_{i/o}$ proteins at early stages of rat brain maturation (Berrendero,F. *et al*., 1998).

The developmental pattern of AEA and 2-AG, two representative eCBs, differs in the brain. Whereas concentrations of AEA increase throughout development until adulthood, fetal levels of 2-AG are similar to those measured in the adult brain (Berrendero,F. 1999).

Manipulating the eCB system, by pre-and/or postnatal administration of cannabinoids or maternal marijuana consumption, has significant consequences on the offspring, such as interference with normal dopamine-dependent motor functions, the hypothalamic-pituitary-adrenal stress axis (Ramos,J.A. *et al*., 2002), memory impairment correlated with a shortening

of hippocampal LTP and reducted extracellular glutamate (Mereu,G. *et al*., 2003), and impairment of higher cognitive functions of the prefrontal cortex (Fried,P.A. *et al*., 2003).

The cerebellum displays a protracted postnatal neurogenesis. It contains the external germinal layer where dividing progenitors are specified to become granule neurons after birth (Lee,A. *et al*., 2005). This brain structure is implicated in motor coordination, cognitive and affective functions. Disruption of cerebellar structure and function is associated with ataxia, autism, and schizophrenia (Rosenberg,R.N. and Grossman,A. 1989; Martin,P. and Albers,M. 1995). The uncontrolled growth of cerebellar precursors results in medulloblastoma (Wechsler-Reya,R. and Scott,M.P. 2001). Cerebellum contains a high density of CB1Rs, and eCB signaling is essential for many of its functions. Our attention focused on synthetic CBR agonist and antagonist influences on postnatal cerebellar neurogenesis, using an *in vitro* model obtained by culturing rat cerebellar granule cells (CGC) in gelatin-coated dishes in a serum-free medium with bFGF and EGF to maintain a mitotic and undifferentiated state (Zusso,M. 2004).

First, the presence of CBR transcripts and proteins in cerebellar neural progenitors at 10 DIV was investigated. This time was chosen for all experiments described in this thesis. Using real time RT-PCR and Western blotting, CB2R expression was demonstrated in cerebellar neural progenitor cells, in agreement with other reports supporting the existence of this protein in the brain, particularly in CNS proliferative regions. Moreover, we found that CB1R mRNA is more highly expressed than CB2R, as expected from previous studies. CB1R protein was visualized by SDS-PAGE and Western blotting, using an antibody corresponding to amino acids 1-150 mapping at the N-terminus of CB1R. The protein band obtained confirmed its glycosylated nature. Within its long N-terminal tail there are two putative N-linked glycosylation sites at positions 77 and 83. CB2R has a relatively short N-terminus (33 amino acids), and has only one glycosylation site at position 11 (Andersson,H. *et al*., 2003). Song *et al*. developed an anti-peptide antiserum raised against the N-terminal 14 amino acids of the CB1R receptor, which was used to detect by immunoblotting the band shift in rat brain membranes following treatment with exo- and endoglycosidases. The authors demonstrated that brain CB1Rs are N-linked glycoproteins with a heterogeneous carbohydrate composition, consisting in part of high mannose or hybrid carbohydrate moieties with terminal mannose residues. When the CB1R N-terminal tail translocates to the luminal side of the ER membrane, the ER's oligosaccharide transferase adds high mannose-type oligosaccharides

(Andersson,H. *et al*., 2003). The apparent molecular weight of mature CB1Rs is 64 kDa, while the deglycosylated isoform is 53 kDa. These authors did not elucidate if the 53 kDa immunoreactive species represents a portion of newly synthesised receptor not co-translationally glycosylated, or a fraction of CB1Rs cleaved of their mannose chain in the Golgi and not further modified (Song,C. and Howlett,A.C. 1995). Glycosylation of GPCR (e.g. D2, β-adrenergic, and A2-adenosine receptors) can be important for the receptor expression and processing, ligand binding, and second messenger coupling.

Cerebellar neural progenitor expression of both CBRs was confirmed by images corresponding to different optical sections of a single Z-stack acquired by confocal microscopy. The two CBRs appeared to display immunolabeling patterns: CB2R was more uniformly distributed intracellularly, being punctate in some regions, while CB1R localization appeared to be more plasma membrane limited. Golgi complex labeling with anti-β-COP antibody did not define further the origin of CB2R synthesis, a possible localization at the secretory pathway level. Recently, CB1Rs, but not CB2Rs, have been reported to localize in specialized membrane microdomains called caveolae (Rimmerman,N. *et al*., 2008). Caveolae (together with clathrin-coated pits) are involved in CB1R agonist-induced or constitutive endocytosis cycling between the plasma membrane and endosomes. The endosomal recycling pathway has been reported to counteract CB1R desensitization, facilitating its recycling and reactivation (Wu,D.F. *et al*., 2008). Caveolae are spatial compartments enriched in components of GPCR signal transduction. They provide a more organized platform for the proper assembly of signaling complexes, also preventing cross-talk between different pathways (Ostrom,R.S. and Insel,P.A. 2004).

Caveolin 1 expression in cerebellar neural progenitor cells was assessed by confocal microscopy. Double labeling with anti-caveolin and anti-CB2R antibodies did not permit one to assign with certainty a localization of the latter in lipid rafts, due to aspecific overlapping of the two immunolabelings. Immunostained images showed a partial co-localization of caveolin 1 with CB1R, in agreement with literature data.

Receptor tyrosine kinases are known to reside in caveolin-rich microdomains enriched in GPCR. A prototype is represented by the Trk (tropomyosin-related kinase) family, whose function is critical to neuron survival, differentiation, and plasticity. Signals from these receptors are initiated by binding of secreted neurotrophins, including BDNF. Trk receptor activation can also occur through a process termed transactivation through GPCR.

Transactivation is independent of neurotrophin binding, occurs at Golgi complex intracellular membranes, exhibits a delayed time course, involves increased Src (v-src sarcoma viral oncogene homolog) family member activity, mobilization of intracellular calcium, and increases in biosynthetic machinery (Rajagopal,R. and Chao,M.V. 2006). Until now there have been few reports of BDNF TrkB receptor transactivation induced by CB1Rs and assembly of CB1R/TrkB receptor complexes in defined membrane compartments (Berghuis,P. *et al*., 2005). Moreover, Aso *et al*. reported hippocampal BDNF levels are a specific target for the impairment in plasticity induced by stress in CB1R knockout mice (Aso,E. *et al*., 2008).

Using the above information as starting point, we investigated the presence of TrkB receptor in cerebellar neural progenitor cells at 10 DIV by immunolabeling, utilizing an antibody against Trk B gp145 raised against amino acids 794-808 of the full-length TrkB gp145 (data not shown). Confocal microscopy was used to show TrkB protein expression in cerebellar neural progenitors and its partial colocalization with CB1R at the caveolae level (data not shown). Further studies on the possible interaction between these two signaling system were not performed because of the complexity of this line of research.

Subsequently, immunocytochemical analysis was used to investigate CBR expression in cerebellar neural progenitor cells under differentiation conditions. A number of authors have reported eCB system expression to be temporally and spatially regulated during brain development, including the postnatal cerebellum (Deshmukh,S. *et al*., 2007; Belue,R.C. *et al*., 1995). A CBR immunofluorescent signal in cells expressing the neuronal marker MAP2 was already evident at the 2nd differentiation day. Labeling intensity increased with progressive maturation of the neuronal phenotype. CBR expression in glial cells (GFAP+) was much less than in MAP2+ cells. These results are in line with evidence showing eCB system involvement in neuronal migration control and axonal guidance (Berghuis,P. *et al*., 2005); moreover, CB1R astrocyte expression has been reported in nucleus accumbens (Rodriguez,J.J. *et al*., 2001), cingulate cortex, medial forebrain bundle, and amigdala, but its expression in cultured astrocytes is still ambiguous. Astrocyte CB1R activation increases the rate of glucose oxidation and ketogenesis and is coupled to less conventional signaling pathways (e.g. sphingomyelin hydrolysis) (Sanchez,C. *et al*., 1998). Navarrete *et al*. demonstrated functional CB1R expression in hippocampal astrocytes and the existence of eCB-mediated neuron-astrocyte communication (Navarrete,M. and Araque,A. 2008). Neuron-

to-astrocyte communication is based on astrocyte expression of different neurotransmitter receptors that, in many cases, are coupled to second messenger pathways. Immunohistochemical studies have shown CB2R expression by perivascular microglia in cerebellar white matter (Nunez,E. *et al*., 2004) and in human fetal astrocytes (Sheng,W.S. *et al*., 2005).

Given the presence of both CBR protein in cerebellar neural progenitor cells the influence of their modulation on proliferation by [^{3}H]-thymidine incorporation assay was examined. We used two synthetic non-selective, high-affinity CBR agonists, WIN 55,212-2 and CP 55,940. WIN 55,212-2 belongs to a group of aminoalkylindole cannabimimetic compounds, and displays moderate selectivity in favour of CB2R (Shim,J.Y. and Howlett,A.C. 2006). The key pharmacophoric elements for the aminoalkylindole agonists at CB1R are the aminoalkyl moiety, the lipophilic aroyl group, and the heterocyclic indole ring; the aroyl moiety group is reported to be important as the steric trigger for inducing CB1R conformational change (Shim,J.Y. and Howlett,A.C. 2006}}. Aminoalkylindoles have a distinct binding domain that overlaps that of other structurally distinct agonists. CP 55,940 belongs to a second group of non-classical cannabinoids; it is a bicyclic analogue of Δ^9-THC and behaves as a full CBR agonist.

A twenty four hour incubation with either 100 nM WIN 55,212-2 or 1000 nM CP 55,940 significantly increased cerebellar neural proliferation (43 ± 22 % and 37 ± 8 %, respectively) *vs* the corresponding vehicle control (Fig. 24). In both cases, the proliferation response was completely inhibited by 1 μM AM 251 (1 h pre-incubation), a selective CB1R antagonist. Our results show that cerebellar neural progenitor proliferation induced by the two synthetic non-selective CBR agonists is entirely mediated by CB1R activation. In fact, the selective CB2R antagonist AM 630 (1 h pre-incubation), in the concentration range used (10-1000 nM), did not affect the radionuclide incorporation values following 24 h agonist treatment.

These data are in agreement with published findings. Aguado *et al*. reported that 30 nM WIN 55,212-2 significantly increased [^{3}H]-thymidine incorporation and BrdU$^+$ cell number in a CB1R-dependent manner in rat embryo cortical progenitor cultures. The cannabinoid agonist significantly increased both the number of neurosphere *per* well and neurosphere size (Aguado,T. *et al*., 2005). Moreover, these authors demonstrated that WIN 55,212-2 increased proliferation of adult cortical neural progenitors. Kim *et al*. reported that 24 h treatment with 100 nM WIN 55,212-2 enhanced BrdU incorporation into neuron-enriched cerebral cortical

cultures (Kim,S.H. *et al*., 2006). Marchalant *et al*. demonstrated that *in vivo* administration of WIN 55,212-2 restores neurogenesis in the aged rat brain. They proposed an anti-inflammatory mechanism of action based on WIN 55,212-2 ability to counteract LPS-induced microglia activation, as they found increased levels of microglia activation associated with aging (Marchalant,Y. *et al*., 2009). Interestingly, both CBR antagonists *per se* did not affect cerebellar neural progenitor proliferation, leading us to conclude that in the nanomolar range these compounds do not behave as inverse agonists, while excluding the existense of an active eCB tone in our *in vitro* model. CBR constitutive activity is still debated with the literature containing contrasting studies. Examples of inverse agonism at CB1R and possible mechanisms are discussed in Chapter 1 (paragraph 1.4).

CB1R involvement in the cannabinoid-mediated proliferative response of cerebellar neural progenitors was confirmed using ACEA, a synthetic highly selective agonist. Twenty four hour incubation with 1 and 10 nM ACEA significantly increased cerebellar neural proliferation (50.59 ± 6.72 % and 35.77 ± 4.48 %, respectively) *vs* the corresponding vehicle control. This effect was completely inhibited by 10 nM AM 251 (1 h pre-incubation).

ACEA is an arachidonic acid derivative, and the effective concentration is in agreement with its $K_{D/I}$ at CB1R (1.4 ± 0.3 nM) (Hillard,C.J. *et al*., 1999). One can speculate that its nanomolar potency is a consequence of structural features, since it differs from AEA in having a chlorine atom instead of an hydroxyl group. This modification in the amide head group was designed to increase the compound's hydrophobicity, thereby providing greater affinity for CB1R compared to AEA.

Our [^{3}H]-thymidine incorporation data are in agreement with other reports. Molina-Holgado *et al*. demonstrated that 200 nM and 1 μM ACEA stimulated neurosphere formation (determined after 7 days in culture) and BrdU incorporation (3 days after a single exposure) compared with control conditions, in cultures of neural stem cells from mouse embyo cortex (E15-16). This effect was completely mediated by CB1R activation (Molina-Holgado,F. *et al*., 2007). Another study reported that chronic rat postnatal treatment with 20 μM ACEA increased radial glia proliferation and the number of gliogenic precursors in the subventricular zone (Arevalo-Martin,A. *et al*., 2007), consistent with cannabinoids exerting a CB1R-dependent gliogenic effect on neural precursor/stem cells in the subgranular zone (Aguado,T. *et al*., 2006). To exclude that ACEA-induced proliferation was mediated by growth factors (EGF and bFGF) added to the culture medium, we performed [^{3}H]-thymidine incorporation in

the absence of mitogenic factors. Cerebellar neural progenitors not only retained their proliferative capacity, but retained CB1R stimulation responsiveness (data not shown).

The mechanisms underlying the action of the selective CB1R agonist ACEA (1 nM) on cerebellar neural progenitor cell proliferation were investigated through Western blotting. MAPK/ERK and Akt were the major intracellular signaling pathways examined, as they are commonly activated by mitogenic stimuli (EGF or neurotrophins like BDNF). Akt is not only involved in cerebellar granule cell survival (Dudek,H. *et al*., 1997), but it plays a role in IGF-1 signaling in fetal cerebellar precursors (Lin,X. and Bulleit,R.F. 1997), affects cell cycle progression, and self-renewal capacity of embryonic stem cells (Watanabe,S. *et al*., 2006) and fetal neural progenitors (Sinor,A.D. and Lillien,L. 2004). Akt regulates adult neural hippocampal progenitor proliferation, transducing intracellular signals from multiple mitogens, including bFGF, Shh, and IGF-1. It is reported that wild-type Akt over-expression reduces glial and neuronal marker expression during adult neural hippocampal progenitor differentiation (Peltier,J. *et al*., 2007).

Cell surface receptor activation by PI3K leads to an increase in phosphatidylinositol-3,4,5-triphosphate which, in turn, recruits Akt to the plasma membrane. Phosphorylation of Tre308 in the catalytic portion of Akt, and Ser473 in the C-terminal regulatory hydrophobic portion result in a fully activated kinase. Once activated, Akt translocates to the nucleus to regulate gene expression. Akt phosphorylates numerous downstream signaling proteins, including Bad apoptosis machinery members, the forkhead transcription factor, the kinase protein Raf; it increases cyclin D1 levels and activates E2F transcription factor, p53, and GSK3-β pathways. Moreover Akt activates CREB and NF-κB. Many authors have reported that cannabinoids activate the PI3K/Akt pathway by acting on both CB1 and CB2 receptors (Sanchez,M.G. *et al*., 2003), and pharmacological stimulation of CB2R activates Akt in mouse neural progenitors (Palazuelos,J. *et al*., 2006). In this regard, Molina-Holgado *et al*. have proposed the involvement of PI3K-Akt signaling in mediating ACEA induced neural proliferation (Molina-Holgado,F. *et al*., 2007).

$G_{i/o}$ protein coupled receptors can activate PI3K/Akt and ERK pathways through Gβγ subunit release via activation of I_B PI3K isoforms, or via transactivation of growth factor tyrosine kinase receptors and subsequent stimulation of I_A PI3K/Akt and ERK pathways. ERK activation is normally associated with the initial activation of a tyrosine kinase-linked receptor. This activates the intracellular G protein Ras and initiates a signaling cascade

beginning with activation of the serine/threonine kinase Raf. Raf activates MAP kinase kinase (MEK) leading to the phosphorylation and activation of MAPK. Mechanisms for the induction of MAPK by CB1R have not been fully elucidated. A proposed mechanism in rat astrocytes involves PI3K activation which, in turn, mediates tyrosine phosphorylation and Raf activation. Alternatively, some authors suggest that a decrease in cAMP levels and consequently in PKA activity may participate in the stimulatory effect of CB1R activation on the MAPK pathway (Derkinderen,P. *et al*., 2003). Jiang *et al*. demonstrated that non-selective CBR agonists promote embryonic and adult hippocampal neural progenitor proliferation via CB1R through activation of the ERK pathway (404 Jiang,W. *et al*., 2005).

We demonstrated that ACEA treatment of cerebellar neural progenitor cells induced a significant activation of Akt at 15 min *vs* control (36.54 ± 7.21 %). Akt phosphorylation persisted for up to 30 min (21 ± 5 %) when was accompanied by a concomitant ERK activation *vs* control (32 ± 4 %). Activation of both kinases was inhibited by the selective CB1R antagonist AM 251. The specificity ACEA-induced ERK and Akt activation was assessed measuring the kinases phosphorylation levels in cultures pretreated with selective MEK (U0126) and PI3K (LY294002) inhibitors. LY294002 is reported to inhibit proliferation of mouse stem cells and to stimulate their differentiation. U0126 (10 μM) completely inhibited ERK phosphorylation both in untreated and ACEA-treated progenitors, but it did not affect Akt protein levels. On the contrary, LY294002 (75 μM) inhibited Akt activation in basal and treated neural progenitor cells. Moreover the PI3K inhibitor reverted to the control level the phospho-ERK increase induced by ACEA, and *per se* reduced phospho-ERK basal levels. Our results thus demonstrate that Akt contributes to basal ERK activation and to CB1R-induced ERK phosphorylation. The contribution of both kinases to cerebellar neural progenitor proliferation was confirmed by [^{3}H]-thymidine incorporation, with both U0126 and LY294002 significantly reducing ACEA-induced and basal proliferation *per se*.

Berghuis *et al*. reported eCBs are chemoattractants for CB1R$^+$ cholecystokinin-expressing interneurons from rat embryonic cortices. AEA modulated the BDNF-induced migration of CB1R$^+$ interneurons in an additive fashion. The AEA-induced migratory response was mediated by Src kinase-dependent TrkB receptor transactivation. Neuronal cell differentiation was associated with recruitment of CB1Rs and TrkB receptors to the axon terminals of developing interneurons. AEA suppressed the BDNF-dependent morphogenesis of interneurons: it inhibited neurite extension and branching, and this effect was abolished by

Src kinase inhibition (Berghuis,P. *et al*., 2005). Williams *et al*. reported that in rat postnatal cerebellar granule neuron cultures, AM 251 inhibited the N-cadherin and bFGF-stimulated neurite outgrowth response. N-cadherin promotes axonal growth during development through a bFGF signaling cascade, whereby bFGF stimulates PLCγ and so the production of DAG. DAG hydrolysis stimulates calcium influx into the growth cones, which is necessary for an axonal growth cone response. ACEA in the low micromolar range stimulated neurite outgrowth via CB1R activation, whose action was downstream from bFGF receptor activation. This signaling cascade required calcium influx through neuronal N- and L-type calcium channels. BDNF stimulated axonal growth by TrkB receptor activation in a DAG-independent fashon (Williams,E.J. *et al*., 2003). Another study reported AEA inhibition of rat embryonic cortical neuron progenitor and PC12 cell differentiation to the mature phenotype through inhibition of NGF-induced ERK activation via CB1R. AEA was reported to inhibit Rap1/B-Raf signaling that would otherwise result in sustained ERK activation and cell differentiation, because AEA decreased cAMP levels to below those necessary for pathway activation (Rueda,D. *et al*., 2002). Moreover, WIN 55,212-2 was reported to stimulate proliferation and astroglial cell differentiation of rat postnatal cortical neural progenitor cultures, exerting a progliogenic action and a concomitant inhibitory effect on neuronal cell differentiation. The eCB system is involved in the control of postnatal and adult hippocampal astrogliogenesis *in vivo*, and reduced astrogliogenesis and increased neurogenesis in CB1R-deficient mice have been demonstrated (Aguado,T. *et al*., 2006). Conceivably, the proliferative effect of the eCB system on neural progenitor cells may result in either astrogliogenesis or neurogenesis, depending on the intensity of cannabinoid stimulation and/or the cellular context in which it is expressed.

ACEA influence on cerebellar neural progenitor differentiation was investigated by evaluating the pattern of relative expression of AUF1 mRNA splice variant transcripts, an ARE binding protein involved in corticogenesis regulation and whose expression is regulated during cerebellar development. Chromatin remodeling and epigenetic mechanisms may bring about rapid changes in brain function, which is particularly important during the postnatal period. Postnatal and adult neurogenesis can be divided into three stages: self-renewal, fate specification and survival of neural precursors; migration and connection with the pre-existing neurons; reorganization in synaptic connectivity between newborn and pre-existing neurons. Epigenetic alterations leading to chromatin remodeling could provide a system to regulate

gene expression at each stage of neurogenesis. Epigenetic mechanisms include histone modifications, polyADP-ribosylation, DNA methylation, and retrotransposition. Lee *et al*. (Lee,C. *et al*., 2008) reported AUF1 proteins are involved in coordinating gene expression in proliferating neuronal precursors/progenitors and differentiating cortical neurons by recruiting chromatin remodeling molecules to AT-rich DNA elements. Moreover, they found that the spatial and temporal pattern of AUF1 expression and histone deacetylase 1 and metastasis-associated protein 2 members of the nucleosome remodeling and histone deacetylase chromatin remodeling complex are similar in the developing rat brain.

In the present study, BDNF was taken as our 'standard' differentiating stimulus. BDNF is one of the critical factors that control granule cell development. It is expressed in the developing cerebellum and increases during the postnatal period, and regulates granule cell migration to the internal granular layer in a TrkB-dependent fashion. BDNF-deficient mice show defects in survival and migration of granule cells during the postnatal period, and exhibit a persistent EGL resulting from impaired granule cell migration out of the EGL (Borghesani,P.R. *et al*., 2002). Cerebellar BDNF expression is non-uniform, with higher levels in the IGL than in the EGL. As such, BNDF functions as an exogenous gradient to promote motogenesis and directed chemotaxis. In response to the BDNF gradient activated TrkB localizes to endosomes toward the leading process facing the gradient, and endosomes determine the polarized movement. Extracellular BDNF binds to and internalizes TrkB in endodomes, inducing migration along the TrkB gradient. Exogenous BDNF stimulates the release of BDNF from migrating granule cells, locally amplifying the BDNF gradient. Autocrine BDNF is required to make the cells competent to respond to an exogenous BDNF gradient and to establish and maintain the polarity of the TrkB endosomes (Zhou,P. *et al*., 2007). Differentiation was studied over a 6-day time frame, because this is the interval necessary for BDNF action on neural progenitor differentiation – as suggested by earlier studies. ACEA at 1 nM, but not higher concentrations significantly affected neural progenitor differentiation *vs* the untreated cells.

AUF1 mRNA expression pattern in cerebellar neural progenitors at 10 DIV is distinct from that in cells under differentiation conditions, and from postnatal cerebellar granule cell cultures that represent the end point of maturation (data not shown). Relative quantities of all four AUF1 transcripts are higher, expecially p40, which is reported to have the major destabilizing action on ARE mRNA (together with p37), and possesses the highest turnover

rate. Our results are in agreement with Hambardzumyan *et al*. since the most abundant transcript in developing cerebellum corresponds to the p40 isoform (Hambardzumyan,D. *et al*., 2009) . During corticogenesis, p40 is the most abundant isoform at the time when $AUF1^{+}$ cells are immunoreactive for proliferation markers. AUF1 mRNA expression pattern in CGC is in agreement with the findings of Hambardzumyan *et al.,* because p37 and p40 expression *vs* p42 and p45 decreases with progression of cerebellar development. The latter 2 isoforms contain exon 7, and are less ubiquitinated (data not shown). Four and 6 days of differentiation induced by BDNF significantly increased expression of all AUF1 splice variants, expecially p45 (see also Hambardzumyan *et al*.). Following 6 differentiation days in the presence of 1 nM ACEA, the AUF1 isoform expression pattern was similar to BDNF although significant differences were minimized. It is tempting to speculate that ACEA influences cerebellar neural progenitor differentiation. However, this will need confirmation by additional experiments that include AM 251 treatment and a study of the expression pattern of gene targets of AUF1 such as Cyclin D1.

A part from these preliminary experiments on differentiation, we can conclude that: cerebellar neural progenitor cells express cannabinoid CB1 and CB2 receptor gene and immunoreactive protein; CB1Rs reside in caveolae–specialized microdomains and their activation stimulates cerebellar neural progenitor proliferation; CB1R-mediated proliferative response involves activation of the mitogen-activated protein kinase/ERK and phosphatidylinositol 3-kinase signaling pathways, which are linked to each other by a cross-talk mechanism.

CHAPTER 5

REFERENCES

Aguado, T., Monory, K., Palazuelos, J., Stella, N., Cravatt, B., Lutz, B., Marsicano, G., Kokaia, Z., Guzman, M. & Galve-Roperh, I. 2005, "The endocannabinoid system drives neural progenitor proliferation", *The FASEB journal : official publication of the Federation of American Societies for Experimental Biology,* vol. 19, no. 12, pp. 1704-1706.

Aguado, T., Palazuelos, J., Monory, K., Stella, N., Cravatt, B., Lutz, B., Marsicano, G., Kokaia, Z., Guzman, M. & Galve-Roperh, I. 2006, "The endocannabinoid system promotes astroglial differentiation by acting on neural progenitor cells", *The Journal of neuroscience : the official journal of the Society for Neuroscience,* vol. 26, no. 5, pp. 1551-1561.

Aguado, T., Romero, E., Monory, K., Palazuelos, J., Sendtner, M., Marsicano, G., Lutz, B., Guzman, M. & Galve-Roperh, I. 2007, "The CB1 cannabinoid receptor mediates excitotoxicity-induced neural progenitor proliferation and neurogenesis", *The Journal of biological chemistry,* vol. 282, no. 33, pp. 23892-23898.

Alger, B.E. 2002, "Retrograde signaling in the regulation of synaptic transmission: focus on endocannabinoids", *Progress in neurobiology,* vol. 68, no. 4, pp. 247-286.

Allen, J.A., Halverson-Tamboli, R.A. & Rasenick, M.M. 2007, "Lipid raft microdomains and neurotransmitter signalling", *Nature reviews.Neuroscience,* vol. 8, no. 2, pp. 128-140.

Andersson, H., D'Antona, A.M., Kendall, D.A., Von Heijne, G. & Chin, C.N. 2003, "Membrane assembly of the cannabinoid receptor 1: impact of a long N-terminal tail", *Molecular pharmacology,* vol. 64, no. 3, pp. 570-577.

Arevalo-Martin, A., Garcia-Ovejero, D., Rubio-Araiz, A., Gomez, O., Molina-Holgado, F. & Molina-Holgado, E. 2007, "Cannabinoids modulate Olig2 and polysialylated neural cell adhesion molecule expression in the subventricular zone of post-natal rats through cannabinoid receptor 1 and cannabinoid receptor 2", *The European journal of neuroscience,* vol. 26, no. 6, pp. 1548-1559.

Aso, E., Ozaita, A., Valdizan, E.M., Ledent, C., Pazos, A., Maldonado, R. & Valverde, O. 2008, "BDNF impairment in the hippocampus is related to enhanced despair behavior in CB1 knockout mice", *Journal of neurochemistry,* vol. 105, no. 2, pp. 565-572.

Bari, M., Battista, N., Fezza, F., Finazzi-Agro, A. & Maccarrone, M. 2005, "Lipid rafts control signaling of type-1 cannabinoid receptors in neuronal cells. Implications for

anandamide-induced apoptosis", *The Journal of biological chemistry,* vol. 280, no. 13, pp. 12212-12220.

Basile, A.S., Hanus, L. & Mendelson, W.B. 1999, "Characterization of the hypnotic properties of oleamide", *Neuroreport,* vol. 10, no. 5, pp. 947-951.

Beltramo, M. & Piomelli, D. 2000, "Carrier-mediated transport and enzymatic hydrolysis of the endogenous cannabinoid 2-arachidonylglycerol", *Neuroreport,* vol. 11, no. 6, pp. 1231-1235.

Belue, R.C., Howlett, A.C., Westlake, T.M. & Hutchings, D.E. 1995, "The ontogeny of cannabinoid receptors in the brain of postnatal and aging rats", *Neurotoxicology and teratology,* vol. 17, no. 1, pp. 25-30.

Benagiano, V., Lorusso, L., Flace, P., Girolamo, F., Rizzi, A., Sabatini, R., Auteri, P., Bosco, L., Cagiano, R. & Ambrosi, G. 2007, "Effects of prenatal exposure to the CB-1 receptor agonist WIN 55212-2 or CO on the GABAergic neuronal systems of rat cerebellar cortex", *Neuroscience,* vol. 149, no. 3, pp. 592-601.

Benito, C., Nunez, E., Tolon, R.M., Carrier, E.J., Rabano, A., Hillard, C.J. & Romero, J. 2003, "Cannabinoid CB2 receptors and fatty acid amide hydrolase are selectively overexpressed in neuritic plaque-associated glia in Alzheimer's disease brains", *The Journal of neuroscience : the official journal of the Society for Neuroscience,* vol. 23, no. 35, pp. 11136-11141.

Benito, C., Tolon, R.M., Pazos, M.R., Nunez, E., Castillo, A.I. & Romero, J. 2008, "Cannabinoid CB2 receptors in human brain inflammation", *British journal of pharmacology,* vol. 153, no. 2, pp. 277-285.

Berghuis, P., Dobszay, M.B., Wang, X., Spano, S., Ledda, F., Sousa, K.M., Schulte, G., Ernfors, P., Mackie, K., Paratcha, G., Hurd, Y.L. & Harkany, T. 2005, "Endocannabinoids regulate interneuron migration and morphogenesis by transactivating the TrkB receptor", *Proceedings of the National Academy of Sciences of the United States of America,* vol. 102, no. 52, pp. 19115-19120.

Berghuis, P., Rajnicek, A.M., Morozov, Y.M., Ross, R.A., Mulder, J., Urban, G.M., Monory, K., Marsicano, G., Matteoli, M., Canty, A., Irving, A.J., Katona, I., Yanagawa, Y., Rakic, P., Lutz, B., Mackie, K. & Harkany, T. 2007, "Hardwiring the brain: endocannabinoids shape neuronal connectivity", *Science (New York, N.Y.),* vol. 316, no. 5828, pp. 1212-1216.

Bernard, C., Milh, M., Morozov, Y.M., Ben-Ari, Y., Freund, T.F. & Gozlan, H. 2005, "Altering cannabinoid signaling during development disrupts neuronal activity", *Proceedings of the National Academy of Sciences of the United States of America,* vol. 102, no. 26, pp. 9388-9393.

Berrendero, F., Garcia-Gil, L., Hernandez, M.L., Romero, J., Cebeira, M., de Miguel, R., Ramos, J.A. & Fernandez-Ruiz, J.J. 1998, "Localization of mRNA expression and

activation of signal transduction mechanisms for cannabinoid receptor in rat brain during fetal development", *Development (Cambridge, England),* vol. 125, no. 16, pp. 3179-3188.

Berrendero, F., Sepe, N., Ramos, J.A., Di Marzo, V., Fernandez-Ruiz, J.J. 1999, "Analysis of cannabinoid receptor binding and mRNA expression and endogenous cannabinoid contents in the developing rat brain during late gestation and early postnatal period", *Synapse,,* vol. 33, no. 3, pp. 181-191.

Bilkei-Gorzo, A., Racz, I., Valverde, O., Otto, M., Michel, K., Sastre, M. & Zimmer, A. 2005, "Early age-related cognitive impairment in mice lacking cannabinoid CB1 receptors", *Proceedings of the National Academy of Sciences of the United States of America,* vol. 102, no. 43, pp. 15670-15675.

Bisogno, T., Berrendero, F., Ambrosino, G., Cebeira, M., Ramos, J.A., Fernandez-Ruiz, J.J. & Di Marzo, V. 1999, "Brain regional distribution of endocannabinoids: implications for their biosynthesis and biological function", *Biochemical and biophysical research communications,* vol. 256, no. 2, pp. 377-380.

Bisogno, T., Howell, F., Williams, G., Minassi, A., Cascio, M.G., Ligresti, A., Matias, I., Schiano-Moriello, A., Paul, P., Williams, E.J., Gangadharan, U., Hobbs, C., Di Marzo, V. & Doherty, P. 2003, "Cloning of the first sn1-DAG lipases points to the spatial and temporal regulation of endocannabinoid signaling in the brain", *The Journal of cell biology,* vol. 163, no. 3, pp. 463-468.

Bisogno, T., Katayama, K., Melck, D., Ueda, N., De Petrocellis, L., Yamamoto, S. & Di Marzo, V. 1998, "Biosynthesis and degradation of bioactive fatty acid amides in human breast cancer and rat pheochromocytoma cells--implications for cell proliferation and differentiation", *European journal of biochemistry / FEBS,* vol. 254, no. 3, pp. 634-642.

Bisogno, T., MacCarrone, M., De Petrocellis, L., Jarrahian, A., Finazzi-Agro, A., Hillard, C. & Di Marzo, V. 2001, "The uptake by cells of 2-arachidonoylglycerol, an endogenous agonist of cannabinoid receptors", *European journal of biochemistry / FEBS,* vol. 268, no. 7, pp. 1982-1989.

Borghesani, P.R., Peyrin, J.M., Klein, R., Rubin, J., Carter, A.R., Schwartz, P.M., Luster, A., Corfas, G. & Segal, R.A. 2002, "BDNF stimulates migration of cerebellar granule cells", *Development (Cambridge, England),* vol. 129, no. 6, pp. 1435-1442.

Bradford, M.M. 1976, "A rapid and sensitive method for the quantitation of microgram quantities of protein utilizing the principle of protein-dye binding", *Analytical Biochemistry,* vol. 72, pp. 248-254.

Buckley, N.E., Hansson, S., Harta, G. & Mezey, E. 1998, "Expression of the CB1 and CB2 receptor messenger RNAs during embryonic development in the rat", *Neuroscience,* vol. 82, no. 4, pp. 1131-1149.

Burstein, S.H., Rossetti, R.G., Yagen, B. & Zurier, R.B. 2000, "Oxidative metabolism of anandamide", *Prostaglandins & other lipid mediators,* vol. 61, no. 1-2, pp. 29-41.

Cadas, H., di Tomaso, E. & Piomelli, D. 1997, "Occurrence and biosynthesis of endogenous cannabinoid precursor, N-arachidonoyl phosphatidylethanolamine, in rat brain", *The Journal of neuroscience : the official journal of the Society for Neuroscience,* vol. 17, no. 4, pp. 1226-1242.

Cadas, H., Gaillet, S., Beltramo, M., Venance, L. & Piomelli, D. 1996, "Biosynthesis of an endogenous cannabinoid precursor in neurons and its control by calcium and cAMP", *The Journal of neuroscience : the official journal of the Society for Neuroscience,* vol. 16, no. 12, pp. 3934-3942.

Calignano, A., La Rana, G., Giuffrida, A. & Piomelli, D. 1998, "Control of pain initiation by endogenous cannabinoids", *Nature,* vol. 394, no. 6690, pp. 277-281.

Carey, M. & Lisberger, S. 2002, "Embarrassed, but not depressed: eye opening lessons for cerebellar learning", *Neuron,* vol. 35, no. 2, pp. 223-226.

Carleton, A., Petreanu, L.T., Lansford, R., Alvarez-Buylla, A. & Lledo, P.M. 2003, "Becoming a new neuron in the adult olfactory bulb", *Nature neuroscience,* vol. 6, no. 5, pp. 507-518.

Carlson, G., Wang, Y. & Alger, B.E. 2002, "Endocannabinoids facilitate the induction of LTP in the hippocampus", *Nature neuroscience,* vol. 5, no. 8, pp. 723-724.

Chevaleyre, V., Takahashi, K.A. & Castillo, P.E. 2006, "Endocannabinoid-mediated synaptic plasticity in the CNS", *Annual Review of Neuroscience,* vol. 29, pp. 37-76.

Citri, A. & Malenka, R.C. 2008, "Synaptic plasticity: multiple forms, functions, and mechanisms", *Neuropsychopharmacology : official publication of the American College of Neuropsychopharmacology,* vol. 33, no. 1, pp. 18-41.

Conti, S., Costa, B., Colleoni, M., Parolaro, D. & Giagnoni, G. 2002, "Antiinflammatory action of endocannabinoid palmitoylethanolamide and the synthetic cannabinoid nabilone in a model of acute inflammation in the rat", *British journal of pharmacology,* vol. 135, no. 1, pp. 181-187.

Costa, B., Comelli, F., Bettoni, I., Colleoni, M. & Giagnoni, G. 2008, "The endogenous fatty acid amide, palmitoylethanolamide, has anti-allodynic and anti-hyperalgesic effects in a murine model of neuropathic pain: involvement of CB(1), TRPV1 and PPARgamma receptors and neurotrophic factors", *Pain,* .

Cravatt, B.F., Prospero-Garcia, O., Siuzdak, G., Gilula, N.B., Henriksen, S.J., Boger, D.L. & Lerner, R.A. 1995, "Chemical characterization of a family of brain lipids that induce sleep", *Science (New York, N.Y.),* vol. 268, no. 5216, pp. 1506-1509.

Davies, S.P., Reddy, H., Caivano, M. & Cohen, P. 2000, "Specificity and mechanism of action of some commonly used protein kinase inhibitors", *The Biochemical journal,* vol. 351, no. Pt 1, pp. 95-105.

Dawson, M.R., Polito, A., Levine, J.M. & Reynolds, R. 2003, "NG2-expressing glial progenitor cells: an abundant and widespread population of cycling cells in the adult rat CNS", *Molecular and cellular neurosciences,* vol. 24, no. 2, pp. 476-488.

Day, T.A., Rakhshan, F., Deutsch, D.G. & Barker, E.L. 2001, "Role of fatty acid amide hydrolase in the transport of the endogenous cannabinoid anandamide", *Molecular pharmacology,* vol. 59, no. 6, pp. 1369-1375.

Derkinderen, P., Valjent, E., Toutant, M., Corvol, J.C., Enslen, H., Ledent, C., Trzaskos, J., Caboche, J. & Girault, J.A. 2003, "Regulation of extracellular signal-regulated kinase by cannabinoids in hippocampus", *The Journal of neuroscience : the official journal of the Society for Neuroscience,* vol. 23, no. 6, pp. 2371-2382.

Deshmukh, S., Onozuka, K., Bender, K.J., Bender, V.A., Lutz, B., Mackie, K. & Feldman, D.E. 2007, "Postnatal development of cannabinoid receptor type 1 expression in rodent somatosensory cortex", *Neuroscience,* vol. 145, no. 1, pp. 279-287.

Devane, W.A., Hanus, L., Breuer, A., Pertwee, R.G., Stevenson, L.A., Griffin, G., Gibson, D., Mandelbaum, A., Etinger, A. & Mechoulam, R. 1992, "Isolation and structure of a brain constituent that binds to the cannabinoid receptor", *Science (New York, N.Y.),* vol. 258, no. 5090, pp. 1946-1949.

Di Marzo, V. 2008, "Targeting the endocannabinoid system: to enhance or reduce?", *Nature reviews.Drug discovery,* vol. 7, no. 5, pp. 438-455.

Di Marzo, V., Sepe, N., De Petrocellis, L., Berger, A., Crozier, G., Fride, E. & Mechoulam, R. 1998, "Trick or treat from food endocannabinoids?", *Nature,* vol. 396, no. 6712, pp. 636-637.

Dinh, T.P., Carpenter, D., Leslie, F.M., Freund, T.F., Katona, I., Sensi, S.L., Kathuria, S. & Piomelli, D. 2002, "Brain monoglyceride lipase participating in endocannabinoid inactivation", *Proceedings of the National Academy of Sciences of the United States of America,* vol. 99, no. 16, pp. 10819-10824.

Dudek, H., Datta, S.R., Franke, T.F., Birnbaum, M.J., Yao, R., Cooper, G.M., Segal, R.A., Kaplan, D.R. & Greenberg, M.E. 1997, "Regulation of neuronal survival by the serine-threonine protein kinase Akt", *Science (New York, N.Y.),* vol. 275, no. 5300, pp. 661-665.

Facchinetti, F., Del Giudice, E., Furegato, S., Passarotto, M. & Leon, A. 2003, "Cannabinoids ablate release of TNFalpha in rat microglial cells stimulated with lypopolysaccharide", *Glia,* vol. 41, no. 2, pp. 161-168.

Facci, L., Stevens, D.A., Pangallo, M., Franceschini, D., Skaper, S.D. & Strijbos, P.J. 2003, "Corticotropin-releasing factor (CRF) and related peptides confer neuroprotection via type 1 CRF receptors", *Neuropharmacology,* vol. 45, no. 5, pp. 623-636.

Farquhar-Smith, W.P., Egertova, M., Bradbury, E.J., McMahon, S.B., Rice, A.S. & Elphick, M.R. 2000, "Cannabinoid CB(1) receptor expression in rat spinal cord", *Molecular and cellular neurosciences,* vol. 15, no. 6, pp. 510-521.

Fedorova, I., Hashimoto, A., Fecik, R.A., Hedrick, M.P., Hanus, L.O., Boger, D.L., Rice, K.C. & Basile, A.S. 2001, "Behavioral evidence for the interaction of oleamide with multiple neurotransmitter systems", *The Journal of pharmacology and experimental therapeutics,* vol. 299, no. 1, pp. 332-342.

Felder, C.C., Nielsen, A., Briley, E.M., Palkovits, M., Priller, J., Axelrod, J., Nguyen, D.N., Richardson, J.M., Riggin, R.M., Koppel, G.A., Paul, S.M. & Becker, G.W. 1996, "Isolation and measurement of the endogenous cannabinoid receptor agonist, anandamide, in brain and peripheral tissues of human and rat", *FEBS letters,* vol. 393, no. 2-3, pp. 231-235.

Fezza, F., Bisogno, T., Minassi, A., Appendino, G., Mechoulam, R. & Di Marzo, V. 2002, "Noladin ether, a putative novel endocannabinoid: inactivation mechanisms and a sensitive method for its quantification in rat tissues", *FEBS letters,* vol. 513, no. 2-3, pp. 294-298.

Fiszman, M.L., Borodinsky, L.N. & Neale, J.H. 1999, "GABA induces proliferation of immature cerebellar granule cells grown in vitro", *Brain research.Developmental brain research,* vol. 115, no. 1, pp. 1-8.

Fowler, C.J. 2007, "The contribution of cyclooxygenase-2 to endocannabinoid metabolism and action", *British journal of pharmacology,* vol. 152, no. 5, pp. 594-601.

Fowler, C.J. 2003, "Plant-derived, synthetic and endogenous cannabinoids as neuroprotective agents. Non-psychoactive cannabinoids, 'entourage' compounds and inhibitors of N-acyl ethanolamine breakdown as therapeutic strategies to avoid pyschotropic effects", *Brain research.Brain research reviews,* vol. 41, no. 1, pp. 26-43.

Fried, P.A., Watkinson, B. & Gray, R. 2003, "Differential effects on cognitive functioning in 13- to 16-year-olds prenatally exposed to cigarettes and marihuana", *Neurotoxicology and teratology,* vol. 25, no. 4, pp. 427-436.

Gallily, R., Breuer, A. & Mechoulam, R. 2000, "2-Arachidonylglycerol, an endogenous cannabinoid, inhibits tumor necrosis factor-alpha production in murine macrophages, and in mice", *European journal of pharmacology,* vol. 406, no. 1, pp. R5-7.

Galve-Roperh, I., Aguado, T., Rueda, D., Velasco, G. & Guzman, M. 2006, "Endocannabinoids: a new family of lipid mediators involved in the regulation of neural cell development", *Current pharmaceutical design,* vol. 12, no. 18, pp. 2319-2325.

Gebremedhin, D., Lange, A.R., Campbell, W.B., Hillard, C.J. & Harder, D.R. 1999, "Cannabinoid CB1 receptor of cat cerebral arterial muscle functions to inhibit L-type Ca2+ channel current", *The American Journal of Physiology,* vol. 276, no. 6 Pt 2, pp. H2085-93.

Golech, S.A., McCarron, R.M., Chen, Y., Bembry, J., Lenz, F., Mechoulam, R., Shohami, E. & Spatz, M. 2004, "Human brain endothelium: coexpression and function of vanilloid and endocannabinoid receptors", *Brain research.Molecular brain research,* vol. 132, no. 1, pp. 87-92.

Gotz, M. & Huttner, W.B. 2005, "The cell biology of neurogenesis", *Nature reviews.Molecular cell biology,* vol. 6, no. 10, pp. 777-788.

Gulyas, A.I., Cravatt, B.F., Bracey, M.H., Dinh, T.P., Piomelli, D., Boscia, F. & Freund, T.F. 2004, "Segregation of two endocannabinoid-hydrolyzing enzymes into pre- and postsynaptic compartments in the rat hippocampus, cerebellum and amygdala", *The European journal of neuroscience,* vol. 20, no. 2, pp. 441-458.

Guzman, M. 2003, "Cannabinoids: potential anticancer agents", *Nature reviews.Cancer,* vol. 3, no. 10, pp. 745-755.

Hajos, N., Ledent, C. & Freund, T.F. 2001, "Novel cannabinoid-sensitive receptor mediates inhibition of glutamatergic synaptic transmission in the hippocampus", *Neuroscience,* vol. 106, no. 1, pp. 1-4.

Hambardzumyan, D., Sergent-Tanguy, S., Thinard, R., Bonnamain, V., Masip, M., Fabre, A., Boudin, H., Neveu, I. & Naveilhan, P. 2009, "AUF1 and Hu proteins in the developing rat brain: implication in the proliferation and differentiation of neural progenitors", *Journal of neuroscience research,* vol. 87, no. 6, pp. 1296-1309.

Harkany, T., Guzman, M., Galve-Roperh, I., Berghuis, P., Devi, L.A. & Mackie, K. 2007, "The emerging functions of endocannabinoid signaling during CNS development", *Trends in pharmacological sciences,* vol. 28, no. 2, pp. 83-92.

Harkany, T., Keimpema, E., Barabas, K. & Mulder, J. 2008, "Endocannabinoid functions controlling neuronal specification during brain development", *Molecular and cellular endocrinology,* vol. 286, no. 1-2 Suppl 1, pp. S84-90.

Hillard, C.J., Manna, S., Greenberg, M.J., DiCamelli, R., Ross, R.A., Stevenson, L.A., Murphy, V., Pertwee, R.G. & Campbell, W.B. 1999, "Synthesis and characterization of potent and selective agonists of the neuronal cannabinoid receptor (CB1)", *The Journal of pharmacology and experimental therapeutics,* vol. 289, no. 3, pp. 1427-1433.

Hohmann, A.G., Suplita, R.L., Bolton, N.M., Neely, M.H., Fegley, D., Mangieri, R., Krey, J.F., Walker, J.M., Holmes, P.V., Crystal, J.D., Duranti, A., Tontini, A., Mor, M., Tarzia, G. & Piomelli, D. 2005, "An endocannabinoid mechanism for stress-induced analgesia", *Nature,* vol. 435, no. 7045, pp. 1108-1112.

Howlett, A.C. 2004, "Efficacy in CB1 receptor-mediated signal transduction", *British journal of pharmacology,* vol. 142, no. 8, pp. 1209-1218.

Howlett, A.C., Barth, F., Bonner, T.I., Cabral, G., Casellas, P., Devane, W.A., Felder, C.C., Herkenham, M., Mackie, K., Martin, B.R., Mechoulam, R. & Pertwee, R.G. 2002, "International Union of Pharmacology. XXVII. Classification of cannabinoid receptors", *Pharmacological reviews,* vol. 54, no. 2, pp. 161-202.

Howlett, A.C. & Fleming, R.M. 1984, "Cannabinoid inhibition of adenylate cyclase. Pharmacology of the response in neuroblastoma cell membranes", *Molecular pharmacology,* vol. 26, no. 3, pp. 532-538.

Howlett, A.C. & Mukhopadhyay, S. 2000, "Cellular signal transduction by anandamide and 2-arachidonoylglycerol", *Chemistry and physics of lipids,* vol. 108, no. 1-2, pp. 53-70.

Huang, S.M., Strangman, N.M. & Walker, J.M. 1999, "Liquid chromatographic-mass spectrometric measurement of the endogenous cannabinoid 2-arachidonylglycerol in the spinal cord and peripheral nervous system", *Zhongguo yao li xue bao = Acta pharmacologica Sinica,* vol. 20, no. 12, pp. 1098-1102.

Huitron-Resendiz, S., Gombart, L., Cravatt, B.F. & Henriksen, S.J. 2001, "Effect of oleamide on sleep and its relationship to blood pressure, body temperature, and locomotor activity in rats", *Experimental neurology,* vol. 172, no. 1, pp. 235-243.

Jiang, W., Zhang, Y., Xiao, L., Van Cleemput, J., Ji, S.P., Bai, G. & Zhang, X. 2005, "Cannabinoids promote embryonic and adult hippocampus neurogenesis and produce anxiolytic- and antidepressant-like effects", *The Journal of clinical investigation,* vol. 115, no. 11, pp. 3104-3116.

Jin, K., Xie, L., Kim, S.H., Parmentier-Batteur, S., Sun, Y., Mao, X.O., Childs, J. & Greenberg, D.A. 2004, "Defective adult neurogenesis in CB1 cannabinoid receptor knockout mice", *Molecular pharmacology,* vol. 66, no. 2, pp. 204-208.

Karlsson, M., Contreras, J.A., Hellman, U., Tornqvist, H. & Holm, C. 1997, "cDNA cloning, tissue distribution, and identification of the catalytic triad of monoglyceride lipase. Evolutionary relationship to esterases, lysophospholipases, and haloperoxidases", *The Journal of biological chemistry,* vol. 272, no. 43, pp. 27218-27223.

Kaslin, J., Ganz, J. & Brand, M. 2008, "Proliferation, neurogenesis and regeneration in the non-mammalian vertebrate brain", *Philosophical transactions of the Royal Society of London.Series B, Biological sciences,* vol. 363, no. 1489, pp. 101-122.

Kawamura, Y., Fukaya, M., Maejima, T., Yoshida, T., Miura, E., Watanabe, M., Ohno-Shosaku, T. & Kano, M. 2006, "The CB1 cannabinoid receptor is the major cannabinoid receptor at excitatory presynaptic sites in the hippocampus and cerebellum", *The Journal of neuroscience : the official journal of the Society for Neuroscience,* vol. 26, no. 11, pp. 2991-3001.

Keren, O. & Sarne, Y. 2003, "Multiple mechanisms of CB1 cannabinoid receptors regulation", *Brain research,* vol. 980, no. 2, pp. 197-205.

Kim, S.H., Won, S.J., Mao, X.O., Ledent, C., Jin, K. & Greenberg, D.A. 2006, "Role for neuronal nitric-oxide synthase in cannabinoid-induced neurogenesis", *The Journal of pharmacology and experimental therapeutics,* vol. 319, no. 1, pp. 150-154.

Klein, T.W., Newton, C., Larsen, K., Lu, L., Perkins, I., Nong, L. & Friedman, H. 2003, "The cannabinoid system and immune modulation", *Journal of leukocyte biology,* vol. 74, no. 4, pp. 486-496.

Koga, D., Santa, T., Fukushima, T., Homma, H. & Imai, K. 1997, "Liquid chromatographic-atmospheric pressure chemical ionization mass spectrometric determination of anandamide and its analogs in rat brain and peripheral tissues", *Journal of chromatography.B, Biomedical sciences and applications,* vol. 690, no. 1-2, pp. 7-13.

Kondo, S., Kondo, H., Nakane, S., Kodaka, T., Tokumura, A., Waku, K. & Sugiura, T. 1998, "2-Arachidonoylglycerol, an endogenous cannabinoid receptor agonist: identification as one of the major species of monoacylglycerols in various rat tissues, and evidence for its generation through CA2+-dependent and -independent mechanisms", *FEBS letters,* vol. 429, no. 2, pp. 152-156.

Kozak, K.R., Gupta, R.A., Moody, J.S., Ji, C., Boeglin, W.E., DuBois, R.N., Brash, A.R. & Marnett, L.J. 2002, "15-Lipoxygenase metabolism of 2-arachidonylglycerol. Generation of a peroxisome proliferator-activated receptor alpha agonist", *The Journal of biological chemistry,* vol. 277, no. 26, pp. 23278-23286.

Kreitzer, A.C. & Regehr, W.G. 2001, "Retrograde inhibition of presynaptic calcium influx by endogenous cannabinoids at excitatory synapses onto Purkinje cells", *Neuron,* vol. 29, no. 3, pp. 717-727.

Kunos, G., Jarai, Z., Batkai, S., Goparaju, S.K., Ishac, E.J., Liu, J., Wang, L. & Wagner, J.A. 2000, "Endocannabinoids as cardiovascular modulators", *Chemistry and physics of lipids,* vol. 108, no. 1-2, pp. 159-168.

Laemmli, U.K. 1970, "Cleavage of structural proteins during the assembly of the head of bacteriophage T4", *Nature,* vol. 227, no. 5259, pp. 680-685.

Lal, A., Mazan-Mamczarz, K., Kawai, T., Yang, X., Martindale, J.L. & Gorospe, M. 2004, "Concurrent versus individual binding of HuR and AUF1 to common labile target mRNAs", *The EMBO journal,* vol. 23, no. 15, pp. 3092-3102.

Lambert, D.M. & Fowler, C.J. 2005, "The endocannabinoid system: drug targets, lead compounds, and potential therapeutic applications", *Journal of medicinal chemistry,* vol. 48, no. 16, pp. 5059-5087.

Lambert, D.M., Vandevoorde, S., Jonsson, K.O. & Fowler, C.J. 2002, "The palmitoylethanolamide family: a new class of anti-inflammatory agents?", *Current medicinal chemistry,* vol. 9, no. 6, pp. 663-674.

Lee, A., Kessler, J.D., Read, T.A., Kaiser, C., Corbeil, D., Huttner, W.B., Johnson, J.E. & Wechsler-Reya, R.J. 2005, "Isolation of neural stem cells from the postnatal cerebellum", *Nature neuroscience,* vol. 8, no. 6, pp. 723-729.

Lee, C., Gyorgy, A., Maric, D., Sadri, N., Schneider, R.J., Barker, J.L., Lawson, M. & Agoston, D.V. 2008, "Members of the NuRD chromatin remodeling complex interact with AUF1 in developing cortical neurons", *Cerebral cortex (New York, N.Y.: 1991),* vol. 18, no. 12, pp. 2909-2919.

Leggett, J.D., Aspley, S., Beckett, S.R., D'Antona, A.M., Kendall, D.A. & Kendall, D.A. 2004, "Oleamide is a selective endogenous agonist of rat and human CB1 cannabinoid receptors", *British journal of pharmacology,* vol. 141, no. 2, pp. 253-262.

Leterrier, C., Bonnard, D., Carrel, D., Rossier, J. & Lenkei, Z. 2004, "Constitutive endocytic cycle of the CB1 cannabinoid receptor", *The Journal of biological chemistry,* vol. 279, no. 34, pp. 36013-36021.

Leterrier, C., Laine, J., Darmon, M., Boudin, H., Rossier, J. & Lenkei, Z. 2006, "Constitutive activation drives compartment-selective endocytosis and axonal targeting of type 1 cannabinoid receptors", *The Journal of neuroscience : the official journal of the Society for Neuroscience,* vol. 26, no. 12, pp. 3141-3153.

Leung, D., Saghatelian, A., Simon, G.M. & Cravatt, B.F. 2006, "Inactivation of N-acyl phosphatidylethanolamine phospholipase D reveals multiple mechanisms for the biosynthesis of endocannabinoids", *Biochemistry,* vol. 45, no. 15, pp. 4720-4726.

Lever, I.J., Robinson, M., Cibelli, M., Paule, C., Santha, P., Yee, L., Hunt, S.P., Cravatt, B.F., Elphick, M.R., Nagy, I. & Rice, A.S. 2009, "Localization of the endocannabinoid-degrading enzyme fatty acid amide hydrolase in rat dorsal root ganglion cells and its regulation after peripheral nerve injury", *The Journal of neuroscience : the official journal of the Society for Neuroscience,* vol. 29, no. 12, pp. 3766-3780.

Levine, J.M., Reynolds, R. & Fawcett, J.W. 2001, "The oligodendrocyte precursor cell in health and disease", *Trends in neurosciences,* vol. 24, no. 1, pp. 39-47.

Lichtman, A.H., Hawkins, E.G., Griffin, G. & Cravatt, B.F. 2002, "Pharmacological activity of fatty acid amides is regulated, but not mediated, by fatty acid amide hydrolase in vivo", *The Journal of pharmacology and experimental therapeutics,* vol. 302, no. 1, pp. 73-79.

Ligresti, A., Bisogno, T., Matias, I., De Petrocellis, L., Cascio, M.G., Cosenza, V., D'argenio, G., Scaglione, G., Bifulco, M., Sorrentini, I. & Di Marzo, V. 2003, "Possible endocannabinoid control of colorectal cancer growth", *Gastroenterology,* vol. 125, no. 3, pp. 677-687.

Lin, X. & Bulleit, R.F. 1997, "Insulin-like growth factor I (IGF-I) is a critical trophic factor for developing cerebellar granule cells", *Brain research.Developmental brain research,* vol. 99, no. 2, pp. 234-242.

Liu, J., Wang, L., Harvey-White, J., Osei-Hyiaman, D., Razdan, R., Gong, Q., Chan, A.C., Zhou, Z., Huang, B.X., Kim, H.Y. & Kunos, G. 2006, "A biosynthetic pathway for anandamide", *Proceedings of the National Academy of Sciences of the United States of America,* vol. 103, no. 36, pp. 13345-13350.

Llano, I., Leresche, N. & Marty, A. 1991, "Calcium entry increases the sensitivity of cerebellar Purkinje cells to applied GABA and decreases inhibitory synaptic currents", *Neuron,* vol. 6, no. 4, pp. 565-574.

Lois, C. & Alvarez-Buylla, A. 1994, "Long-distance neuronal migration in the adult mammalian brain", *Science (New York, N.Y.),* vol. 264, no. 5162, pp. 1145-1148.

Lopez-Gallardo, M., Llorente, R., Llorente-Berzal, A., Marco, E.M., Prada, C., Di Marzo, V. & Viveros, M.P. 2008, "Neuronal and glial alterations in the cerebellar cortex of maternally deprived rats: gender differences and modulatory effects of two inhibitors of endocannabinoid inactivation", *Developmental neurobiology,* vol. 68, no. 12, pp. 1429-1440.

Maccarrone, M., Attina, M., Cartoni, A., Bari, M. & Finazzi-Agro, A. 2001, "Gas chromatography-mass spectrometry analysis of endogenous cannabinoids in healthy and tumoral human brain and human cells in culture", *Journal of neurochemistry,* vol. 76, no. 2, pp. 594-601.

Maccarrone, M., Fiorucci, L., Erba, F., Bari, M., Finazzi-Agro, A. & Ascoli, F. 2000, "Human mast cells take up and hydrolyze anandamide under the control of 5-lipoxygenase and do not express cannabinoid receptors", *FEBS letters,* vol. 468, no. 2-3, pp. 176-180.

Mackie, K. 2006, "Cannabinoid receptors as therapeutic targets", *Annual Review of Pharmacology and Toxicology,* vol. 46, pp. 101-122.

Mackie, K. & Hille, B. 1992, "Cannabinoids inhibit N-type calcium channels in neuroblastoma-glioma cells", *Proceedings of the National Academy of Sciences of the United States of America,* vol. 89, no. 9, pp. 3825-3829.

Malan, T.P.,Jr, Ibrahim, M.M., Vanderah, T.W., Makriyannis, A. & Porreca, F. 2002, "Inhibition of pain responses by activation of CB(2) cannabinoid receptors", *Chemistry and physics of lipids,* vol. 121, no. 1-2, pp. 191-200.

Marchalant, Y., Brothers, H.M. & Wenk, G.L. 2009, "Cannabinoid agonist WIN-55,212-2 partially restores neurogenesis in the aged rat brain", *Molecular psychiatry,* vol. 14, no. 12, pp. 1068-1069.

Maresz, K., Carrier, E.J., Ponomarev, E.D., Hillard, C.J. & Dittel, B.N. 2005, "Modulation of the cannabinoid CB2 receptor in microglial cells in response to inflammatory stimuli", *Journal of neurochemistry,* vol. 95, no. 2, pp. 437-445.

Marsicano, G., Goodenough, S., Monory, K., Hermann, H., Eder, M., Cannich, A., Azad, S.C., Cascio, M.G., Gutierrez, S.O., van der Stelt, M., Lopez-Rodriguez, M.L., Casanova, E., Schutz, G., Zieglgansberger, W., Di Marzo, V., Behl, C. & Lutz, B. 2003, "CB1 cannabinoid receptors and on-demand defense against excitotoxicity", *Science (New York, N.Y.),* vol. 302, no. 5642, pp. 84-88.

Martin, P. & Albers, M. 1995, "Cerebellum and schizophrenia: a selective review", *Schizophrenia bulletin,* vol. 21, no. 2, pp. 241-250.

McFarland, M.J., Porter, A.C., Rakhshan, F.R., Rawat, D.S., Gibbs, R.A. & Barker, E.L. 2004, "A role for caveolae/lipid rafts in the uptake and recycling of the endogenous cannabinoid anandamide", *The Journal of biological chemistry,* vol. 279, no. 40, pp. 41991-41997.

Mechoulam, R., Ben-Shabat, S., Hanus, L., Ligumsky, M., Kaminski, N.E., Schatz, A.R., Gopher, A., Almog, S., Martin, B.R. & Compton, D.R. 1995, "Identification of an endogenous 2-monoglyceride, present in canine gut, that binds to cannabinoid receptors", *Biochemical pharmacology,* vol. 50, no. 1, pp. 83-90.

Mechoulam, R., Fride, E., Hanus, L., Sheskin, T., Bisogno, T., Di Marzo, V., Bayewitch, M. & Vogel, Z. 1997, "Anandamide may mediate sleep induction", *Nature,* vol. 389, no. 6646, pp. 25-26.

Mechoulam, R., Gaoni, Y. 1965, "The isolation and structure of cannabinolic, cannabidiolic and cannabigerolic acids", *Tetrahedron Letters,* vol. 9, pp. 5771-5772.

Mereu, G., Fa, M., Ferraro, L., Cagiano, R., Antonelli, T., Tattoli, M., Ghiglieri, V., Tanganelli, S., Gessa, G.L. & Cuomo, V. 2003, "Prenatal exposure to a cannabinoid agonist produces memory deficits linked to dysfunction in hippocampal long-term potentiation and glutamate release", *Proceedings of the National Academy of Sciences of the United States of America,* vol. 100, no. 8, pp. 4915-4920.

Mikasova, L., Groc, L., Choquet, D. & Manzoni, O.J. 2008, "Altered surface trafficking of presynaptic cannabinoid type 1 receptor in and out synaptic terminals parallels receptor desensitization", *Proceedings of the National Academy of Sciences of the United States of America,* vol. 105, no. 47, pp. 18596-18601.

Molina-Holgado, F., Pinteaux, E., Moore, J.D., Molina-Holgado, E., Guaza, C., Gibson, R.M. & Rothwell, N.J. 2003, "Endogenous interleukin-1 receptor antagonist mediates anti-inflammatory and neuroprotective actions of cannabinoids in neurons and glia", *The Journal of neuroscience : the official journal of the Society for Neuroscience,* vol. 23, no. 16, pp. 6470-6474.

Molina-Holgado, F., Rubio-Araiz, A., Garcia-Ovejero, D., Williams, R.J., Moore, J.D., Arevalo-Martin, A., Gomez-Torres, O. & Molina-Holgado, E. 2007, "CB2 cannabinoid receptors promote mouse neural stem cell proliferation", *The European journal of neuroscience,* vol. 25, no. 3, pp. 629-634.

Moody, J.S., Kozak, K.R., Ji, C. & Marnett, L.J. 2001, "Selective oxygenation of the endocannabinoid 2-arachidonylglycerol by leukocyte-type 12-lipoxygenase", *Biochemistry,* vol. 40, no. 4, pp. 861-866.

Mu, J., Zhuang, S.Y., Kirby, M.T., Hampson, R.E. & Deadwyler, S.A. 1999, "Cannabinoid receptors differentially modulate potassium A and D currents in hippocampal neurons in culture", *The Journal of pharmacology and experimental therapeutics,* vol. 291, no. 2, pp. 893-902.

Murillo-Rodriguez, E., Giordano, M., Cabeza, R., Henriksen, S.J., Mendez Diaz, M., Navarro, L. & Prospero-Garcia, O. 2001, "Oleamide modulates memory in rats", *Neuroscience letters,* vol. 313, no. 1-2, pp. 61-64.

Navarrete, M. & Araque, A. 2008, "Endocannabinoids mediate neuron-astrocyte communication", *Neuron,* vol. 57, no. 6, pp. 883-893.

Nunez, E., Benito, C., Pazos, M.R., Barbachano, A., Fajardo, O., Gonzalez, S., Tolon, R.M. & Romero, J. 2004, "Cannabinoid CB2 receptors are expressed by perivascular microglial cells in the human brain: an immunohistochemical study", *Synapse (New York, N.Y.),* vol. 53, no. 4, pp. 208-213.

Okano, H. & Sawamoto, K. 2008, "Neural stem cells: involvement in adult neurogenesis and CNS repair", *Philosophical transactions of the Royal Society of London.Series B, Biological sciences,* vol. 363, no. 1500, pp. 2111-2122.

Ortar, G., Ligresti, A., De Petrocellis, L., Morera, E. & Di Marzo, V. 2003, "Novel selective and metabolically stable inhibitors of anandamide cellular uptake", *Biochemical pharmacology,* vol. 65, no. 9, pp. 1473-1481.

Ostrom, R.S. & Insel, P.A. 2004, "The evolving role of lipid rafts and caveolae in G protein-coupled receptor signaling: implications for molecular pharmacology", *British journal of pharmacology,* vol. 143, no. 2, pp. 235-245.

Ozaita, A., Puighermanal, E. & Maldonado, R. 2007, "Regulation of PI3K/Akt/GSK-3 pathway by cannabinoids in the brain", *Journal of neurochemistry,* vol. 102, no. 4, pp. 1105-1114.

Palazuelos, J., Aguado, T., Egia, A., Mechoulam, R., Guzman, M. & Galve-Roperh, I. 2006, "Non-psychoactive CB2 cannabinoid agonists stimulate neural progenitor proliferation", *The FASEB journal : official publication of the Federation of American Societies for Experimental Biology,* vol. 20, no. 13, pp. 2405-2407.

Peltier, J., O'Neill, A. & Schaffer, D.V. 2007, "PI3K/Akt and CREB regulate adult neural hippocampal progenitor proliferation and differentiation", *Developmental neurobiology,* vol. 67, no. 10, pp. 1348-1361.

Pertwee, R.G. 2005, "Inverse agonism and neutral antagonism at cannabinoid CB1 receptors", *Life Sciences,* vol. 76, no. 12, pp. 1307-1324.

Petrosino, S., Ligresti, A. & Di Marzo, V. 2009, "Endocannabinoid chemical biology: a tool for the development of novel therapies", *Current opinion in chemical biology,* vol. 13, no. 3, pp. 309-320.

Piomelli, D., Beltramo, M., Glasnapp, S., Lin, S.Y., Goutopoulos, A., Xie, X.Q. & Makriyannis, A. 1999, "Structural determinants for recognition and translocation by the anandamide transporter", *Proceedings of the National Academy of Sciences of the United States of America,* vol. 96, no. 10, pp. 5802-5807.

Piomelli, D., Giuffrida, A., Calignano, A. & Rodriguez de Fonseca, F. 2000, "The endocannabinoid system as a target for therapeutic drugs", *Trends in pharmacological sciences,* vol. 21, no. 6, pp. 218-224.

Rajagopal, R. & Chao, M.V. 2006, "A role for Fyn in Trk receptor transactivation by G-protein-coupled receptor signaling", *Molecular and cellular neurosciences,* vol. 33, no. 1, pp. 36-46.

Ramos, J.A., De Miguel, R., Cebeira, M., Hernandez, M. & Fernandez-Ruiz, J. 2002, "Exposure to cannabinoids in the development of endogenous cannabinoid system", *Neurotoxicity research,* vol. 4, no. 4, pp. 363-372.

Rimmerman, N., Hughes, H.V., Bradshaw, H.B., Pazos, M.X., Mackie, K., Prieto, A.L. & Walker, J.M. 2008, "Compartmentalization of endocannabinoids into lipid rafts in a dorsal root ganglion cell line", *British journal of pharmacology,* vol. 153, no. 2, pp. 380-389.

Rodriguez de Fonseca, F., Ramos, J.A., Bonnin, A. & Fernandez-Ruiz, J.J. 1993, "Presence of cannabinoid binding sites in the brain from early postnatal ages", *Neuroreport,* vol. 4, no. 2, pp. 135-138.

Rodriguez, J.J., Mackie, K. & Pickel, V.M. 2001, "Ultrastructural localization of the CB1 cannabinoid receptor in mu-opioid receptor patches of the rat Caudate putamen nucleus", *The Journal of neuroscience : the official journal of the Society for Neuroscience,* vol. 21, no. 3, pp. 823-833.

Rosenberg, R.N. & Grossman, A. 1989, "Hereditary ataxia", *Neurologic clinics,* vol. 7, no. 1, pp. 25-36.

Ross, R.A., Craib, S.J., Stevenson, L.A., Pertwee, R.G., Henderson, A., Toole, J. & Ellington, H.C. 2002, "Pharmacological characterization of the anandamide cyclooxygenase

metabolite: prostaglandin E2 ethanolamide", *The Journal of pharmacology and experimental therapeutics,* vol. 301, no. 3, pp. 900-907.

Rubino, T., Forlani, G., Vigano, D., Zippel, R. & Parolaro, D. 2004, "Modulation of extracellular signal-regulated kinases cascade by chronic delta 9-tetrahydrocannabinol treatment", *Molecular and cellular neurosciences,* vol. 25, no. 3, pp. 355-362.

Rueda, D., Navarro, B., Martinez-Serrano, A., Guzman, M. & Galve-Roperh, I. 2002, "The endocannabinoid anandamide inhibits neuronal progenitor cell differentiation through attenuation of the Rap1/B-Raf/ERK pathway", *The Journal of biological chemistry,* vol. 277, no. 48, pp. 46645-46650.

Safo, P.K., Cravatt, B.F. & Regehr, W.G. 2006, "Retrograde endocannabinoid signaling in the cerebellar cortex", *Cerebellum (London, England),* vol. 5, no. 2, pp. 134-145.

Sanchez, C., Galve-Roperh, I., Rueda, D. & Guzman, M. 1998, "Involvement of sphingomyelin hydrolysis and the mitogen-activated protein kinase cascade in the Delta9-tetrahydrocannabinol-induced stimulation of glucose metabolism in primary astrocytes", *Molecular pharmacology,* vol. 54, no. 5, pp. 834-843.

Sanchez, M.G., Ruiz-Llorente, L., Sanchez, A.M. & Diaz-Laviada, I. 2003, "Activation of phosphoinositide 3-kinase/PKB pathway by CB(1) and CB(2) cannabinoid receptors expressed in prostate PC-3 cells. Involvement in Raf-1 stimulation and NGF induction", *Cellular signalling,* vol. 15, no. 9, pp. 851-859.

Sarkar, B., Xi, Q., He, C. & Schneider, R.J. 2003, "Selective degradation of AU-rich mRNAs promoted by the p37 AUF1 protein isoform", *Molecular and cellular biology,* vol. 23, no. 18, pp. 6685-6693.

Schmid, P.C., Paria, B.C., Krebsbach, R.J., Schmid, H.H. & Dey, S.K. 1997, "Changes in anandamide levels in mouse uterus are associated with uterine receptivity for embryo implantation", *Proceedings of the National Academy of Sciences of the United States of America,* vol. 94, no. 8, pp. 4188-4192.

Schmid, P.C., Schwartz, K.D., Smith, C.N., Krebsbach, R.J., Berdyshev, E.V. & Schmid, H.H. 2000, "A sensitive endocannabinoid assay. The simultaneous analysis of N-acylethanolamines and 2-monoacylglycerols", *Chemistry and physics of lipids,* vol. 104, no. 2, pp. 185-191.

Sheng, W.S., Hu, S., Min, X., Cabral, G.A., Lokensgard, J.R. & Peterson, P.K. 2005, "Synthetic cannabinoid WIN55,212-2 inhibits generation of inflammatory mediators by IL-1beta-stimulated human astrocytes", *Glia,* vol. 49, no. 2, pp. 211-219.

Shim, J.Y. & Howlett, A.C. 2006, "WIN55212-2 docking to the CB1 cannabinoid receptor and multiple pathways for conformational induction", *Journal of chemical information and modeling,* vol. 46, no. 3, pp. 1286-1300.

Showalter, V.M., Compton, D.R., Martin, B.R. & Abood, M.E. 1996, "Evaluation of binding in a transfected cell line expressing a peripheral cannabinoid receptor (CB2): identification of cannabinoid receptor subtype selective ligands", *The Journal of pharmacology and experimental therapeutics,* vol. 278, no. 3, pp. 989-999.

Simon, G.M. & Cravatt, B.F. 2006, "Endocannabinoid biosynthesis proceeding through glycerophospho-N-acyl ethanolamine and a role for alpha/beta-hydrolase 4 in this pathway", *The Journal of biological chemistry,* vol. 281, no. 36, pp. 26465-26472.

Sinor, A.D. & Lillien, L. 2004, "Akt-1 expression level regulates CNS precursors", *The Journal of neuroscience : the official journal of the Society for Neuroscience,* vol. 24, no. 39, pp. 8531-8541.

Skaper, S.D., Facci, L., Dilani, D., Leon, A. & Toffano, G. 1990, *Culture and use of primary and clonal neural cells. In: P.M. Conn, Editor, Methods in Neurosciences,* .

Skaper, S.D., Buriani, A., Dal Toso, R., Petrelli, L., Romanello, S., Facci, L. & Leon, A. 1996, "The ALIAmide palmitoylethanolamide and cannabinoids, but not anandamide, are protective in a delayed postglutamate paradigm of excitotoxic death in cerebellar granule neurons", *Proceedings of the National Academy of Sciences of the United States of America,* vol. 93, no. 9, pp. 3984-3989.

Smith, P.B., Compton, D.R., Welch, S.P., Razdan, R.K., Mechoulam, R. & Martin, B.R. 1994, "The pharmacological activity of anandamide, a putative endogenous cannabinoid, in mice", *The Journal of pharmacology and experimental therapeutics,* vol. 270, no. 1, pp. 219-227.

Song, C. & Howlett, A.C. 1995, "Rat brain cannabinoid receptors are N-linked glycosylated proteins", *Life Sciences,* vol. 56, no. 23-24, pp. 1983-1989.

Spoto, B., Fezza, F., Parlongo, G., Battista, N., Sgro', E., Gasperi, V., Zoccali, C. & Maccarrone, M. 2006, "Human adipose tissue binds and metabolizes the endocannabinoids anandamide and 2-arachidonoylglycerol", *Biochimie,* vol. 88, no. 12, pp. 1889-1897.

Stefano, G.B., Bilfinger, T.V., Rialas, C.M. & Deutsch, D.G. 2000, "2-Arachidonyl-Glycerol Stimulates Nitric Oxide Release from Human Immune and Vascular Tissues and Invertebrate Immunocytes by Cannabinoid Receptor 1", *Pharmacological research : the official journal of the Italian Pharmacological Society,* vol. 42, no. 4, pp. 317-322.

Straiker, A. & Mackie, K. 2005, "Depolarization-induced suppression of excitation in murine autaptic hippocampal neurones", *The Journal of physiology,* vol. 569, no. Pt 2, pp. 501-517.

Straiker, A., Stella, N., Piomelli, D., Mackie, K., Karten, H.J. & Maguire, G. 1999, "Cannabinoid CB1 receptors and ligands in vertebrate retina: localization and function of an endogenous signaling system", *Proceedings of the National Academy of Sciences of the United States of America,* vol. 96, no. 25, pp. 14565-14570.

Suarez, J., Bermudez-Silva, F.J., Mackie, K., Ledent, C., Zimmer, A., Cravatt, B.F. & de Fonseca, F.R. 2008, "Immunohistochemical description of the endogenous cannabinoid system in the rat cerebellum and functionally related nuclei", *The Journal of comparative neurology,* vol. 509, no. 4, pp. 400-421.

Sugiura, T., Kobayashi, Y., Oka, S. & Waku, K. 2002, "Biosynthesis and degradation of anandamide and 2-arachidonoylglycerol and their possible physiological significance", *Prostaglandins, leukotrienes, and essential fatty acids,* vol. 66, no. 2-3, pp. 173-192.

Torrisani, J., Unterberger, A., Tendulkar, S.R., Shikimi, K. & Szyf, M. 2007, "AUF1 cell cycle variations define genomic DNA methylation by regulation of DNMT1 mRNA stability", *Molecular and cellular biology,* vol. 27, no. 1, pp. 395-410.

Trushina, E., Du Charme, J., Parisi, J. & McMurray, C.T. 2006, "Neurological abnormalities in caveolin-1 knock out mice", *Behavioural brain research,* vol. 172, no. 1, pp. 24-32.

Van Sickle, M.D., Duncan, M., Kingsley, P.J., Mouihate, A., Urbani, P., Mackie, K., Stella, N., Makriyannis, A., Piomelli, D., Davison, J.S., Marnett, L.J., Di Marzo, V., Pittman, Q.J., Patel, K.D. & Sharkey, K.A. 2005, "Identification and functional characterization of brainstem cannabinoid CB2 receptors", *Science (New York, N.Y.),* vol. 310, no. 5746, pp. 329-332.

Wang, V.Y. & Zoghbi, H.Y. 2001, "Genetic regulation of cerebellar development", *Nature reviews.Neuroscience,* vol. 2, no. 7, pp. 484-491.

Watanabe, S., Umehara, H., Murayama, K., Okabe, M., Kimura, T. & Nakano, T. 2006, "Activation of Akt signaling is sufficient to maintain pluripotency in mouse and primate embryonic stem cells", *Oncogene,* vol. 25, no. 19, pp. 2697-2707.

Wechsler-Reya, R. & Scott, M.P. 2001, "The developmental biology of brain tumors", *Annual Review of Neuroscience,* vol. 24, pp. 385-428.

Williams, E.J., Walsh, F.S. & Doherty, P. 2003, "The FGF receptor uses the endocannabinoid signaling system to couple to an axonal growth response", *The Journal of cell biology,* vol. 160, no. 4, pp. 481-486.

Wilson, I.G. 1997, "Inhibition and facilitation of nucleic acid amplification", *Applied and Environmental Microbiology,* vol. 63, no. 10, pp. 3741-3751.

Wilson, I.G. 1997, "Inhibition and facilitation of nucleic acid amplification", *Applied and Environmental Microbiology,* vol. 63, no. 10, pp. 3741-3751.

Wonders, C.P., Anderson, S.A. 2006, "The origin and specification of cortical interneurons", *Nature reviews Neuroscience,* vol. 7, no. 9, pp. 687-696.

Yoshida, T., Fukaya, M., Uchigashima, M., Miura, E., Kamiya, H., Kano, M. & Watanabe, M. 2006, "Localization of diacylglycerol lipase-alpha around postsynaptic spine suggests close proximity between production site of an endocannabinoid, 2-arachidonoyl-glycerol,

and presynaptic cannabinoid CB1 receptor", *The Journal of neuroscience : the official journal of the Society for Neuroscience,* vol. 26, no. 18, pp. 4740-4751.

Zhou, P., Porcionatto, M., Pilapil, M., Chen, Y., Choi, Y., Tolias, K.F., Bikoff, J.B., Hong, E.J., Greenberg, M.E. & Segal, R.A. 2007, "Polarized signaling endosomes coordinate BDNF-induced chemotaxis of cerebellar precursors", *Neuron,* vol. 55, no. 1, pp. 53-68.

Zucker, R.S. & Regehr, W.G. 2002, "Short-term synaptic plasticity", *Annual Review of Physiology,* vol. 64, pp. 355-405.

Zusso, M., Debetto, P., Guidolin, D., Barbierato, M., Manev, H. & Giusti, P. 2008, "Fluoxetine-induced proliferation and differentiation of neural progenitor cells isolated from rat postnatal cerebellum", *Biochemical pharmacology,* vol. 76, no. 3, pp. 391-403.

Zusso, M., Debetto, P., Guidolin, D. & Giusti, P. 2004, "Cerebellar granular cell cultures as an in vitro model for antidepressant drug-induced neurogenesis", *Critical reviews in neurobiology,* vol. 16, no. 1-2, pp. 59-65.

ACKNOWLEDGEMENTS

Desidero innanzitutto ringraziare il Prof. Giusti che mi ha accompagnata e guidata in questo percorso formativo post-lauream, dandomi l'opportunità di appassionarmi al mondo della ricerca e di nutrire la mia curiosità.

Desidero ringraziare il Dott. Stephen Skaper per l'aiuto datomi nella stesura di questa tesi, per le sue lezioni d'inglese, la sua attività di supervisore critico nei miei esperimenti, e per il suo sano umorismo.

Desidero ringraziare tutti i componenti del lab.di Neuropsicofarmacologia, ed in particolare il Dott. Massimo Barbierato per le sue lezioni di biologia molecolare e per la pazienza con cui mi ha seguita nel lavoro sperimentale svolto assieme

Desidero ringraziare i miei genitori, mamma Lucia e papà Piero, per i numerosi sacrifici fatti per darmi la possibilità di studiare e di arricchirmi come persona, nonché per tutti i loro insegnamenti e per la grande pazienza e comprensione dimostratami.

Desidero ringraziare Andrea per essermi stato vicino e per tutto il suo amore.

Infine, ma non di minor rilievo, rivolgo un grazie a Maria perché con la sua preghiera mi ha sempre sorretta e mi ha trasmesso una grande forza.